

Towards Rapid Electrochemical Test System of Polyanilino-Laccase-on-Gold Enzyme Nanobiosensor for Water Estrogens



By

Sinazo Qakala



A thesis submitted in partial fulfilment of the requirements for the degree of

Magister Scientiae in Nanoscience

Faculty of Science

University of the Western Cape

Cape Town, South Africa

Supervisor: Prof Emmanuel I Iwuoha

Co-supervisor: Dr Tesfaye T Waryo

November 2013

Page Left Blank



Towards Rapid Electrochemical Test System of Polyanilino-Laccase-on-Gold Enzyme Nanobiosensor for Water Estrogens

Sinazo Qakala

KEYWORDS

17 α -ethnylestradiol

17 β -estradiol

Estriol

Estrone

Laccase (*Trametes versicolor*)

Gold nanoparticles

Cyclic voltammetry

Polyaniline

Enzyme biosensor

Endocrine Disrupting Compounds



Page Left Blank



Abstract

Current water treatment technologies do not remove many endocrine disruptor compounds (EDCs) such as 17α -ethynylestradiol (EE2) in its entirety, and the amount of these pollutants that continues to enter the aquatic environment through wastewater effluents is still capable of causing harmful health effects. Therefore the development of simpler and more sensitive biosensor system for detection of EE2 must be developed which have high responsiveness, low cost and easy handling. Therefore the aim of this study was to work towards the development of rapid test system of polyaniline-laccase on gold enzyme nanobiosensor (PANI-PSSA/Lac/Glu) for water estrogens. Preliminary studies were first done on the materials used in this study: estrogens, laccase, gold nanoparticles (AuNPs), and electropolymerized PANI-PSSA. Laccase was shown to be active towards EE2 and the enzyme could be stored for over three months. EE2 solution also could be used for over three months. Buffer used in this study was found to be suitable. Phosphoric acid (H_3PO_4) was a suitable electrolyte than hydrochloric acid (HCl) to be used for the electropolymerization of aniline and was used because it has same ions as the McIlvaine buffer (McIIB) which the post-deposition CVs indicated the formation of electrochemically very stable film. AuNPs were successfully synthesized and its size was identified to be less than 22 nm. McIIB used for testing electrochemical properties of AuNP. CVs of GC/PANI-PSSA and GC/PANI-PSSA/Au showed no difference before and after exposure to aq. EE2 solution, an indication of being re-usable and could also serve as stable immobilising platform in laccase biosensor. When interrogating with electrochemical impedance spectroscopy (EIS), the charge transfer resistance (R_{ct}) of both GC/PANI-PSSA and GC/PANI-PSSA/Lac/Glu showed an average increase by about 2.4% and 21% before and after exposure of EE2, respectively. This shows that the GC/PANI-PSSA/Lac/Glu was a functional EE2 biosensor and showing a positive step towards achieving a re-usable biosensor for EE2 as a model water estrogen. Future work

will focus on exploring different ways of improving the biosensor's surface regeneration and its sensitivity to EE2.



Page Left Blank



Declaration

I declare that **Towards Rapid Electrochemical Test System of Polyanilino-Laccase-On-Gold Enzyme Nanobiosensor for Water Estrogen** is my own work, that it has not been submitted for any degree or examination in any other University, and that all the sources I have used or quoted have been indicated and acknowledged by complete references.

Ms Sinazo Qakala

Signed _____



November 2013

Page Left Blank



Acknowledgements

Firstly I would like to thank God for giving me the strength throughout my studies, and indeed for being my rock throughout my project.

I would also like to thank **National Nanoscience Postgraduate Teaching and Training Programme (NNPTTP), Department of Science and Technology (DST)** for funding my masters' project.

I would like to thank my supervisor **Professor Emmanuel I. Iwuoha** for believing in me and for giving me this opportunity, really appreciated.

I would like to appreciate my co-supervisor **Dr Tesfaye T. Waryo** for his leadership, supervision, guidance, motivation he has bestowed in me during my masters project and for editing my thesis and for contributing to my research development.

I am truly grateful to the **Department of Physics and Structural Biotechnology** for the use of their equipment.

I would like to thank **Christopher Sunday, Abebaw A. Tsegaye, Valentine Anye** and all **sensor lab researchers**, for assisting me.

I would also like to thank my family **Khunjulwa, Phumlani, Asandiswa, Unathi, Nobudlelwane, Siphenathi, Ncedikhaya, Olwethu, Lindelwa Qakala** and friends especially **Michael Menemene** your support meant a lot to me.

My mom, pillar of my strength, **Vuyiswa Qakala**: your love, support and prayers meant a lot to me. Thank you for believing in me all these years. Love you Ntumbeza.

My son, **Ovayo Qakala**, you were my inspiration and you brought joy everyday into my life, thank you baby.

To my partner **Lwanduyolo Dlela**, thank you for your support, love, prayers and encouragement, really appreciated Shweme.



DEDICATION

This work is dedicated to my mom Vuyiswa Qakala, my son Ovayo Qakala and my partner Lwanduyolo Dlela.



Page Left Blank

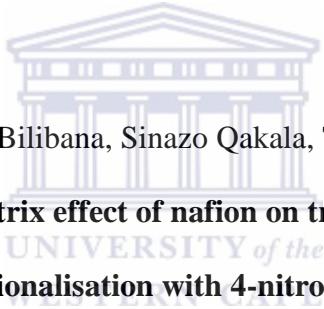


CONFERENCES AND PUBLICATIONS

CONFERENCES

Sinazo Qakala, Emmanuel Iwuoha, Tesfaye Waryo, Laccase biosensor rapid test systems for water estrogens: preliminary UV/vis absorption, fluorescence, and cyclic voltammetry studies, *13th Topical Meeting of the International Society of Electrochemistry*, from 7 to 10 April 2013, CSIR ICC, Pretoria, South Africa. (<http://topical13.ise-online.org/general/PRETORIA-program.pdf>).

PUBLICATIONS



Christopher E. Sunday, Mawethu Bilibana, Sinazo Qakala, Tesfaye Waryo, et al., Emmanuel I. Iwuoha, **Modulation of the matrix effect of nafion on tris(bipyridine) ruthenium(II) electrochemical probes by functionalisation with 4-nitrophenylazo graphene-gold nanocomposite**, *Electrochimica Acta*, Published online 7 January 2014 (<http://dx.doi.org/10.1016/j.electacta.2013.12.143>).

Sinazo Qakala, Tesfaye T. Waryo, Christopher E. Sunday, Priscilla G. Baker, Emmanuel I. Iwuoha, **Electropolymerization of aniline is possible in phosphoric acid in the presence of polystyrene sulfonic acid dopant**, being submitted to the *International Journal of Electrochemical Sciences*.

Sinazo Qakala, Tesfaye T. Waryo, Emmanuel I. Iwuoha, **Recent electrochemical laccase biosensors and prospect of applications to water estrogen determination – a review**, book chapter in preparation

Page Left Blank



TABLE OF CONTENT

Title Page	i
Keywords	iii
Abstract	v
Declaration	viii
Acknowledgement	x
Dedication	xii
Conferences and Publications	xiv
Table of Contents	xvi
List of Abbreviations	xxii
List of Figures	xxiv
List of Tables	xxix
1. <u>CHAPTER I: INTRODUCTION</u>	1
1.1. Problem Statement	1
1.2. Aim and Objectives	3
1.3. Thesis Layout	4
2. <u>CHAPTER II: LITERATURE REVIEW</u>	
2.1. Endocrine System	5
2.1.1. Endocrine disrupting Compound	5

2.1.2. 17alpha-ethinylestradiol and associated compounds	6
2.1.2.1. Structure of endocrine disrupting compounds	7
2.1.2.2. Classes of endocrine disrupting compounds	7
2.1.2.3. Human Exposure of 17alpha-ethinylestradiol	8
2.1.2.4. Health effects of 17alpha-ethinylestradiol	9
2.1.2.5. Effect of 17alpha-ethinylestradiol in the environment ...	9
2.2. Enzymes	11
2.2.1. Classification and types of enzymes	12
2.2.2. Structural and functional features of laccase (<i>Trametes Versicolor</i>)	13
2.2.2.1. Laccase active site	15
2.2.2.2. Application of laccase	17
2.3. Biosensor	19
2.3.1. Classification and types of biosensor	20
2.3.2. Enzyme-based electrochemical biosensor	22
2.4. Gold nanoparticles	22
2.4.1. Properties of gold nanoparticles.....	23
2.4.2. Application of gold nanoparticles.....	24
2.5. Conducting polymers	25
2.5.1. Polyaniline	27
3. <u>CHAPTER III: PRINCIPLES OF SELECTED ANALYTICAL METHODS ...</u>	31
3.1. Electrochemical techniques	31
3.1.1. Cyclic Voltammetry	31
3.1.2. Electrochemical Impedance Spectroscopy (EIS)	35
3.2. Spectroscopy techniques	
3.2.1. Ultraviolet-Visible Spectroscopy	36

3.2.2. Transmission electron microscopy	37
4. <u>CHAPTER IV: EXPERIMENTAL</u>	39
4.1. Chemicals and Materials	39
4.2. Reagent Solutions	
4.2.1. Preparation of McIlvaine buffer	40
4.2.2. Preparation of laccase solution	41
4.2.3. Preparation of laccase solution for the SDS-PAGE	41
4.2.4. Preparation of stock solutions of the Estrogens	41
4.2.5. Preparation of other solutions	42
4.3. Synthesis of Gold Nanoparticles.....	42
4.4. Distillation of aniline	43
4.5. Instruments	43
4.5.1. Electrochemical Measurements	43
4.5.2. UV/Vis Absorption and Fluorescence Measurements	44
4.5.3. Electrophoresis (SDS-PAGE)	44
4.5.4. Microscopic Imaging (TEM & SEM).....	44
4.6. Preliminary Studies	45
4.6.1. Electroactivity of the Estrogens at GC, Au, and Pt Electrodes	45
4.6.2. UV/Vis Absorption and Fluorescence Spectra of the Estrogens and Laccase	45
4.6.3. Verification of the Enzymatic Activity of Laccase in Solution	45
4.6.4. Testing of Electroactivity of Laccase in Solution and as Drop-Coated Film on GC, Au, and Pt Electrodes	46
4.6.5. Electroactivity of Drop-Coated AuNP Film	47

4.6.6. Electropolymerization and Characterization of Polyaniline Films (GC/PANI-PSSA)	47
4.7. Electrochemical Laccase Biosensor Studies	48
4.7.1. Preparation of GCE/PANI-PSSA	48
4.7.2. Electroactivity of Dissolved Laccases at GCE/PANI-PSSA	48
4.7.3. Preparation of GCE/PANI-PSSA/ Laccase	48
4.7.4. Preparation of GCE//PANI-PSSA/AuNP	48
4.7.5. Preparation of GCE//PANI-PSSA/AuNP-Lac	48
4.7.6. Preparation of GCE//PANI-PSSA/Lac-Glu	49
4.7.7. Preparation of GCE//PANI-PSSA/AuNP-Glu-Laccase	49
4.8. Cyclic voltammetric Sensing of E2 with Laccase Biosensors	50
4.9. Electrochemical Impedance Sensing of E2 with the Laccase Biosensors	50
5. <u>CHAPTER V: RESULTS AND DISCUSSION</u>	51
5.1. Preliminary Studies of Estrogens, Gold Nanoparticles, and Laccase	51
5.1.1. Estrogens	51
5.1.1.1. UV/ Vis Spectra of Aq. Estrogens Solutions	51
5.1.1.2. UV/ Vis Fluorescence Spectra of the Estrogens	53
5.1.1.3. Electroactivity of the Estrogens at GC, Au, and Pt Electrodes	54
5.1.1.4. Effect of storage	56
5.1.1.5. Summary	58
5.1.2. Laccase	58
5.1.2.1. Purity and Molecular Weight of Laccase	58
5.1.2.2. UV/ Vis Absorption Spectrum of Laccase in McIIB (pH 4.9)	60

5.1.2.3.	Laccase Activity on EE2 in McIIB (pH 4.9) as Monitored with UV/ Vis Absorption.....	60
5.1.2.4.	Laccase Activity on EE2 as Monitored with UV/ Vis Fluorescence	61
5.1.2.5.	Electrochemical properties of laccase on GCE, AuE and PtE	62
5.1.2.6.	Effect of storage on Laccase activity.....	64
5.1.2.7.	Summary	65
5.1.3.	Gold Nanoparticles	66
5.1.3.1.	UV/ Vis Absorption Spectrum of AuNP	66
5.1.3.2.	TEM Images, SAED, EDX, and Size Distribution AuNP....	68
5.1.3.3.	SEM Images of AuNP, Laccase, & Au-Laccase	73
5.1.3.4.	TEM images of AuNP, Laccase, AuNP-Laccase	73
5.1.3.5.	Electroactivity of AuNP films	75
5.1.3.6.	Summary	75
5.1.4.	Polyaniline/ Polystyrene Sulfonic Acid Composite Films	76
5.1.4.1.	Electro-co-polymerization and CV Characterization in Aq. HCl	76
5.1.4.2.	Electro-co-polymerization and CV Characterization in Aq. H ₃ PO ₄	77
5.1.4.3.	CV Characterization of GC/PANI-PSSA in McIlvaine Buffer	79
5.1.4.4.	Electroactivity of EE2 at GC/PANI-PSSA in McIlvaine Buffer	80
5.1.4.5.	Electroactivity of Dissolved Laccase on GC/PANI-PSSA in McIlvaine Buffer	81

5.1.4.6.	Electroactivity of Drop-Coated Laccase on GC/PANI-PSSA in McIlvaine Buffer	82
5.1.4.7.	Response of GC/PANI-PSSA/Lac to EE2 in McIlB under Aearobic and non-Aearobic Conditions	83
5.1.4.8.	Summary	84
5.2.	Cyclic Voltammetric Amperometric Laccase Biosensor Studies	85
5.2.1.	Response of GC/PANI-PSSA to EE2	85
5.2.2.	Response of GC/PANI-PSSA/ Lac/ Glu to EE2	86
5.2.3.	Response of GC/PANI-PSSA/ Au/ Lac/ Glu to EE2	88
5.2.4.	Summary and Comparison of Platforms	89
5.3.	Electrochemical Impedance Laccase Biosensor Studies	90
5.3.1.	Response of GC/PANI-PSSA to EE2	91
5.3.2.	Response of GC/PANI-PSSA/ Lac/ Glu to EE2	94
5.3.3.	Summary and Comparison of Platforms	96
6.	<u>CHAPTER VI SUMMARY CONCLUSIONS AND RECOMMENDATIONS</u>	97
6.1.	Summary Conclusions	97
6.2.	Recommendation for Future Work	97
7.	<u>BIBLIOGRAPHY</u>	99

LIST OF ABBREVIATIONS AND SYMBOLS

ΔE_p : Peak potential separation

AuE : Gold electrode

C : Capacitance

CPE : Constant phase element

E1 : Estrone

E2 : 17 β -estradiol

E3 : Estriol

EDC : Endocrine disrupting compounds

EE2 : 17 α -ethnylestradiol

E_{pa} : Anodic peak potential

E_{pc} : Cathodic peak potential

GCE : Glassy carbon electrode

HRTEM : High resolution transmission electron microscopy

I_{pa} : Anodic peak current

I_{pc} : Cathodic peak current

McIlB : McIlvaine buffer



PAGE : Polyacrylamide gel electrophoresis

PANI : Polyaniline

PtE : Platinum electrode

R_{ct} : Charge transfer resistance

R_s : Solution Resistance

SAED : Selected-area electron diffraction

SDS : sodium dodecyl sulphate

SEM : Scanning electron microscopy

TEM : Transmission electron microscopy

UV/ Vis : Ultraviolet – Visible

Z_{im} : Imaginary impedance

Z_{re} : Real impedance



LIST OF FIGURES

Figure 1:	Chemical structure of some natural E1, E2, E3, Eq, 17a-Eqn and synthetic estrogenic EE2 compounds	7
Figure 2:	Laccase (<i>Trametes Versicolor</i>) enzyme structure	14
Figure 3:	Illustration of the active site of laccase showing the relative orientation of the copper atoms	15
Figure 4:	The proposed reaction mechanism of dioxygen reduction to water by laccase	16
Figure 5:	Schematic diagram of a biosensor	20
Figure 6:	Structures of conductive polymers	26
Figure 7:	Chemical structure of polyaniline	27
Figure 8:	Three different forms of PANI depending on oxidation state	28
Figure 9:	A photograph an electrochemical cell consisting of three electrodes	31
Figure 10:	Atypical cyclic voltammogram showing peak parameters (E_{pc} , E_{pa} , i_{pc} , i_{pa})	32
Figure 11:	UV/ Vis spectrometer	36
Figure 12:	Flow chart used for testing surface regeneration and reproducibility of CVs of PANI-PSSA, PANI-PSSA/Lac/Glu and PANI-PSSA/Au/Lac/Glu before and after exposure to aq. EE2	50

Figure 13:	UV/ Vis absorption spectra of estrogens 0.1 mM (aq.)	51
Figure 14:	UV/ Vis fluorescence spectra of aq. solutions of the estrogens (0.1 mM each) at an excitation wavelength of $\lambda_{ex} = 280$ nm	53
Figure 15:	CV of EE2 in 1 mM McIIB (pH 4.9) using A) glassy C electrode, B) gold electrode and C) platinum electrode	55
Figure 16:	Time lapse UV/ Vis absorption spectra of EE2/ lac mixture in McIIB (pH 4.9)	57
Figure 17:	Electrophoretograms of laccase developed on a 10% SDS-PAGE gel ...		59
Figure 18:	UV/ Vis absorption spectrum of laccase (0.1 mM) in McIIB	60
Figure 19:	Time-laps UV/ Vis absorption spectra before and after addition of laccase (1 mM) to EE2 (1 mM) solution in McIIB (pH 4.9)	61
Figure 20:	Time-lapse UV/ Vis fluorescence spectra of before and after addition of laccase (0.01 mM) to a solution of EE2 (1 mM) in modified McIIB	62
Figure 21:	CVs of laccase films on Au, GC and Pt electrodes in McIIB at scan rates of 10 and 100 mV/ s	63
Figure 22:	Time-laps UV/ Vis absorption spectra of reaction mixtures containing Laccase 1×10^{-3} mM (0.1 mg/ml) and EE2 (1 mM) from stock solutions of different ages in McIIB:	65

Figure 23:	UV/ Vis absorption spectra of the Au nanoparticles solution used in this study	67
Figure 24:	HR-TEM images of the gold nanoparticles	68
Figure 25:	Graph showing size distribution of the gold nanoparticles used in the study	69
Figure 26:	(A) HR-TEM images of the AuNPs (inset: size distribution histogram); (B) SAED pattern.	70
Figure 27:	EDX spectrum of AuNP	71
Figure 28:	a) SEM images gold nanoparticle b) Laccase at 200 nm and c) EDX	72
Figure 29:	TEM images of laccase, (laccase + AuNP) mixture, and EDS of (laccase + AuNP)	74
Figure 30:	CV of drop coated AuNP in McIlB	75
Figure 31:	Electropolymerization CV (10 cycles at 50 mV/ s) of Aniline (50 mM) on GCE in presence of PSSA (25 mM) in aq. HCl (1 M)	76
Figure 32:	CV of GCE/PANI-PSSA in fresh portion of aq. 1 M HCl at scan rate of 50 mV/ s	77
Figure 33:	Electropolymerization CV (10 cycles at 50 mV/ s) of Aniline (50 mM) on GCE in presence of PSSA (25 mM) in aq. H ₃ PO ₄ (1 M)	78
Figure 34:	CV of GC/PANI/PSSA film in aq. H ₃ PO ₄ (1000 mM) overlaid with the back ground CV of GCE	79

Figure 35:	Overlay of three-cycle CVs of GC/PANI/PSSA film in McIlB (1 M)	79
Figure 36:	CV of GC/PANI-PSSA in McIlB without (red) and with (green) dissolved EE2 (1 mM)	80
Figure 37:	CVs of GC/PANI-PSSA at a scan rate of 100 mV/ s in McIlB before (black) and after (after) addition of laccase (1 mM)	81
Figure 38:	CVs of GC/PANI-PSSA and GC/PANI-PSSA/Lac	83
Figure 39:	Set of CVs of GC/PANI-PSSA recorded at 25 mV/ s in McIlB before and after a 60 s dip in water blank or in aq. EE2 (1 mM) for four successively repeated experiments	86
Figure 40:	Set of CVs of GC/PANI-PSSA/Lac/Glu recorded at 25 mV/ s in McIlB before and after a 60 s dip in water-blank or in aq. EE2 (1 mM) sample for four successively repeated experiments	87
Figure 41:	Set of CVs of GC/PANI-PSSA/Au/Lac/Glu recorded at 25 mV/ s in McIlB before and after a 60 s dip in water blank or in aq. EE2 (1 mM) for three successively repeated experiments	89
Figure 42:	Equivalent circuit model for GC/PANI-PSSA and PANI-PSSA/Lac/Glu in McIlB.	90
Figure 43:	Impedance (Nyquist) plots for GC/PANI-PSSA at dc bias potential (E_{dc}) of 8.5 mV in McIlB before and after 60 s exposure to water or to aq. EE2 for three consecutive cycles with thorough rinsing with water between each cycle	92

Figure 44: Impedance (Nyquist) plots for GC/PANI-PSSA/Lac/Glu at dc bias potential (E_{dc}) of 0.11 V in McIlB before and after 60 s exposure to water or to aq. EE2 for three consecutive cycles with thorough rinsing with water between each cycle..... 94



LIST OF TABLES

Table 1:	Diagnostic tests for electrochemical reversibility of a redox couple using cyclic voltammetry	33
Table 2:	UV/ Vis absorption peaks of estrogens at concentrations (c) of 0.1 mM (aq.) in cuvettes with path lengths (l) of 1 cm in McIIB (pH 4.9)	52
Table 3:	Summary of UV/ Vis fluorescence peaks of the estrogens (0.1 mM) at excitation wavelength $\lambda_{ex} = 280$ nm in aqueous solution	54
Table 4:	Equivalent circuit and kinetic parameters estimated using the EIS data for GC/PANI-PSSA in McIIB before and after exposure to aq. EE2 solution	93
Table 5:	Equivalent circuit and kinetic parameters estimated using the EIS data for GC/PANI-PSSA/ Lac-Glu in McIIB before and after exposure to aq. EE2 solution	95

Page Left Blank



CHAPTER I: INTRODUCTION

1.1 Problem Statement

Over the last several years, there have been some concerns about environmental chemicals that disrupt normal endocrine functions in living organisms including humans [1]. These environmental chemicals together are well known as endocrine disrupting compounds (EDCs). EDCs may imitate modulate and block hormone synthesis. Most of these chemicals act as agonists of estrogen receptors. The concern behind these steroids for the aquatic environment is due to their endocrine disruption potential, and these are mainly estrogens and contraceptives, including 17β -estradiol (E2), 17α -ethynylestradiol (EE2), estrone (E1), estriol (E3) and mestranol (MeEE2). It has been proven that these estrogenic compounds can mimic the natural estrogens by binding to estrogen receptors and interfering with endocrine signalling pathways [2]. When these estrogens are present in the environment above a certain concentration (threshold limit value), can cause adverse health effects on wildlife [3]. Hormone steroids enter the environment by being excreted by all humans as well as animals from their bodies through sewage discharge and animal waste disposal. Adding to that, synthetic estrogens widely used in oral contraceptives and hormone replacement therapy is consumed in humans and after excretion enters the wastewater stream [4]. Municipal wastewater is the main disposal pathway for human waste born estrogenic compounds [3]. These steroids in have been detected in effluents of sewage treatment plants (STPs) and surface water. They may interfere with the normal functioning of endocrine systems that will end up affecting reproduction and development in wildlife [5].

This thesis focuses on 17α -ethynylestradiol (EE2), the synthetic estrogen. 17α -ethynylestradiol is an active component in oral contraceptive pills. It is also an active ingredient of preparations aimed at managing menopausal and postmenopausal syndrome.

17 α -ethynylestradiol is excreted from the human body in high amounts and released via sewage treatment plant effluent into aquatic environments. In fish, estrogen receptors have strong binding affinities for EE2. Therefore exposure to this chemical raises the possibility of adverse neuroendocrine responses in aquatic animals. 17 α -ethynylestradiol is also used in physiological replacement therapy deficiency conditions for the treatment of prostate and breast cancer [6].

The presence of chemical compounds of estrogenic activity in the natural environment has raised interest worldwide since mixtures of these compounds are excreted by women, man, animals and they have always been present in the environment [1] According to literature data, estrogenic sexual hormones are present in water environment in a very low concentrations about 3 pM (1 ng/ L) from organisms being physiologically active. Several studies have reported that estrogen levels in source and finished drinking water showed that EE2 is below the limit of detection (LOD) 0.16 pM (0.05 ng/ L). However, in 2004, EE2 and natural steroid estrogens were not detected in drinking water above the LOD of 1 pM (0.3 ng/ L) [7]. Other studies have showed EE2 was detected in 9 of 10 effluent samples in different countries with a maximum concentration of 140 pM (42 ng/ L). Therefore this shows that the range is below the limit of detection of 140 pM (42 ng/ L) [5].

There is a problem identified involving routine analysis of hormones in surface and polluted water. This is caused by the fact that there are no good procedures to determine these compounds in such low concentrations. The conventional techniques for removal of EDCs include membrane bioreactors, ozonation and sand filtration. However, the disadvantage of these analysis methods was that none of these conventional water treatment processes are totally efficient in removing EDCs [8]. A wide range of estrogenic contaminants has been detected in the aquatic environment. Among these natural and synthetic steroid estrogens

typically present in municipal sewage-treatment plant (STP) effluents are the most potent. Detection of estrogens in the environment has raised concerns in recent years because of the potential of these compounds to affect both wildlife and humans [9].

Looking at the adverse effects of the estrogenic compounds mentioned above, there is an urgent need to detect and control estrogenic activity especially in the aquatic environment. At the moment there are varieties methods used for estrogens' detection. Mostly are analytical and biological detection methods. In earlier times, estrogenic contaminations were identified and measured by classical analytical techniques such as LC-tandem mass spectrometry (LC-MS/MS), gas chromatography–mass spectrometry (GC-MS), liquid chromatography-mass spectrometry (LC-MS), high performance liquid chromatography (HPLC/MS) and enzyme-linked immunosorbent assays (ELISA). The sensitivity, accuracy and high reproducibility of these analytical methods make them the most excellent tools for estrogens screening. However, these techniques are time consuming because of sample preparation and operationally expensiveness as highly skilled operators routinely required. Moreover, they cannot be performed easily outside the laboratory and they are restricted to a limited set of substances like environmental chemicals with estrogenic activities [10-11]. Therefore, many researchers have been showing interest in trying to develop simpler and more sensitive biosensor-based methods. Biosensors can have fast response to analytes, hence high sample through put rates, low cost and they are easy to operate [12].

1.2 Aim and Objectives

General objectives

The aim of this work was to focus towards developing rapid test system of polyaniline-laccase on gold enzyme nanobiosensor for water estrogens.

Specific objectives

The main objective of the project is to:

- Prepare chemically gold nanoparticles and AuNP/laccase composite;
- Characterize the synthesized gold nanoparticles using transmission electron microscopy (TEM), scanning electron microscopy (SEM), (uv-vis spectroscopy (Uv-Vis) and cyclic voltammetry (CV);
- Prepare electrochemically and characterize poly (glu-co-aniline), polyaniline/ Lac, polyaniline/ AuNP, poly (aniline)/AuNP-Lac, pol (glu-co-aniline)/ Lac and poly (glu-co-aniline)/AuNP/ laccase, films;
- Fabricate the composite PANI/ Glutaraldehyde-AuNPs-Lac;
- Develop a nanobiosensor using EE2 enzyme for detection of estrogen and
- Apply the biosensor.

However, as the title of the thesis, the project went, reasonably within the constraints faced during the lab work, as far as testing the viability of the platform in question for an electrochemical transduction of the enzymatic breakdown of a model estrogen by the enzyme laccase. It was explored if changes in parameters of cyclic voltammetry and electrochemical impedance spectra before and after the enzymatic reaction could be related qualitatively with the presence of the model estrogen in aqueous media.

1.3 Thesis layout

This dissertation is presented in six chapters including the introduction. Chapter II contains a literature of endocrine system, biosensor, enzymes gold nanoparticles and polymers. Chapter III briefly describes the principles of selected analytical techniques. Chapter IV is the experimental part. Chapter V is the results and discussion. Chapter VI presents the conclusions and recommendation from this work. Then section VII is the bibliography. This

thesis focuses towards developing rapid test system of polyaniline-laccase on gold enzyme nanobiosensor for water estrogens.

CHAPTER II: LITERATURE REVIEW

2.1 Endocrine System

Endocrine system is a collection of glands which secret chemicals and different type of hormones that regulate metabolism, tissue function, development and growth, sleep, mood and reproduction. Endocrine is a Greek word; endo- means within and crinis is secrete, [13]. Hormones are chemical messengers produced by endocrine glands. These hormones transfer information from one set of cells to the other, in order o coordinate functions of the different parts of the body. There are several classes of hormones that exist like steroids, amino acids derivatives, polypeptides and proteins [14].

2.1.1 Endocrine disrupting compounds

An endocrine disrupting compound (EDCs) is one interferes with the function of the endocrine system [15-16]. EDCs are of different group of compounds from dioxins, persistent organic pollutant such as DDT and PCB, polychlorinated biphenyls, phenols, pesticides and phthalates to natural and synthetic hormones [2].

EDCs mimic modulate and block hormone synthesis, which many of them act as agonists of estrogen receptors. EDCs pose a serious threat due to an estrogenic potential activity that they mimic. Looking at the detection of these chemicals within the natural system, it is therefore necessary to protect public and environmental health. Instruments such as HPLC or GC/MS are very sensitive for the detection these chemical and have been used intensively for the last several decades. However, these instruments are very complicated to perform and may

require a long time for analysis. To address these challenges, many researchers have been trying to develop simpler and more sensitive biosensor system for chemical sensing [12].

Estradiol is the major estrogen which followed after estrone and estriol. They are produced primarily in the ovaries. The role the estrogen is to organise the normal development and function of the female genitalia and breasts. During the stage of puberty, estrogen promotes growth of the breasts, uterus and vagina. Besides, it ascertains the pattern of fat deposition spread in the body which determine the typical shape of a female. Furthermore, estrogen controls development of the secondary sexual characteristics and regulate pubertal growth or the growth of the adult height. When it comes to women, estrogens function as regulating the menstrual cycle, contributing to the hormonal standard of pregnancy and maintaining female libido [14].

2.1.2 17α -ethinylestradiol and associated compounds

Ethinylestradiol was the first orally active synthetic steroidal estrogen, synthesized in 1938 by Hans Herloff Inhoffen and Walter Hohlweg at Schering AG in Berlin. 17α -ethinylestradiol is a synthetic hormone. It is a derivative of the natural hormone estradiol. Ethinylestradiol is an orally bio-active estrogen used in almost all modern formulations of combined oral contraceptive pills and it is one of the most commonly used medications [17]. The natural estrogen 17β -estradiol (E2), estrone (E1), estriol (E3), are those mostly known endocrine disrupting chemicals (EDCs) that have been entering water systems via human and animal waste products. Even when they present at trace concentrations of ng/L, endocrine disrupting compounds can interfere with the regulatory network in humans and wildlife [8].

2.1.2.1 Structure of endocrine disrupting compounds

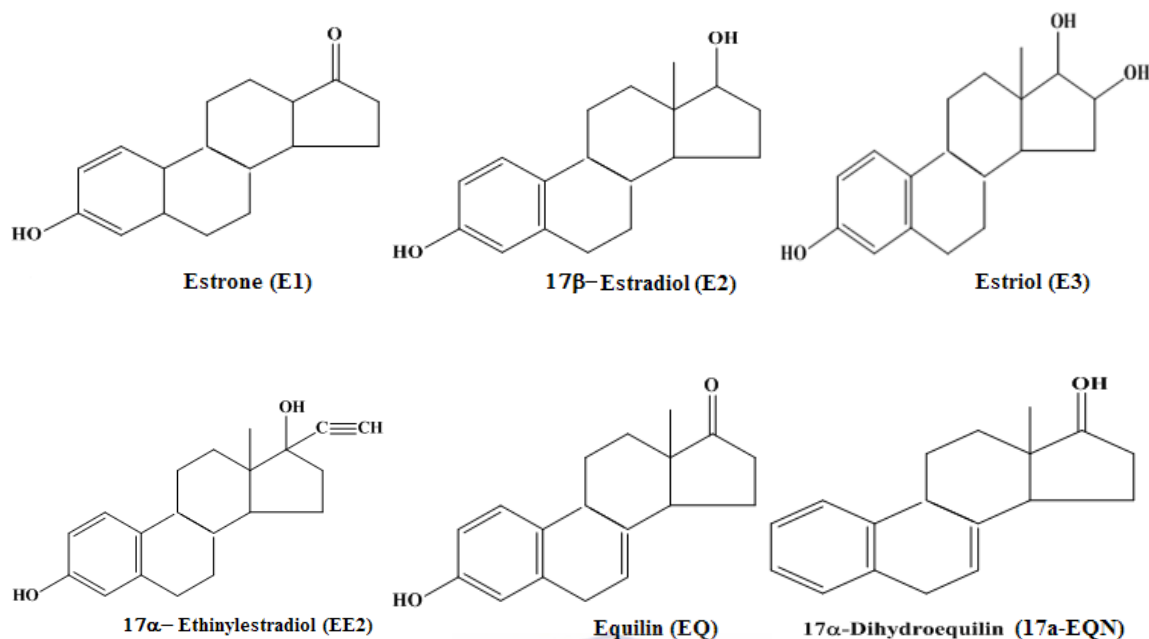


Figure 1: Chemical structure of some natural Estrone (E1), 17β-estradiol (E2), Estriol (E3), Equilin (EQ), 17α-dihydroequilin (17a-Eqn) and synthetic estrogenic (17α-ethinylestradiol (EE2)) compounds [3].

Most of these estrogenic compounds consist of the phenolic benzene ring in their molecular structure, which is essential for the high-affinity binding of estrogenic compounds with the specific binding sites on estrogen receptor (ER). Natural estrogens have the same tetracyclic network consisting of a phenolic, two cyclohexene and one cyclopentane ring. For the different configuration of the D-ring, various compounds can be formed [18].

2.1.2.2 Classes of endocrine disrupting compounds

Endocrine disrupting compounds (EDCs) which interfere with functioning of the endocrine system are classified as natural and synthetic compounds. 17β-estradiol belongs to EDCs is an important compound of the pharmaceutical product. It also found as a by product in medicinal products [4]. On the other hand, E2 is found as additives and pesticides in animal

feed. Although these compounds are found in very little amount in the environment, their effect is very huge on marine animals and humans [19-20]. 17α -ethinylestradiol is mostly utilised as an active compound in birth control pills [21]. It has been used as active ingredient used in formulations for managing menopausal and postmenopausal syndrome. In addition to this, 17α -ethinylestradiol was used in physiological replacement therapy in deficiency conditions, and in treatment of prostate and breast cancer [6].

Three of the estrogens E1, E3 and E2 are natural while EE2 is a synthetic hormone. Among these compounds EE2 and E2 are the most powerful estrogenic substances followed by E1 and E3. When these compounds are found in the environment above a certain concentration limit, and then they can have an adverse health effect on wildlife. These natural and synthetic estrogens enter the aquatic ecosystem via effluents from municipal sewage treatment plants (STPs) [6]. Municipal waste water is said to be the main disposal pathway for the human waste born estrogenic compounds. One of the major health effects associated with exposure of different fish species to estrogenic compounds; is that they change their sexual development and mating behaviour. Some studies on some of the estrogen compound have also reported lower sperm count, change in male reproductive health and breast cancer [3].

2.1.2.3 Human Exposure of 17α -ethinylestradiol

Despite the compelling evidences on wildlife, the adverse health effects of estrogenic hormones on human are still a debatable issue. Some studies have reported lower sperm count, declining male reproductive health and breast cancer as an aftermath of increased exposure to endogenous and exogenous estrogenic compounds [22].

Estrogens and estrogenic compounds released into the environment with wastewater effluent can move out of the water and flow down into riverbed sediments [22]. This finding is

important because it showed that hormones and chemicals can reach and may contaminate shallow groundwater. People can be exposed to the pollutants by drinking the water or irrigating using the water [22]. There is also a possibility that EDCs may be affecting the reproductive health and possibly of humans [23-24]. Moreover, there is a possibility that it could lead to vaginal cancer [25].

2.1.2.4 Health effects of 17 α -ethinylestradiol

Several studies on 17 α -ethinylestradiol have shown that the major health effects associated with exposure of different fish species to this estrogenic compound include the change in sexual development, presence of intersex species and also the change in mating behaviour [3]. Chronic exposure of fathead minnows to environmentally relevant concentration of EE2 in an experimental lake area resulted in feminization of the males through vitellogenin production that led to a near collapse of the species in the lake. Also early exposure to EE2 at a concentration of 33 pM (9.86 ng/L) resulted in diminished courting behavior of female zebrafish [26].

2.1.2.5 Effect of 17 α -ethinylestradiol in the environment

Endocrine disrupting substances, EE2 has the potential to unfavourably affect the sensitive hormone pathways that modulate reproductive functions. For example, aquatic organisms adverse effects may be shown in terms of reduced fertility and egg production in female fish and feminization of male fish [1, 27]. Exposure to EE2 may cause a variety of other effects which include induced production of vitellogenin in male fish, alteration in gene expressions and change in sex ratio of progeny [28-29]. When studies were done on the effect of EE2 on various aquatic organisms, the outcome indicated that EE2 toxicity change over a wide range

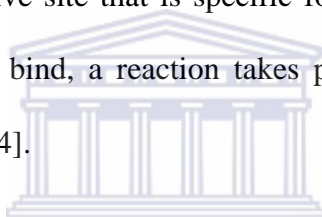
of concentrations. In principle, toxicity is a function of the type of aquatic organism, length of exposure to the contaminant, its life stage and the end point used in the study [17, 30].

17 α -ethinylestradiol (EE2) is the synthetic estrogen. It is an active component of oral contraceptive pills, following excretion by humans and is also considered as the major contributor to the total estrogenicity of sewage effluent [31]. Hormone replacement therapy (HRT), which involves the oral intake of progesterone, estrogens and testosterone, can contribute to the total estrogenicity of municipal wastewater [22]. There are two points that the hormone can enter to the environment, firstly through effluents from waste water treatment plants (WWTPs) and non-point sources, which is surface run-off from agricultural operations. Therefore EE2 is one of the estrogens that enter sewage treatment plants in a conjugated, inactive form. Once it is in the treatment plants, it is split into an active form via bacterial breakdown and then it enters natural waters, which are the streams and rivers. However, EE2 remains relatively stable during the activated sludge process used in sewage plants, thus avoiding breakdown and elimination [26].

Various research groups have reported that estrogen levels in source and finished drinking water in the UK and U.S, primarily show that EE2 is below the limit of detection (LOD) 0.16 pM (0.05 ng/L). In other studies, Germany and UK Environment Agency, came to the conclusion from the data available through 2004 that EE2 and natural steroid estrogens were not detected in drinking water above the LOD of 1 pM (0.3 ng/ L) [7]. However EE2 was detected in 9 of 10 effluent samples in different countries with a maximum concentration of 0.14 nM (42 ng/ L), therefore it shows that it ranges below the limit of detection of 0.141 nM (42 ng/ L) [5].

2.2 Enzymes

One of the important benefits obtained from the intensive research in biochemistry since the 1940`s according to literature, is the use of enzymes for the diagnosis test of disease [32]. Enzymes have provided the basis for the field of clinical chemistry. Specificity is one of the properties of enzymes that make them as important as diagnostic and research tools and they exhibit relative to the reactions they catalyze. A few enzymes exhibit absolute specificity; that is, they will catalyze only one particular reaction. Other enzymes will be specific for a particular type of chemical bond or functional group [33]. Enzymes are proteins and used to change the chemical properties of other molecules. Therefore this is done by catalyzing a reaction. The enzyme has an active site that is specific for a certain molecule or substrate. When the enzyme and substrate bind, a reaction takes place. The effect on the substrate depends on the type of enzyme [34].



Most of the enzymes are much larger than the substrates they act on and so only a small portion of the enzyme (around 2–4 amino acids) is directly involved in catalysis. Because of these properties, enzymes are one of the most important biomolecules which has an extensive range of applications in industrial and biomedical field. That is why today enzymes are considered as one of the most important widely used molecules. As they are very selective catalysts, then they can greatly accelerate both the rate and specificity of metabolic reactions including the digestion of food [35]. Enzyme-catalysed reactions offer faster rates than traditional biochemical processes, because enzymes decrease the energy required for biochemical reactions. Enzymes have been used for decades to analyse the concentration of different analytes. Their commercial availability at high purity levels makes them very attractive for mass production of enzyme sensors. The main limitations of enzymes that affect their activity and application are pH, ionic strength, chemical inhibitors and temperature.

Most of the enzymes used in biosensor fabrication are oxidases that consume dissolved oxygen and produce hydrogen peroxide [36].

2.2.1 Classifications and types of enzymes

Enzymes have been classified into six groups by the Nomenclature Committee of the International Union of Biochemistry and Molecular Biology (NC-IUBMB). They are oxidoreductases, transferases, hydrolases, lyases, isomerase, and ligases [37]. Also enzymes can be classified by the kind of chemical reaction they catalyse. The different types of enzymes listed below are briefly described.

Oxidoreductases: - these are enzymes that transfer electrons in the form of hydride ions or hydrogen atoms. Example: Dehydrogenases Oxidases.

Transferases: - these are type of enzymes that catalyze group transfer reactions. This involves the transfer of a group of atoms from one molecule to another. An example would be moving a phosphoryl group from ATP to glucose. Example: Transaminase Kinases.

Hydrolases: - They are class of enzymes that transfer functional groups to water. Example: Estrases Digestive enzymes.

Lyases: - these are enzymes that move groups to double bonds or remove groups to form double bonds. Example: Decarboxylases Aldolases.

Isomerase:-this type of enzyme produces isomeres of a molecule by moving groups of atoms within a molecule. Example: Phospho hexo isomerase, Fumarase.

Ligases: - are enzymes that catalyze condensation reactions during ATP cleavage to form bonds between a carbon atom and either another carbon atom, sulphur, oxygen, or nitrogen.

Example: Citric acid synthetase [38].

2.2.2 Structure and function of the laccase enzyme

Laccase (benzenediol oxygen oxidoreductases; EC 1.10.3.2) is one of the very few enzymes that have been studied since the end of 19th century [39]. According to the studies done, an enzyme of this group was first described by Yoshida [40]. It was first demonstrated in the exudates of *Rhus vernicifera*, which is the Japanese lacquer tree. Few years down the line, it was also demonstrated in fungi [41]. Laccases are polyphenol oxidases which belong to the family of multicopper oxidases [42-43]. The most noticeable representatives of this family include ascorbate oxidase and mammalian plasma ceruloplasmin[44-46]. Laccase are glycoproteins, which are everywhere in nature and also they have been reported in higher plants and almost every fungus that has been examined for them. You can find laccase in plants like trees, turnips, apples, cabbages, potatoes, asparagus, pears, beets and in some several other vegetables [47]. A multi-copper enzyme, shown in Figure 3, contains four Cu atoms per molecule and organized into three different copper sites. Therefore they catalyze the one electron oxidation of four reducing-substrate molecules connected with the four-electron reduction of molecular oxygen to water molecules [48-49]

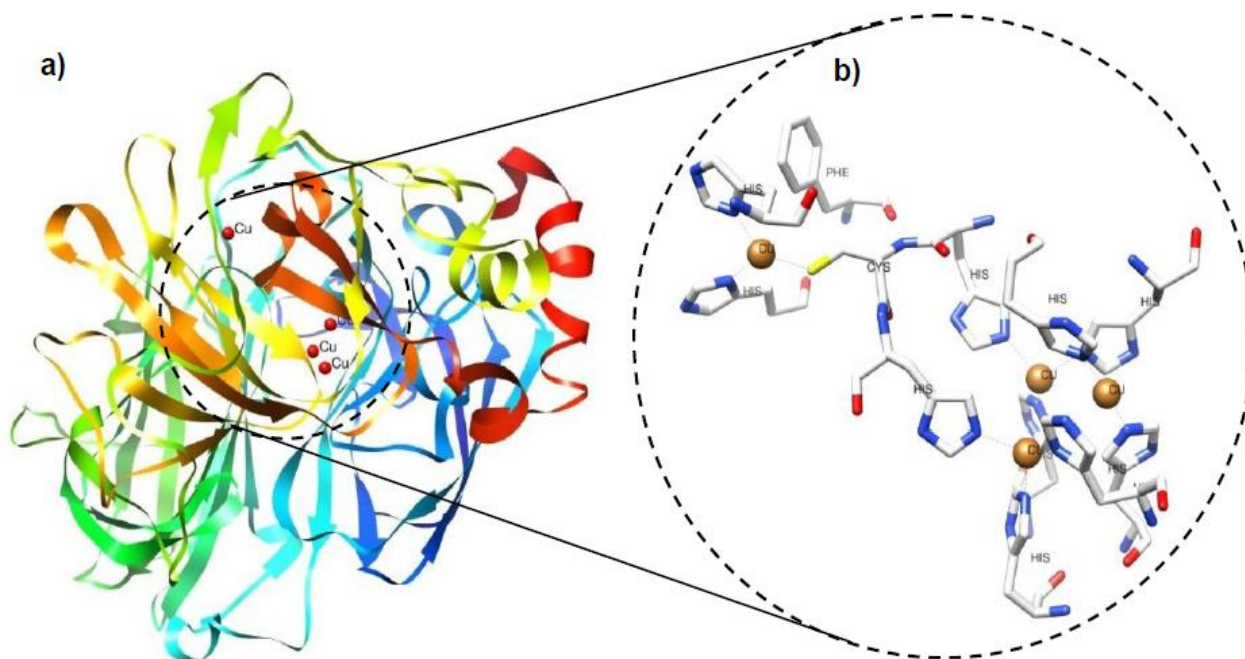


Figure 2: a) Three-dimensional X-ray structure of laccase (*Trametes Versicolor*) b) Active site of laccase, showing copper atoms and amino acids that coordinate those copper [49].

Laccases can reduce oxygen straight to water in a four-electron transfer step without intermediate formation of soluble hydrogen peroxide in the cost of one-electron oxidation of a variety of substrates, for example phenolic compound [50-51]. As it is well known that phenolic compounds establish a large group of organic pollutants, usually spread throughout the environment [52]. Laccases have a specific wide substrate and also a great potential for the determination of phenolic compounds. Laccase shows a wide specificity in the process of oxidizing many compounds, mostly of phenolic type and also can be used for decontamination of a number of aquatic and terrestrial xenobiotics, industrial waste-waters and also as for biotechnological treatment of industrial products. When there is a presence of mediators, laccase usually play a role in the oxidation of non-phenolic substrates [53].

Figure 3, shows the laccase monomer which consists of three domains. Domain 2 represents the residues involved in substrate binding. Therefore T2 and T3 coppers are between domain

3 and 1 while T1 copper is situated in domain 3. This main structure of laccase is connected by two disulfide bonds [49].

2.2.2.1 Laccase active site

The function of laccase depends on the Cu atoms distributed over three different binding sites. Cu atoms in laccase structure play a vital role in the catalytic mechanism of the enzyme. There are three major steps in laccase catalysis process. The first one is Type 1 Cu is reduced by a reducing substrate, which can be further oxidized. During this step the electron is transferred internally from Type 1 Cu to a trinuclear cluster made up of the Type 2 and Type 3 Cu atoms. Then on these trinuclear cluster sites, O₂ molecule is reduced to water [54].

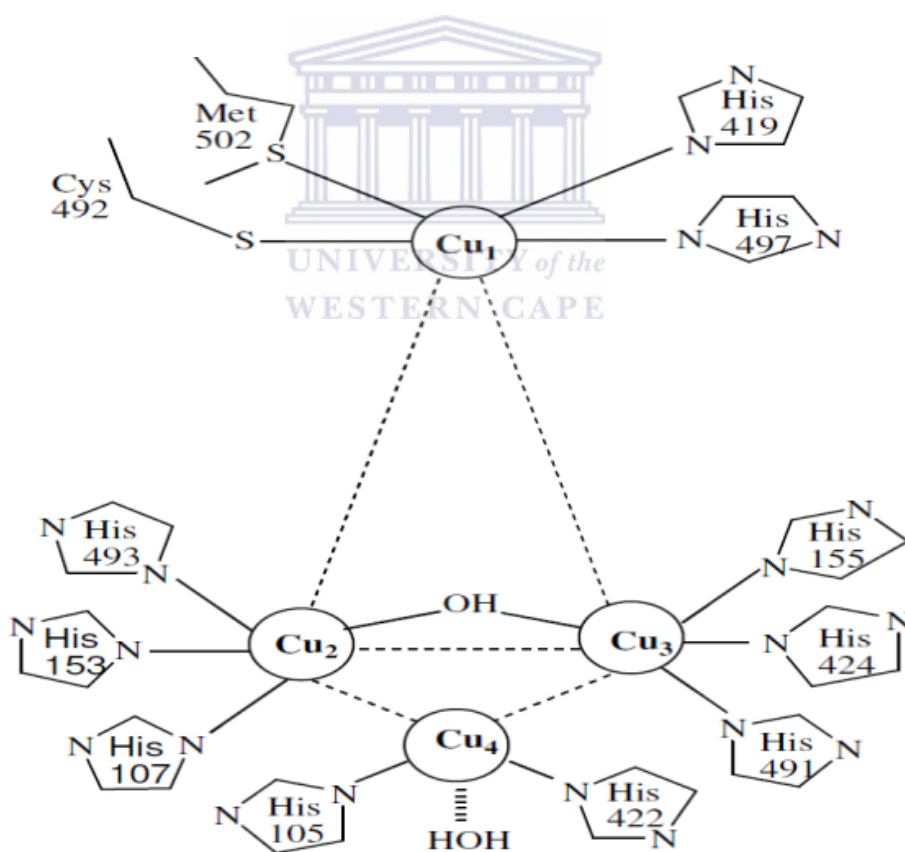


Figure 3: Illustration of the active site of laccase showing the relative orientation of the copper atoms [54].

Oxygen molecule binds to the trinuclear cluster for the asymmetric activation and it is also assumed that the O_2 binding pocket appears to limit the access of oxidizing agents other than O_2 . It is important to notice that H_2O_2 is not detected outside of laccase during steady state laccase catalysis indicating four electron reduction of O_2 to water is occurring during this process. Overall a one-electron substrate oxidation is coupled to a four-electron reduction of oxygen. This shows the reaction mechanism is not straightforward. It seems that laccase operate as a battery, storing electrons from individual substrate oxidation reaction to decrease molecular oxygen. In addition to this, it appears that bound oxygen intermediates are involved in this reaction mechanism [55].

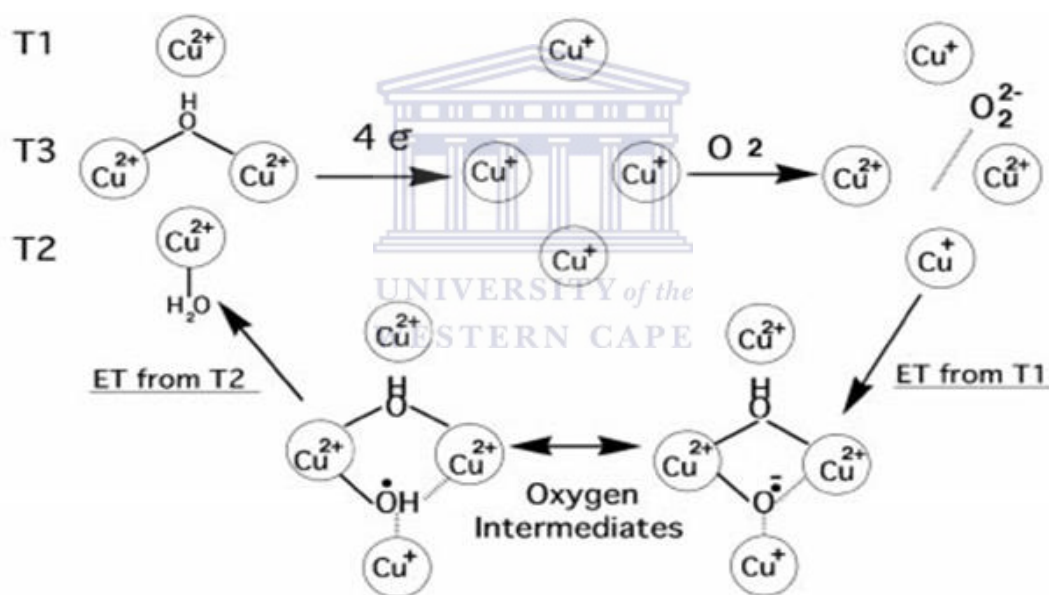


Figure 4: The proposed reaction mechanism of dioxygen reduction to water by laccase [55].

The mechanism proposed in figure 4 shows a clarification of what was already thought to happen at laccase active sites, and the need to obtain four electrons to reduce one oxygen molecule to two molecules of water. In the intermediate state, T1 and T3 coppers are oxidised while both T2 coppers are bridged by a hydroxide or oxide ion. The proton sources to form water from the hydroxide ion are usually the substrate, bulk water or certain amino acids near

the active center. Furthermore, the intermediate radicals appeared to be in equilibrium with H^+ depending on the pH. Therefore one of the oxygen atoms is converted to the linking hydroxide and another to the radical species bound to the trinuclear centre. The reaction ends when the final electron is transferred to the intermediate radical to form hydroxide ion or the interchangeable water molecule bound to T2 copper [49].

2.2.2.2 Laccase applications

Laccase is applicable in many industrial processes of the phenolic compounds. For example they are used to manufacture plastics, dyes, paper, drugs, pesticides and antioxidants. Phenols are breakdown products from natural organic compounds such as humic substances, lignins and tannins. Many studies showed that certain phenols and related aromatic compounds are highly toxic, carcinogenic and allergenic due to their toxic effects. Therefore, their determination and removal in the environment are of great importance [53]. So, massive industrial applications of laccases have been proposed. These include pulp and paper, textile, organic synthesis, environmental, food, pharmaceuticals and nanobiotechnology [54].

Waste Detoxification and Decontamination

Laccase has been mostly utilised to oxidatively detoxify or it can also remove several aromatic xenobiotic and pollutants found in industrial waste and contaminated soil and water. Therefore laccase catalysis could result indirect degradation or polymerization/immobilization. Reported reactions directly degraded by laccase include direct dechlorination, cleavage of aromatic rings, mineralization of polycyclic aromatic hydrocarbons, decolorization of pulp or cotton mill effluent and bleaching of textile dyes [44].

Textile Industry

Many reports indicated that laccases have been used to substitute severe chemicals in hair dyes in a way that dye origin are oxidised by laccase to achieve the colouring agent wanted. It has been also reported that laccase stop back-staining of dyed or printed textiles. Looking at the medical side of applications, laccase enzymes start to enter in the treatment of various conditions [49]. Reasons why laccase is used in commercial textile applications are to improve the whiteness in conventional bleaching of cotton and recently in biostoning. Possible benefits of the application include energy, chemicals and water saving. Laccases also has the potential of bleaching indigo-dyed denim fabrics to lighter shades [54, 56].

Food Industry

Carbohydrates, unsaturated fatty acids, thiols consist of proteins and phenols are the substrate of laccase and they are very important constituents of various foods and beverages. Polyphenol removals must be selective to avoid an unwanted change in the wine's organoleptic characteristics. Wine stabilization is one of the main applications of laccase in the food industry as it substitutes to physical-chemical adsorbents. The flavour quality of vegetable oils can be improved with laccase by removing dissolved oxygen [54]. Besides, these enzymes have been used as dough and bread improving agents. It was also surprisingly suggested that when you add laccase to the dough used for producing baked products, it may be used as an oxidizing agent on the dough components and serve to improve the strength of gluten structures in dough or baked products. As a result of this, laccase improve crumb structure and increase volume [44].

Medicine or Pharmaceutical industry

Laccase is involved in a variety of applications like, medical diagnosis and pharmaceutical industry. Laccase also has an application in the agriculture area by clearing pesticides,

herbicides and some of the explosives in soil. Another interesting application of laccase is in the preparation of some important drugs, like anticancer drugs and in some cases it is added in some cosmetics to reduce their toxicity. Therefore laccase system would reduce the offensive molecules or even kill the microbes that generate them [44]. Laccase also has the ability to form polymers of value able importance. Therefore many body, domestic and industrial odours are caused by sulphides and ammonia or other organic compounds. Being able to oxidize several sulphur containing compounds and thiols, laccase have been studied for deodorants application.

2.3 Biosensor

Biosensors consist of a biological component called bioreceptor. The bioreceptor is the first necessary constituent of a biosensor, which consist of enzyme, antibodies, organelles, receptor, tissue or cells from either plants or animals either closely connected to or joined within a transducer device (for example a kind of electrode) to produce a signal proportional to the analyte concentration [36]. Therefore the transducer will finally convert the biochemical reaction into a countable and measurable response signal which can be further enlarged, processed and stored for later analysis [57-58]. This signal transducer is the second important part of a biosensor [59]. The specific class of transducer active is based on the parameter which are measured, for example, electrochemical (amperometric, potentiometric and conductometric), optical (colormetric, luminescence and fluorescence) or calorimetric (thermistor) signals [10].

Biosensors can be classified as enzymatic biosensors, genosensors, and immunosensors, to mention a few. They can also be divided into few categories depending on the transduction process, such as electrochemical, optical, piezoelectric, and thermal/calorimetric biosensors. Among these different kinds of biosensors, the electrochemical biosensors are the most

common class and commercialized devices of biomolecular electronics [18]. In this chapter, we will focus on the enzyme-based electrochemical biosensors since enzyme electrodes have attracted ever-increasing attentions due to the potential applications in many areas.

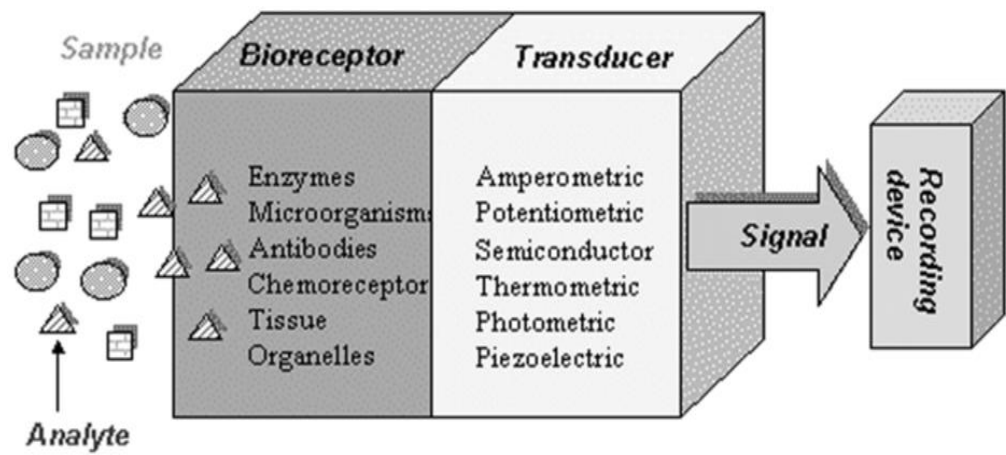


Figure 5: Schematic diagram of a biosensor. A biosensor is made up of a bioreceptor and a transducer [60].



2.3.1 Classes of biosensors

Thermometric biosensors

Thermometric biosensors are constructed by combining enzymes with temperature sensors. When the analyte is exposed to the enzyme, heat of reaction of the enzyme is measured and is calibrated against the analyte concentration [61].

Potentiometric biosensors

Unlike the electrochemical biosensor, the potentiometric biosensors are based on ion-selective electrodes (ISE) and ion-sensitive field effect transistors (ISFET). The main output signal is possibly due to ions gathered at the ion-selective membrane interface. Therefore the current flowing through the electrode is almost equal to zero [62]. The potentiometric measurements involve the determination of the potential difference between an indicator and

a reference electrode or two reference electrodes separated by a perm selective membrane, when there is no significant current owing between them. In this case an ion-selective electrode (ISE) is used as a transducer, which is an electrochemical sensor based on thin films or selective membranes as recognition elements. The most common potentiometric devices are pH electrodes or gas selective electrodes. The potential differences between the indicator and reference electrode are proportional to the logarithm of the ion activity or concentration [63].

Amperometric biosensor

Unlike the potentiometric biosensor, amperometric biosensors are sensitive and more suitable for the mass production. Amperometric biosensors use the working electrode usually either a noble metal or a screen-printed layer covered by the biorecognition component. Carbon paste with an embedded enzyme is another economic option [64]. When the potential is applied, conversion of electroactive species produced in the enzyme layer occurs at the electrode and therefore the resulting current is measured. The amperometric biosensors utilise two or three electrode configurations. In the past it consists of only reference and working (containing immobilized biorecognition component) electrodes. The amperometric biosensors are more of the advantage and are usually used on a large scale analytes such as glucose and lactate [62].

Impedimetric or Conductometry biosensor

Many enzyme reactions, such as that of urease, and many biological membrane receptors may be monitored by ion conductometric or impedimetric devices, using interdigitated microelectrodes [63]. Such devices follow either impedance (Z) or its components resistance (R), capacitance (C) and inductance which typically has only a minimal influence in a typical electrochemical setup [62].

2.3.2 Enzyme-based electrochemical biosensors

Enzyme-based electrochemical biosensors are based on enzymatic catalysis of a reaction which produces ions. On this electrochemical biosensor, the sensor substrate contains three electrodes: a reference electrode, a working electrode, and a counter electrode. In this case, a counter electrode may also be present as an ion source. The target analyte acts in the reaction that takes place on the active electrode surface. So the ions produced in the reaction generate a potential that is subtracted from that of the reference electrode to produce a signal. Electrochemical biosensors are usually based on potentiometry and amperometry methods [61].

Enzyme-based electrochemical biosensors have been mostly used widely in our lives, such as health care, food safety and environmental monitoring. The sensitive detection of phenolic compound is an important topic for environmental research because phenolic compounds often exist in the wastewater of many industries are the cause of the rise of many problems for our living environment as many of them are very toxic [18]. Recently there is a strong interest in the development of laccase-based biosensors using nanomaterials, because of their unique and particular properties [65-66].

2.4 Gold nanoparticles

In recent years, there has been a dynamic application of various nanomaterials in the development of biosensors. Nanomaterials are generally referred to the materials with dimensions ranging from 1 to 100 nm, which have some special physicochemical characteristics resulting from their small size structures. Gold nanoparticles (GNPs) have been used for many biological applications due to their chemical stability, biocompatibility and unique optical properties [67]. The gold surface chemistry eases the coating,

functionalization and integration of GNPs with a host of biomolecular moieties. Therefore the GNPs have the ability to carry several therapeutic agents and biomolecules including DNA, proteins, peptides, and low molecular weight compounds. It can also enter across different barriers through small capillaries into individual cells [68].

Gold nanoparticles could provide a stable immobilization for biomolecules retaining their bioactivity, the electron transfer between the redox and the surfaces of electrode system make it to be more conductive. There is also a great interest shown on the study done on gold-based enzyme biosensor [69]. Gold nanoparticles are normally synthesized in two ways either chemical route or electrodeposition. The gold nanoparticles are usually absorbed in different ways in order to improve the fabrication or performance of biosensor. The surface of the electrode roughens by gold nanoparticles to improve the interaction of enzyme with the electrode. An example studied for this application is the construction of enzyme-based biosensor for the detection of concentration of indinavir drug (ARV) in the blood. In this study, the gold nanoparticle will be used for the construction of the enzyme-based biosensor [70].

2.4.1 Properties of gold nanoparticles

Nanoparticles can be shaped from many materials and have a wide functional diversity very different from bulk materials with their electronic, catalytic and optical properties originating from their quantum scale dimensions. These confinement effects of nanomaterials often produce greatly improved and potentially controllable properties [71]. They are notable due to their intrinsic properties which include biocompatibility, low cytotoxicity and immunogenicity, good electronic conductivity and chemical stability [72].

Gold nanoparticles with large surface area and good electronic properties may provide a stable surface for enzyme immobilization. They can act as conduction centers to facilitate transfer of the electrons. They are spherically shaped with a diameter of several tens of nanometers in size in comparable to the large biological molecules [73]. Recently they have been also used for the study and development of nanoplatforms as sensing surfaces and has been concentrating mostly on the areas of analytical science and electrochemical sensors [74].

2.4.2 Applications of gold nanoparticles

Gold nanoparticles (AuNP) are a very important and frequently used in nanotechnology, mainly due to their surface plasmon resonance (SPR), their easy of surface functionalization or Bioconjugation and their chemical stability and biocompatibility [75]. AuNP determine optical, electrical, chemical and biological properties [67].

Colloidal gold nanoparticles (AuNP) have been shown that they increase mass sensitivity in biosensing detection by attaching analytes such as proteins, peptides and oligonucleotides to the nanoparticles. Polyvinylidene difluoride (PVDF) polymer is well established as a substrate demonstrating its high affinity of binding proteins. As such, it has been used as continuous thin films in both physical and chemical sensors [76].

In electrochemical bioassays, AuNPs are used to connect enzymes to electrode surfaces and are able to mediate electrochemical reactions as redox catalysts. The particles also strengthen recognition signals for biological processes. With AuNPs new biosensors with improvements in sensibility, selectivity, easy fabrication and low cost have been developed [49].

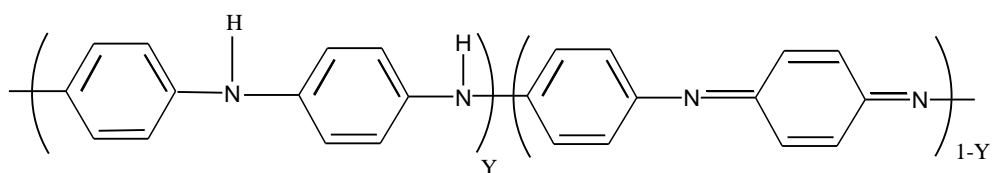
Immobilization process has been used for improving enzyme activity and stability in aqueous media and more recently in non-aqueous media. Enzyme immobilization is important in

biotechnological processes for high operational stability and durability, easy separation of products and their low cost for industrial applications [18, 73]. The selection of support matrix and designing the carrier are very important in enzyme immobilization. Recently, nanostructured materials have found a broad application as a matrix for enzyme immobilization [75]. This make the gold nanoparticles more attractive in their use as host matrixes as they are spherically shaped with a diameter of several tens of nanometers in size. Therefore with the size of thousand times smaller than cells, these nanoparticles offer a variety of biomedical applications including cancer diagnosis, radiotherapy, drug and gene delivery, sensors and biosensors, and controlling and suppressing of bacterial growth [73].

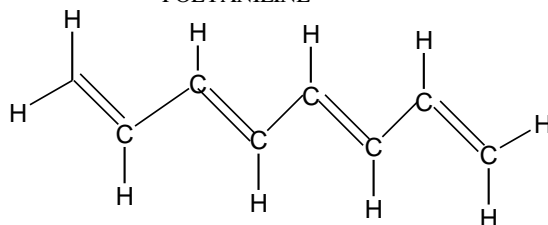
2.5 Conducting Polymers

Conjugated conducting polymers are being discarded for their traditional roles as electric insulators to literally take charge as conductors with a range of novel applications [77]. Research on conducting polymers intensified soon after the discovery of poly(sulphur nitride) by Greene and Street in 1975 which becomes superconducting at low temperatures[78]. Conducting polymers contain π -electron backbone, which is responsible for their uncommon electronic properties such as low energy optical transitions, electrical conductivity, low ionization potential and high electron affinity [79]. This extended π -conjugated system of the conducting polymers has single and double bonds alternating along the polymer chain. [77].

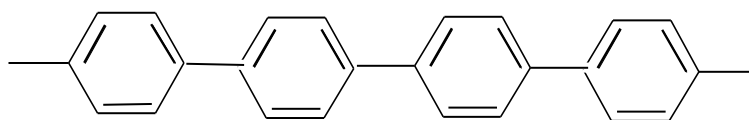
Conducting polymers show better electrical conductivity by several orders of magnitude by doping. Therefore the energy storage mechanism of the conducting polymers was explained by the fact that these polymers were able to lower their energy by altering their bonds which caused the production of energy of up to 1.5 eV making them a higher energy semiconductor [80]. Conductive polymers are composed of different classes, which are poly(acetylene)s, poly(pyrole)s, poly(thiophene)s, poly(terthiophene)s, poly(aniline)s, poly(fluorine)s.



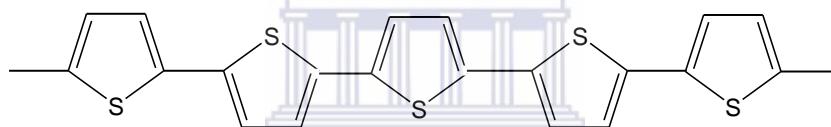
POLYANILINE



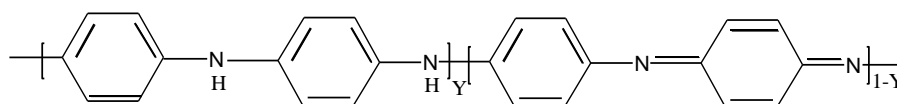
POLYACETYLENE



POLYPHENYLENE



POLYTHIOPHENE



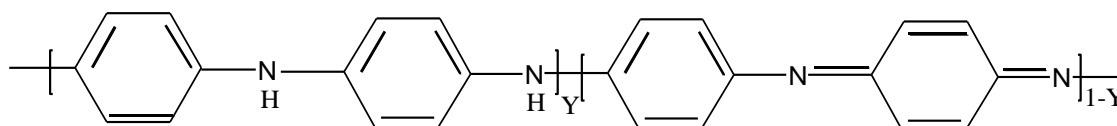
POLYANILINE

Figure 6: Structures of conductive polymers

Polyaniline has been shown to be the most conducting polymer studied due to its high environmental stability, controllable electrical conductivity and interesting redox properties associated with chain nitrogen. The potential applications of polyaniline include organic lightweight batteries, microelectronics, electrochromic displays, electromagnetic shielding and sensors [81].

2.5.1 Polyaniline

Polyaniline can be prepared by chemical or electrochemical oxidation of aniline. It is the most synthesized, studied, popular and widely used electrically conducting polymer. Polyaniline (PANI) is one of the most studied conductive polymers due to its easy synthesis, environmental stability, simple doping/dedoping, high conductivity and several unique properties [82]. Its ease of preparation, light weight, low cost, better electronic and optical properties, highly stable in air, its soluble in various solvents, and its good processibility [83] made PANI more popular and attractive polymer. On the other hand, PANI can be used in many applications, such as electromagnetic interference (EMI) shielding, electro-catalysts, rechargeable battery, light-emitting diodes (LEDs), chemical sensor, biosensor, corrosion devices and microwave absorption [84].



POLYANILINE

Figure 7: Chemical structure of polyaniline

During the synthesis of polyaniline, the aniline monomer - a known cheap organic compound - can be polymerized by chemical or electrochemical oxidation using water as solvent. The resulting polyaniline polymer is environmental stable, can be doped using a variety of p- or n- dopants or using protonic inorganic or organic acids and has many applications. However, the low solubility of the doped polymer in most organic solvents, the poor mechanical properties and low processability are major drawbacks for practical use and many efforts have tried to surpass these difficulties. The synthesis of the conducting polyaniline blends and composites is a cheap method that combines the processability of the insulated polymers and electrical and redox properties of the polyaniline [85].



Page left blank



CHAPTER III: PRINCIPLES OF SELECTED ANALYTICAL METHODS

3.1 Electrochemical techniques

3.1.1 Cyclic Voltammetry (CV)

Cyclic voltammetry (CV) is performed by using the potential of a working electrode and measuring the resulting current. Cyclic voltammetry system consists of an electrolysis cell, a potentiostat, a current-to-voltage converter, and a data transfer system. The electrolysis cell consists of a working electrode, counter electrode, reference electrode, and electrolytic solution. The working electrode's potential is varied linearly with time, while the reference electrode maintains a constant potential. The counter electrode on the other hand conducts electricity from the signal source to the working electrode. The purpose of the electrolytic solution is to provide ions to the electrodes during oxidation and reduction.

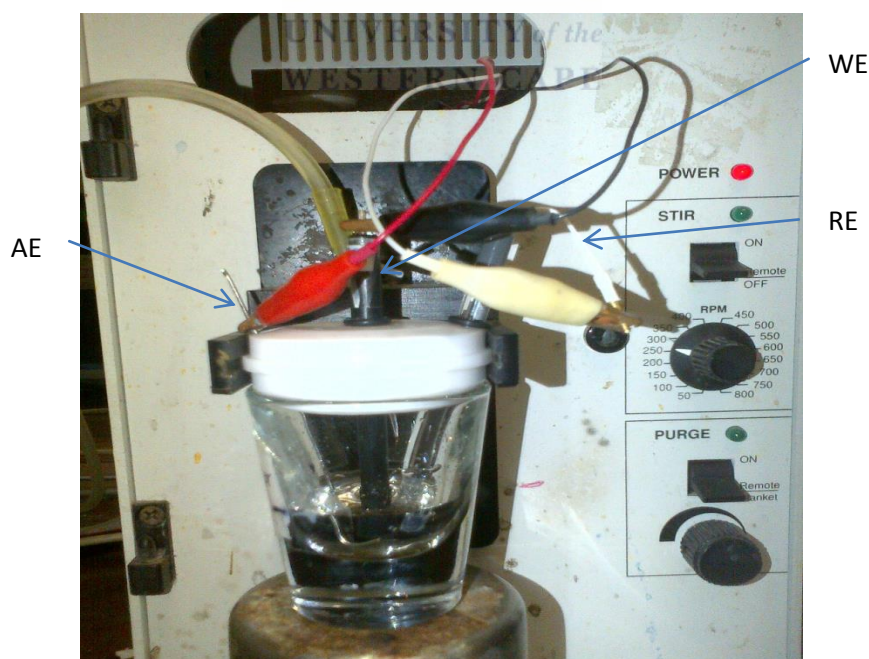


Figure 9: A photograph an electrochemical cell consisting of three electrodes (Abducted from lab experiment)

Figure 9 depicts a picture of a three electrode cell connected to the potentiostat: Black is the working electrode (WE), platinum wire is the counter electrode (AE) and the white one is the reference electrode (RE). CV is used for the study of redox processes, for understanding reaction intermediates, and for obtaining information on stability of reaction products.

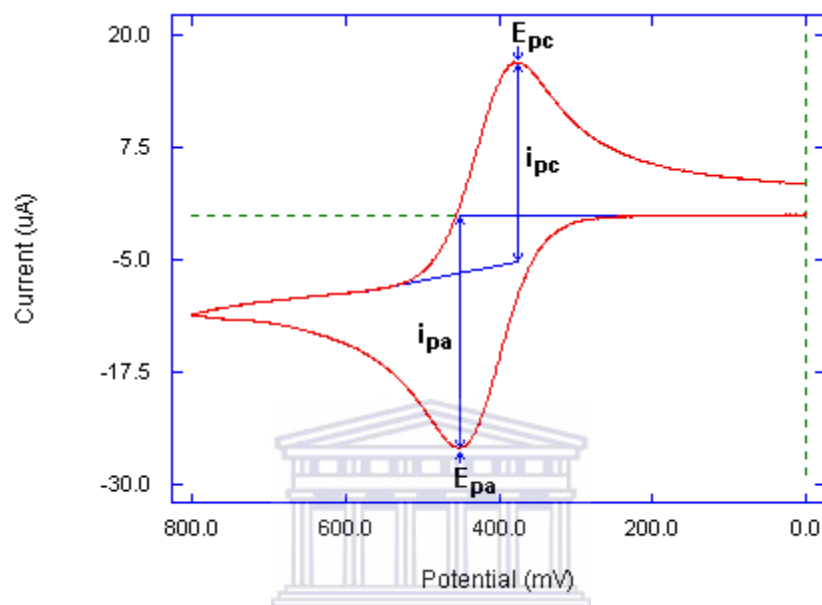


Figure 10: Atypical cyclic voltammogram showing peak parameters ($E_{p,a}$, $E_{p,c}$, $i_{p,c}$, $i_{p,a}$) [33].

Figure 10 shows two parts; the upper (cathodic) peak represent the reduction reaction, $O + ne \rightarrow R$ and the lower part (anodic) peak represent the oxidation electrode reaction, $R \rightarrow O + ne$ [87]. When the redox system throughout the potential scan is in equilibrium, then the redox process is reversible.

Table 1: Diagnostic tests for electrochemical reversibility of a redox couple using cyclic voltammetry [87]

1	$I_{pc} = I_{pa}$
2	E_{pc} and E_{pa} are independent of the scan rate v
3	$E^{\circ'}$ is positioned midway between E_{pc} and E_{pa} , therefore $E^{\circ'} = (E_{pa} + E_{pc})/2$
4	I_p is proportional to $v^{1/2}$
5	The separation between E_{pc} and E_{pa} is $59/n$ mV for an n -electron couple

One of the most important equations in electrochemistry is Randles-Sevcik equation, this equation describes the reversible process of the reactions occurring at the electrode surface [87].

$$I_{pc} = 0.4463nFA \left(\frac{nF}{RT} \right)^{1/2} D^{1/2} v^{1/2} c_{analyte}$$



$$I_{pa} = 0.4463nFA \left[\frac{nF}{RT} \right]^{1/2} C_{Red}^{bulk} D_{Red}^{1/2} v^{1/2}$$

Where I_p is the peak current, A is the electrode area, n is the number of electrons transferred, D is the diffusion coefficient, v is the speed at which the potential is scanned, $c_{analyte}$ is the bulk concentration, $R = 8.314 \text{ K}^{-1}$ is the general gas constant and T is the temperature in K.

And also another equation used for reversible electrode reaction is:

$$\Delta E_p = E_{pa} - E_{pc} = 2.3 \left(\frac{RT}{nF} \right) = \frac{58}{n} \text{ mV at } 25 \text{ }^\circ\text{C}$$

For the irreversible reaction:

$$|E_{pc} - E_{p/2}| = 1.86 \left(\frac{RT}{\alpha_c n_\alpha F} \right) = \frac{47.7}{\alpha_c n_\alpha} \text{ mV at } 25^\circ\text{C}$$

$$i_{pc} = 0.4958 \times nF \times \left(\frac{\alpha n F}{RT} \right)^{1/2} A D_0^{1/2} v^{1/2} C_0^{bulk}$$

$$E_{pc} = E^{o'} - \frac{RT}{\alpha n F} \left[0.780 + \frac{2.3}{2} \log \left[\frac{(1-\alpha)nFD_R}{RT(k^0)^2} \right] \right] + \frac{2.3RT}{2(1-\alpha)nF} \log v$$

Where k^0 is the standard heterogeneous rate constant, α is the transfer coefficient and $E^{o'}$ is the formal potential.

For a quasi-reversible:

$$\psi = \left[\frac{RT}{nFD_{OX}\pi} \right]^{1/2} \left[\frac{D_{OX}}{D_{Red}} \right]^{\alpha/2} k^0 v^{-1/2}$$

Where ψ Nicholson's parameter with numerically calculated values as a function of $nx\Delta E$ for each scan rate.

Reversible process:- occurs when an electroactive species in solution is oxidized or reduced in a forward scan and reduced (or oxidized) in the backward scan. This type of system is in equilibrium throughout the potential scan.

Irreversible process:- is the process where the reaction goes one-way, the most common is when only a single oxidation or reduction peak with a weak or no reverse peak is observed. Irreversible processes are a result of slow electron transfer or chemical reactions at the surface of the working electrode. Besides, a large peak potential separation (>200 mV) if there is a peak in the reverse scan also indicates the irreversible of a reaction,

Quasi-reversible process:- shows both of the behaviour of the reversible and irreversible processes.

For the thin film, the is irreversible reaction and the following current-potential relations are used:

$$i_{pc} = \frac{\alpha n^2 F^2 A \Gamma}{2.718 RT} v$$

$$i_{pa} = \frac{(1-\alpha)n^2 F^2 A \Gamma}{2.718 RT} v$$

$$E_{pc} = E^{\circ} - 2.3 \frac{RT}{\alpha n F} \log \left(\frac{RTk^{\circ}}{\alpha n F v} \right)$$

$$E_{pa} = E^{\circ} + 2.3 \frac{RT}{(1-\alpha)n F} \log \left(\frac{RTk^{\circ}}{(1-\alpha)n F v} \right)$$



3.1.2 Electrochemical Impedance Spectroscopy (EIS)

Electrochemical Impedance Spectroscopy (EIS) is the technique where the cell or electrode impedance is plotted vs frequency. In modern practice, the impedance is usually measured with lock-in amplifiers or frequency-response analysers, which are faster and more convenient than impedance bridges [88].

3.2 Spectroscopy techniques

3.2.1 Ultraviolet-Visible (UV/ Vis) Spectroscopy

Uv-visible spectroscopy helps in the identification of unknown compounds, specific functional groups and nature of carbon chain, unsaturation and examination of poly nuclear compounds.

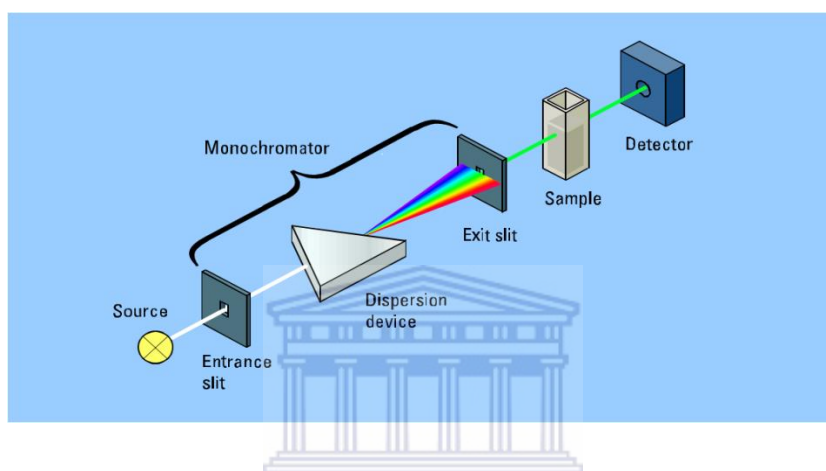


Figure 11: UV/ Vis spectrophotometer [89]

Uv-visible spectrometer consists of the light source the deuterium arc lamp, yields a good intensity continuum in the uv region and provides useful intensity in the visible region and a detector which convert a light signal into an electrical signal. Ideally, it should give a linear response over a wide range with low noise and high sensitivity.

The principles of UV/ Vis absorption spectroscopy is based on Beer's and Lambert's Law which states that the fraction of incident radiation absorbed is proportional to the number of absorbing molecules in its path [90]. When the radiation passes through a solution, the amount of light absorbed or transmitted is an exponential function of the molecular concentration of the solute and also a function of length of the path of radiation through the sample. Therefore:

$$A = \text{Log}\left(\frac{I_o}{I}\right) = \epsilon cl$$

Where

A = absorbance

I_o = intensity of the incident light (or the light intensity passing through a reference cell)

I = Intensity of light transmitted through the sample solution

c = concentration of the solute in mol L⁻¹

l = path length of the sample in cm

ϵ = extinction coefficient



In this thesis, this technique will be used to check the activity of an enzyme and measure its effectiveness as a catalyst and also to characterise the gold nanoparticles.

3.2.2 Transmission electron microscopy (TEM)

Transmission electron microscopy uses high energy electrons (up to 300 kV accelerating voltage) which are accelerated to nearly the speed of light. The electron beam behaves like a wave front with wavelength about a million times shorter than light waves. When an electron beam passes through a thin-section specimen of a material, electrons are scattered. A sophisticated system of electromagnetic lenses focuses the scattered electrons into an image or a diffraction pattern, or a nano-analytical spectrum, depending on the mode of operation.

Page Left Blank



CHAPTER IV: EXPERIMENTAL

4.1 Chemicals and Materials

- 17 α -ethynylestradiol (EE2) (Sigma Aldrich, $\geq 98\%$, Product # E4876)
- 17 β -estradiol (Sigma Aldrich, $\geq 98\%$, Product # E8875)
- Acetic acid glacial (B&M Scientific \geq Product #)
- Aniline (Sigma Aldrich, 99%, Product # 132934)
- Citric acid (Sigma Aldrich, ≥ 99.5 -102%, Product # 33114)
- Coomassie blue removal (Sigma Aldrich, Product # 27813)
- Equilin (EQ) (Sigma Aldrich, Product # E8126)
- Estriol (E3) (Sigma Aldrich, $\geq 97\%$, Product # E1253)
- Estrone (E1) (Sigma Aldrich, $\geq 99\%$, Product # E9750)
- Ethanol absolute (Sigma Aldrich, $\geq 99.8\%$, Product # 34870)
- Glutaraldehyde (Sigma Aldrich, ≥ 50 wt %, Product # 340855)
- Gold Chloride (Sigma Aldrich, $\geq 99.8\%$, Product # 34923)
- Hydrochloric acid (Sigma Aldrich, $\geq 37\%$, Product # 258148)
- Laccase (*Trametes Versicolor*) (Sigma Aldrich, ≥ 10 U/mg, Product # 51639)
- Phosphoric acid (Sigma Aldrich, ≥ 18 wt%, Product # W290017)
- Poly (4-styrenesulfonic acid) (Sigma Aldrich, ≥ 18 wt%, Product # 561223)
- Sodium Borohydride (Sigma Aldrich, $\geq 99,999$ Product # 254169)
- Sodium Chloride (Sigma Aldrich, $\geq 99.5\%$, Product # S7653)
- Sodium Phosphate dibasic dihydrate (Sigma Aldrich, ≥ 99.5 , Product # 30412)
- Sodium citrate tribasic dihydrate (Sigma Aldrich, $\geq 98\%$, Product # C0909)

4.2 Reagent solutions

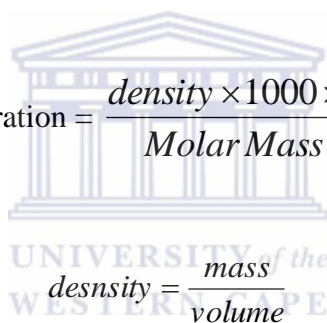
An ultrapure de-ionized water (18 MΩ cm) produced by a reverse osmosis/ ion-exchange combined water purification system (Rios TM 3/ Synergy, Millipore) was used for the preparation of all reagent solutions and experimental steps where necessary.

Preparation of solutions

Solutions for the procedure were prepared using different analytical formulas such as the following equations for the preparation and dilutions of solutions:

$$C_1V_1 = C_2V_2$$

$$\text{Concentration} = \frac{\text{density} \times 1000 \times \text{purity}}{\text{Molar Mass} \times 100}$$



$$C = M \times MW \times V$$

4.2.1 Preparation of modified McIlvaine buffer

McIlvaine buffer (McIIB) was prepared according to Tanaka et al. (2009)[91] with some modification, by dissolving citric acid ($C_6H_8O_7 \cdot H_2O$) and 3.5597 of sodium phosphate dibasic dihydrate ($HNa_2O_4P \cdot 2H_2O$) separately in 100 mL of 20% (v/v) ethanol/water mixture each. The pH meter was then calibrated with standard solutions. Then the pH of the citric acid was found to be 1.68 and disodium phosphate was found to be 9.68 at a temperature of 20.2 °C. Then both were mixed each by a volume of 40 mL and the McIlvaine buffer was measured at

pH 4.99. The buffer solution was used and stored in a refrigerator at 18 °C for not more than a week.

4.2.2 Preparation of laccase (*Trametes Versicolor*) enzyme stock solution

10 mM laccase stock solution was prepared by dissolving 0.0100 g of laccase in 1 mL of 50% (v/v) ethanol/ water. The resulting turbid solution was then centrifuged at 10000 -14000 rpm for about 10 minutes. The clear light-orange supernatant solution was decanted off into a brown vial and stored in a fridge at +4 °C and used for not more than 3 weeks.

4.2.3 Preparation of laccase solutions for SDS-PAGE

All reagents and experimental activities were provided and handled by the Structural Biotechnology Unit (University of the Western Cape). The running gel (10% SDS-PAGE) was already prepared and laccase was diluted with phosphate buffer, the other with water and lastly with ethanol. Two samples of the blank were prepared using 50% v/v ethanol and water and phosphate buffer. Therefore after, the concentration of the five samples was checked using Nanodrop spectrophotometer. To those solutions, 10 µL of SDS (sodium dodecyl sulphate) was added on top. Thereafter it was boiled at 95 °C using a digital heat block for 5 minutes and after that it was taken for centrifuge because it was too concentrated. Therefore all 5 solutions were poured on separate markers. Experiment ran for 60 minutes. After that, the gel was stained with Coomassie blue solution and put in a microwave for 2 minutes. Then it was immediately taken out and de-stained with 50% water/ethanol for overnight. Therefore the molecular weight and purity was successfully identified.

4.2.4 Preparation of stock solutions of the Estrogens

10 mL of 10 mM stock solutions of each estrogens were prepared in a 40/60 (v/v) absolute ethanol/ water by weighing out 30 mg 17 α -ethynylestradiol, 27.5 mg 17 β -estradiol, 27.9 mg

estrone, 30 mg estriol and 26.8 mg Equilin. The sample solutions thus prepared were always stored at 18 °C in a fridge.

4.2.5 Preparation of other solutions

10 mL of 3 M aq. NaCl was prepared by weighing 1.753 g of sodium chloride.

100 mL of 1 M aq. HCl solution was prepared by diluting an 8.21 mL aliquot of conc. HCl (37%).

100 mL of 1 M aq. H₃PO₄ solution was prepared by diluting an 11.5 mL aliquot of 18wt% H₃PO₄.

About 5 mM aq. glutaraldehyde stock solution was prepared by diluting 9.8 µL of the 50 wt % glutaraldehyde with 1 mL of water in a brown vial.

3 mL of 300 mM aq. NaBH₄ was prepared by weighing 0.283g of sodium Borohydride.

1 mL of 0.5 mM aq. HAuCl₄ solution was prepared by diluting 10.85 µL of the gold chloride with 25 mL of water in a brown vial.

4.3 Synthesis of Gold Nanoparticles

Gold nanoparticles were synthesized according to Kimling et al., 2006 [92] with some modification. Before the experiment started, all cleaned glassware was rinsed with water. 10 mL of ROP-DDI water was transferred into a round bottom flask and 5 mL of 0.1 M aq. sodium citrate was added into it. The solution was stirred for 5 minutes. Then 1 mL of 0.5 mM HAuCl₄ was added and with continuous stirring while nitrogen gas was used to remove dissolved oxygen for 10 minutes. In the hydrogen gas head space, 3 mL of 0.3 M sodium Borohydride (NaBH₄) was injected drop-wise into the solution and allowed to be stirred for

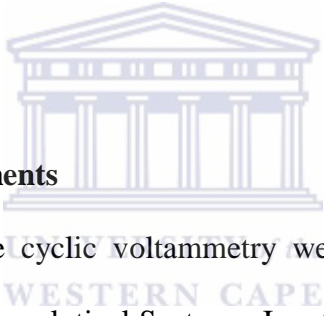
30 minutes. The resulting deep wine red coloured solution was immediately centrifuged to separate the nanoparticles from the excess reactants, reagents, and the solvent (water). The residue was then cleaned by re-suspending in water and re-centrifuging for three consecutive times. The cleaned residue of the cleaned nanoparticles was then re-suspended in 1 mL of water and always kept in the fridge at + 4 °C as a stock solution from which working solutions were prepared by further dilutions when necessary.

4.4 Distillation of aniline

The commercially provided aniline was purified before use by distillation according to the experimental set-up of Ruh and Rosette [93].

4.5 Instruments

4.5.1 Electrochemical measurements



Electrochemical experiments like cyclic voltammetry were carried out using BAS 100B electrochemical analyzer from Bioanalytical Systems, Inc. (West Lafayette, USA); also using PalmSens operated with PalmTrace PC software (PalmSens, Utrecht, The Netherlands) with an three-electrode electrochemical cell set-up with a platinum wire as the counter electrode, Ag/ AgCl (3.0 M NaCl) as the reference electrode and glassy carbon electrode ($d = 0.3$ cm), gold electrode ($d = 0.16$ cm) and platinum electrode ($d = 0.16$ cm) as a working electrode and computers were connected to the machine for recording the results.

Electrochemical impedance measurements (EIS) were recorded with Zahner IM6ex (Zhaner, Germany) at an amplitude of 10 mV within frequency range of 100 mHz to 100 kHz using the same electrodes mentioned above.

The electrode was cleaned by polishing with alumina powder of 1.0, 0.3 and 0.05 μm using polishing pads for 5 minutes. After polishing, the electrode was sonicated firstly with ethanol for 10 minutes and after with distilled water for another 10 minutes in order to remove any particles of the powder on the electrode surface. The experiments were carried out at controlled room temperature (about 22 $^{\circ}\text{C}$) using McIlB solution (pH 4.99). Unless otherwise indicated all electrochemical measurements were preceded by purging of the supporting electrolyte with argon (Afrox, South Africa) for about 10 minutes before commencement of measurement and keeping of a blanket of the gas over the head space of the solution during the measurement. No Ar-purging was employed when the immobilized enzyme was used to directly catalyze the oxidation of the estrogens under aerobic condition.

4.5.2 UV/ Vis Molecular absorption and Fluorescence Measurements

The UV/ Vis spectra were recorded on a Nicolet Evolution 100 Spectrometer (Thermo Electron Corporation, UK). Fluorescence spectra of samples were recorded using Horiba NanoLog™ 3-22- TRIAX (USA), with emission monochromators at a slit width of 5 nm.

4.5.3 Electrophoresis (SDS-PAGE)

Molecular weight and purity of the Laccase dissolved in ethanol and phosphate solutions were determined with SDS-PAGE with mini-protean system (Bio-Rad, California). Before this measurement the actual concentrations of laccase in these solutions were estimated using NanoDrop ND-1000 Spectrophotometer with a computer interface to the NanoDrop and the boiling was carried out using VWR Digital Heatblock (VWR, Pennsylvania).

4.5.4 Microscopic Imaging (TEM & SEM)

Transmission electron microscopy (TEM) analysis of the AuNPs and laccase samples, which were first drop-coated and dried onto copper or nickel grids, were done using a Tecnai G2 F20X-Twin MAT 200 kV Field Emission High Resolution Transmission Electron

Microscope (HRTEM) from FEI (Eindhoven, Netherlands). Additionally SEM images of the AuNPs were obtained with Zeiss Auriga HRSEM analyzer using the secondary electron (SE) mode at different voltages different resolution.

4.6 Preliminary Studies

4.6.1 Electroactivity of the EE2 as model estrogen on GC, Au, and Pt electrodes

Potential windows of each electrode in McIIB were first established by running cyclic voltammograms (CV) at 100 mV/ s scan rate: gold electrode (AuE) 1.3 to -0.8 V, glassy carbon electrode (GCE) 1.4 to -1.4 V and platinum electrode (PtE) 1.4 to -0.6 V. Three-cycle CVs were then recorded with each electrode in 5 mL McIIB before and after adding 50 μ L aliquot of the stock solution of EE2 to work at 1 mM concentration of the model estrogen. This was done to check the electrochemical activities of EE2 at these electrodes.

4.6.2 UV/ Vis Absorption and Fluorescence Spectra of the Estrogens and Laccase

100 μ L of the 10 mM of EE2 stock solution was poured into a 2 mL centrifuge tube and then 900 μ L of McIIB was added to the same centrifuge tube to obtain a 1 mM EE2 working solution. 700 μ L of that mixture was then added to a 700 μ L cuvette and UV/ Vis absorption spectra were recorded using McIIB both as a blank and as reference (or diluent).

During measurements of the UV/ Vis emission fluorescence spectra 30 μ L of a stock solution was diluted to 3000 μ L. For all estrogens McIIB was used as the blank and water as the reference (or diluents). For the enzyme, McIIB was again used both as a blank and as the reference (or diluents).

4.6.3 Verification of the Enzymatic Activity of Laccase in Solution

100 μ L of the 10 mM of EE2 stock solution was poured into a 2 mL centrifuge tube and then 900 μ L of McIIB was added to the same centrifuge tube to obtain a 1 mM EE2 working

solution. 700 μL of that mixture was then added to a 700 μL cuvette and UV/ Vis absorption spectra were recorded using McIIB both as a blank and as reference (or diluent). After that was done, the solution was transferred back to the centrifuge tube. Then 10 μL aliquot from the laccase stock solution was spiked into the above 1000 μL EE2 solution and a timer was started immediately in order to monitor the oxidation of the latter at intervals of time. The concentration and activity of the enzyme in the resulting reaction mixture was estimated to be 0.10 nM (0.01 mg/ mL) and 1 U, respectively (as calculated based on supplier's declaration of assay on the original container of the enzyme). As time went by, the reaction mixture was observed to get cloudy confirming the oxidation of EE2 and formation of a precipitated polymeric product. Therefore the reaction was cleared by centrifugation (5 minutes) every time before taking samples for recording the spectra. Spectra were recorded at different intervals, from 0 to 90 minutes.

4.6.4 Testing of Electroactivity of Laccase in Solution and as Drop-Coated Film on GC, Au, and Pt Electrodes

For the preparation of drop-coated films of laccase, a working solution of the enzyme was firstly prepared as 60 μL lac from the 10 mM stock solution +500 μL of ethanol and 500 μL McIIB. There after volume of 4 μL of laccase was drop-coated onto GC, Pt, and Au electrode surfaces, and then let dry for 15 minutes under a day-light lamp. Then each were transferred to the electrochemical cell containing 5 mL of McIIB to run three-cycle CVs at scan rates of 10 and 100 mV/ s within the same potential windows for recording the CVs of the estrogens. The CVs of dissolved laccase were also laccase were also checked at a concentration of 1 μM after spiking an aliquot of a 10 μM secondary stock solution of the enzyme.

4.6.5 Electroactivity of Drop-Coated AuNP Film

4 μL of the AuNP stock solution was drop-coated on the GCE and let dry in air under a day-light lamp for about 20 minutes. The electrode with the AuNP film was then transferred to an electrochemical cell containing 5 mL McIIB to record a three-cycle CV between $E = 1.35$ to -1.4 V at a scan rates of 10 mV/ s and 100 mV/ s.

4.6.6 Electropolymerization and characterization of polyaniline/ polystyrene sulfonic acid composite films on glassy carbon electrode (GC/PANI-PSSA)

Before the electro-polymerisation of aniline on the pre-cleaned glassy carbon electrode, a background CV was recorded between the initial potential of $E = -0.2$ V to a final potential of $E = 1.1$ V at a scan rate of 50 mV/ s for 3 cycles in a 5 mL aq. HCl (1000 mM) or H_3PO_4 (1000 mM) supporting electrolytes. Then 23 μL of pure aniline and 125 μL of PSSA (18wt%) were added to the supporting electrolyte in order to carry out the electropolymerization process at concentrations of 50 mM aniline and of 25 mM PSSA. The electropolymerization was carried out with the same setting of CV but now for 5 cycles, resulting in the deposition of greenish PANI-PSSA film. Then that modified electrode with PANI-PSSA was gently rinsed first with fresh portion of the supporting electrolyte used and then with water. This was done to remove any unreacted aniline that may be loosely adsorbed onto the modified electrode. Then electropolymerization solution was discarded, and the CV-based confirmation and characterization of the produced PANI-PSSA film was carried out in a fresh 5 mL aq. HCl or H_3PO_4 in the electrochemical cell. Then, the film was removed and rinsed again with water, and transferred to cell containing 5 mL McIIB in order to carry out another set of CV measurements to check the electrochemical stability and electrode kinetic characteristics of the film under the condition suitable for the laccase biosensor. In the latter case CVs were recorded at several scan rates in the potential range of -1 to 0.7 V.

4.7 Electrochemical Laccase Biosensor Studies

4.7.1 Preparation of GCE/PANI-PSSA

Cleaning of the GC electrode, the electro-polymerization of the mixture of aniline and PSSA, and post-electropolymerization CV diagnostic experiments were done the same way as described previously. Before testing the use of the resulting GC/PANI-PSSA platform with the enzyme, the electrochemical response of the former to EE2 was established by recording CVs in the potential range of -1 to 0.7 V in the presence of 1 mM of EE2 in 5 mL McIlB.

4.7.2 Electroactivity of Dissolved Laccase at GCE/PANI-PSSA

The electrochemical response of the GC/PANI-PSSA to EE2 was tested by recording CVs in the potential range of -1 to 0.7 V in the presence of 1 mM of Laccase in 5 mL McIlB.

4.7.3 Preparation of GCE/PANI-PSSA/ LAC

4 μ L of laccase was drop coated onto the GC/PANI-PSSA and dried under a day-light lamp for 15 minutes. There after it was transferred to the cell containing 5 mL McIlvaine buffer to record three-cycle CVs in the potential range -1 to 0.7 V and scan rate of 25 mV/ s, with or without Ar-purging as well in the absence or in the presence of EE2 (0.1 mM).

4.7.4 Preparation of GCE/PANI-PSSA/ AuNP

4 μ L of AuNP stock solution was drop coated onto the GC/PANI-PSSA and dried under a day-light lamp for 15 minutes. There after it was transferred to the cell containing 5 mL McIlB to record three-cycle CVs in the potential range -1 to 0.7 V and scan rate of 25 mV/ s in the absence or in the presence of EE2 (0.1 mM).

4.7.5 Preparation of GCE/PANI-PSSA/ AuNP/ LAC

4 μ L AuNP was first drop-coated onto the GC/PANI-PSSA and dried in air under a day-light lamp for 15 minutes. After it dried out, then 4 μ L of laccase was drop-coated over the AuNP

layer and dried in air under a day-light lamp for 15 minutes. There after it was immediately characterised in the 5 mL McIlvaine buffer in the presence of oxygen (i.e., with Ar-purging) in the potential range between -1 V to 0.7 V a scan rate of 25 mV/ s for 3 cycles for investigation of electrochemical behaviour. Additional CVs were recorded after spiking the stock solution of EE2 to obtain 0.1 mM concentration.

4.7.6 Preparation of GCE/PANI-PSSA/ LAC/ GLU

4 μ L glutaraldehyde was first drop-coated onto the GC/PANI-PSSA and dried in air under a day-light lamp for 15 minutes. After it dried out, then 4 μ L of laccase was drop-coated over the glutaraldehyde layer and dried in air under a day-light lamp for 15 minutes. There after it was immediately characterised in the 5 mL McIlvaine buffer in the presence of oxygen (i.e., with Ar-purging) in the potential range between -1 V to 0.7 V a scan rate of 25 mV/ s for 3 cycles for investigation of electrochemical behaviour. Additional CVs were recorded in the presence of stock solution of EE2 to obtain 0.1 mM concentration.

4.7.7 Preparation of GCE//PANI-PSSA/AuNP/ LAC/ GLU

4 μ L AuNP was first drop-coated onto the GC/PANI-PSSA and dried in air under a day-light lamp for 15 minutes. After it dried out, then 4 μ L of laccase was drop-coated over the AuNP layer and dried in air under a day-light lamp for 15 minutes. After that one dried, then 4 μ L of glutaraldehyde was drop-coated over the AuNP and laccase layer and dried in air under a day-light lamp for 15 minutes. There after it was immediately characterised in the 5 mL McIlvaine buffer in the presence of oxygen (i.e., with Ar-purging) in the potential range between -1 V to 0.7 V a scan rate of 25 mV/ s for 3 cycles for investigation of electrochemical behaviour. Additional CVs were recorded after spiking the stock solution of EE2 to obtain 0.1 mM concentration.

4.8 Cyclic Voltammetric Sensing of EE2 with Laccase Biosensors

For PANI-PSSA, PANI-PSSA/Lac/Glu and PANI-PSSA/AuNp/Lac/Glu, electropolymerization was done with the same procedure as discussed in 4.5.6 and stability check as well. Therefore after procedure, sensing was done as follows:

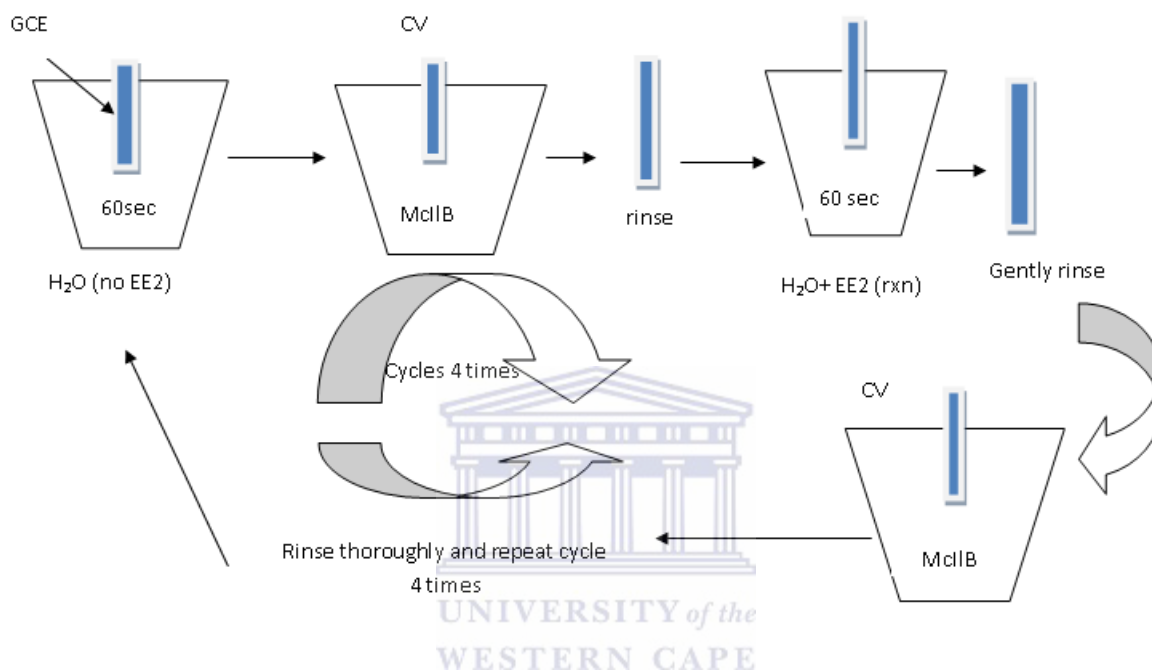


Figure 12: Flow chart used for testing surface regeneration and reproducibility of CVs of PANI-PSSA, PANI-PSSA/Lac/Glu and PANI-PSSA/Au/Lac/Glu before and after exposure to aq. EE2

4.9 Electrochemical Impedance Sensing of EE2 with the Laccase Biosensors

For the electrochemical impedance, same procedure as in 4.7 was done at a frequency of 100 mHz to 100 kHz and amplitude of 10 mV.

CHAPTER V: RESULTS AND DISCUSSION

5.1 Preliminary Studies of Estrogens, Gold Nanoparticles, and Laccase

5.1.1 Estrogens

5.1.1.1 UV/ Vis Spectra of Aq. Estrogens Solutions

The UV/ Vis absorption spectra of the estrogens (E1, E2, E3, EE2 and EQ) were recorded between 190 nm - 1100 nm at bandwidth of 2 nm. Figure 13 shows an overlay of the obtained spectra. The estrogens absorb within similar range of wavelengths from 194 to 293 nm. The characteristics and chromophores of the various peaks observed have been summarized in Table 2.

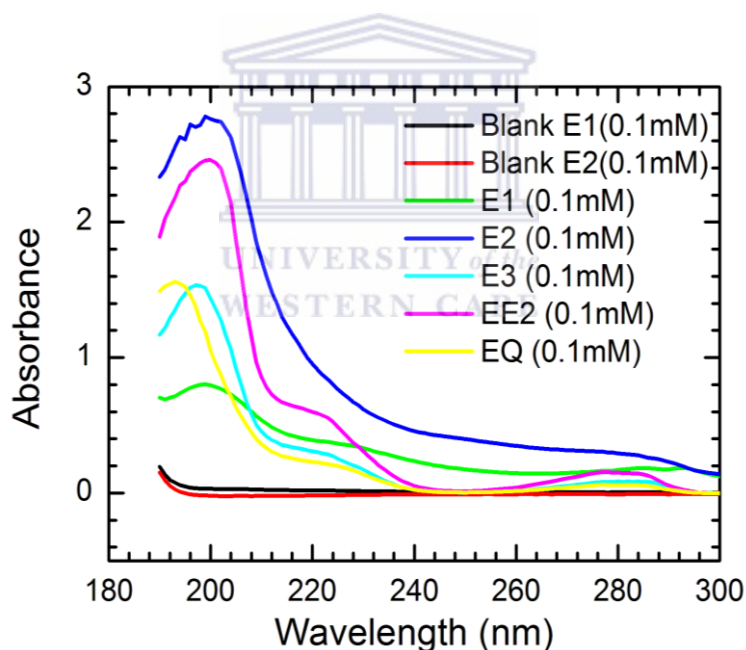


Figure 13: UV/ Vis absorption spectrum of estrogens in 0.1 mM aq.

The molar absorptivity were estimated as per the Beer-Lambert law ($\epsilon = A/ cl$) where A = absorbance, c = molar concentration in mM, and l = light path length through the sample. Four peaks at 199, 231, 285 and 293 nm for E1 were observed from the spectra with an extinction coefficient of 7.9, 1.8 and 3.5 $\text{mM}^{-1} \text{cm}^{-1}$. The second peak at 231 nm appeared to be very broad and this is due to the benzene ring. At 199 nm a slightly sharp peak was

observed, this is due to $\pi \rightarrow \pi^*$ transition. E2 showed one absorption peak at 197 nm due to $\pi \rightarrow \pi^*$ transition within the formation in the benzaldehyde ring [94].

Table 2: UV/ Vis absorption peaks of estrogens at concentrations (c) of 0.1 mM (aq.) in cuvettes with path lengths (l) of 1 cm in McIlB (pH 4.9)

Estrogen	No of peaks	$\lambda_{\max}/$ nm	A	$\epsilon/$ mM ⁻¹ cm ⁻¹	Origin of peak (chromophore)	Ref.
E1	2	199	0.79	7.9	>C=O	[95]
		231	0.35	3.5	-C=C-C=C-	[95]
		285	0.18	1.8	>C-OH	[95]
		293	0.18	1.8	≥C-OH	[95]
E2	1	197	2.74	27.4	Ar	[95]
EE2	4	200	2.47	24.7	Ar	[95]
		222	0.57	5.7	?	
		277	0.16	1.6	Ar-OH	[95]
		284	0.14	1.4	Ar	[95]
E3	3	197	1.53	15.3	Ar	[95]
		222	0.29	2.9	?	?
		277	0.083	0.83	Ar-OH	[95]
		286	0.083	0.83	Ar-OH	[95]
EQ	4	194	1.55	15.5	C=O, Ar-H	[95]
		222	0.20	2	?	?
		277	0.061	0.61	Ar-OH	[95]
		284	0.058	0.58	Ar-H	[95]

E2 has one absorption peak. EE2 with four absorption peaks within the formation at the benzaldehyde and phenol ring. Peaks were sharp, some broad. E3 showed four absorption peaks at 197 to 286 nm with a weak absorption due to $n \rightarrow \pi^*$ transition and at 197 nm a sharp peak is formed. For Equilin, four absorption peaks were observed at 194, 222, 277 and 284 nm.

5.1.1.2 UV/ Vis Fluorescence Spectra of the Estrogens

The fluorescence spectra of the estrogens (E1, E2, E3, EE2 and EQ) were recorded between 295 nm - 545 nm at the excitation wavelength of $\lambda_{ex} = 280$ nm. According to Figure 14A and B, the respective prominent peaks were: EE2 ($\lambda_{max} = 304$), E3 ($\lambda_{max} = 318$), E2 ($\lambda_{max} = 305$), EQ ($\lambda_{max} = 310, 362$), and E1 ($\lambda_{max} = 309, 420$). These λ_{max} confirm that some of the estrogens emit almost at the same region as in the UV/ Vis spectra.

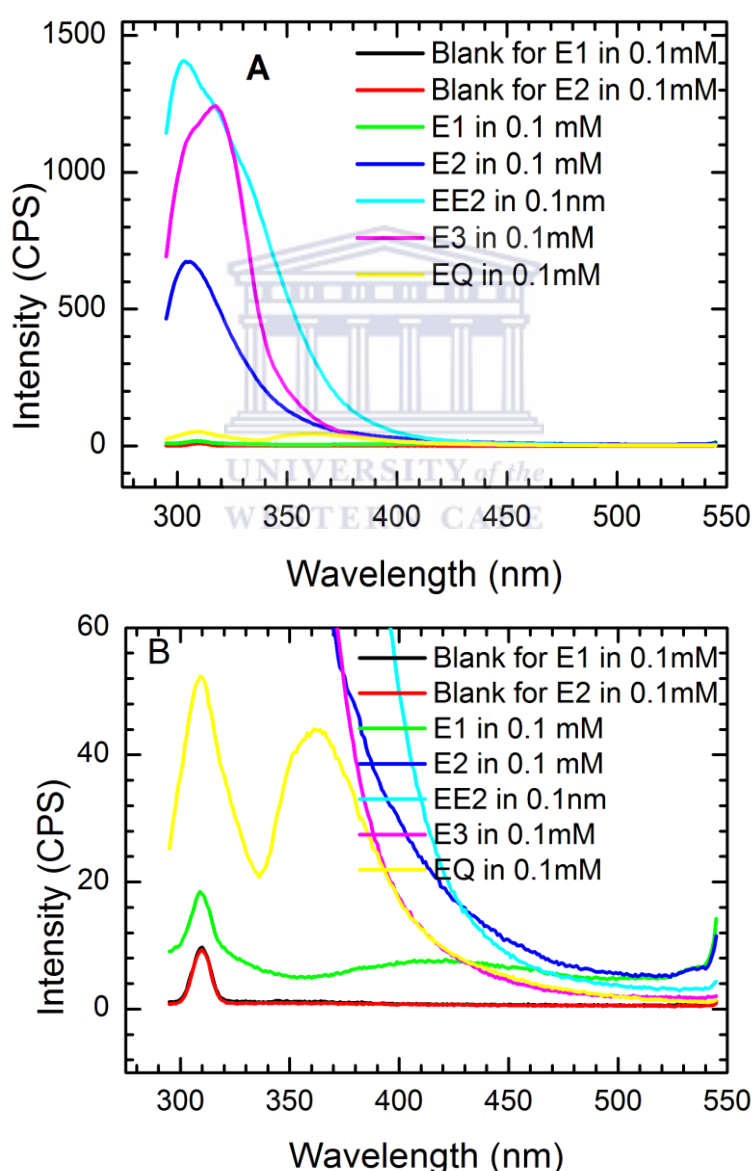
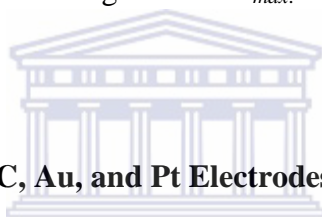


Figure 14: (A) UV/ Vis fluorescence spectra of aq. solutions of the estrogens (0.1 mM each) at an excitation wavelength of $\lambda_{ex} = 280$ nm. B: zoomed-in view.

Table 3: Summary of UV/ Vis fluorescence peaks of the estrogens (0.1 mM) at excitation wavelength $\lambda_{ex} = 280$ nm in aqueous solution

Estrogen	No of peaks	λ_{max} / nm	Intensity/ 10^3 C.P.S.
E1	2	309	10.6
		420	7.87
E2	1	305	665
EE2	1	304	1400
E3	1	318	1240
EQ	2	310	41.7
		362	43.5

Table 3 shows the intensity of all estrogens and λ_{max} . E1 with 7.86 and EE2 having the highest intensity of 1400.



5.1.1.3 Electroactivity EE2 at GC, Au, and Pt Electrodes

The cyclic voltammograms in Figure 15A, B, C were respectively recorded within different working ranges with GCE ($E = 1.35$ to -1.4 V), AuE ($E = 1.3$ to -0.8 V) and PtE ($E = 1.4$ to -0.55 V) at a scan rate of 10 mV/ s in the presence of EE2 on different electrodes was used to study the electrochemical properties of EE2. One new anodic peak of about 0.9 V was observed at a potential of 0.9 V when using GCE. The peak height decreased on subsequent scans and no reverse peak was observed because EE2 is not only irreversibly electroactive but also products which caused electrode fouling were formed. Looking at the CVs recorded with the Au electrode (Fig 15B), an increase in the background anodic peak at 0.79 V was observed in the first cycle, which shows a possible oxidation of EE2 at this potential with no obvious reverse peak. Since this peak and the other background peaks also decreased with successive scan, EE2 was oxidized irreversibly and AuE surface fouled like the GC was.

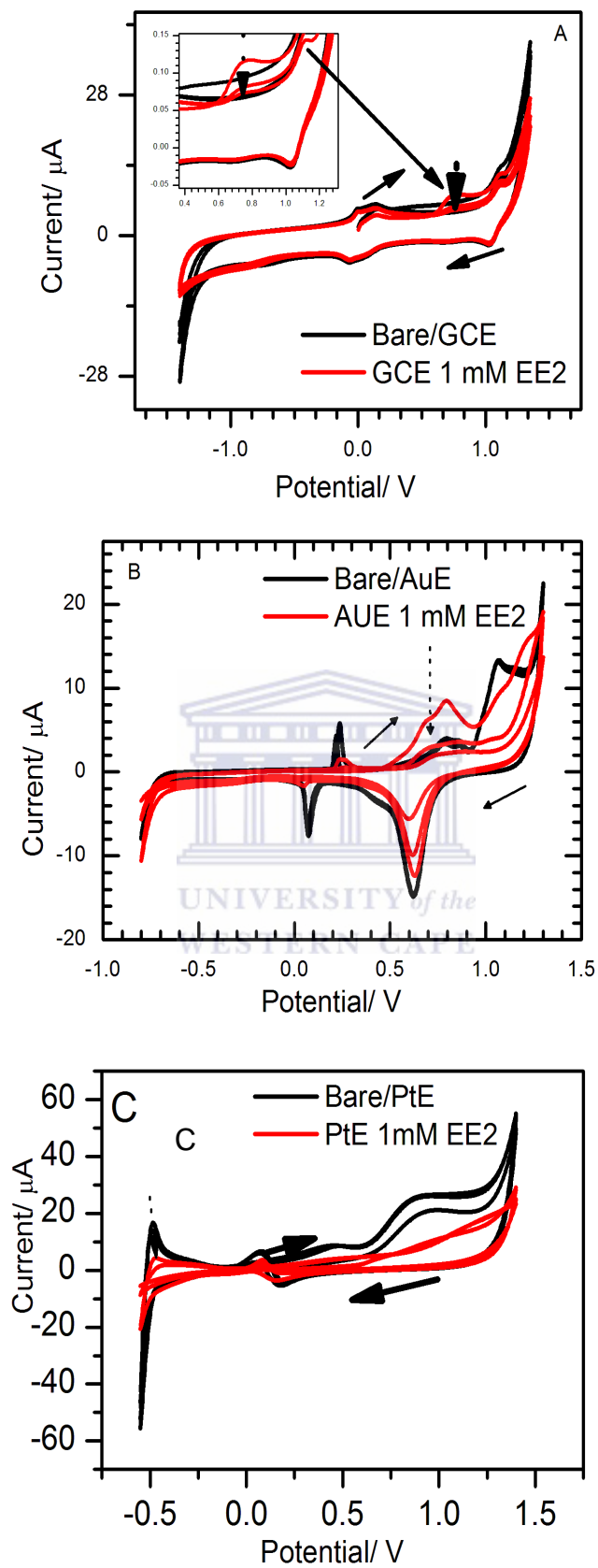


Figure 15: CV of EE2 in 1 mM McIIB (pH 4.9) using A) glassy C electrode, B) gold electrode and C) platinum electrode. Scan rate: 100 mV/ s

No peak was observed at the PtE in the presence of EE2, but it appeared to adsorb without reaction as evidenced by the drastic decrease in the background current of the electrode. Based on these results the GCE was the lectrode least passivated in the presence of EE2.

5.1.1.4 Effect of storage

UV/ Vis absorption spectra were recorded check the effect of time of storage of EE2. Figure 16A and B show overlay of spectra obtained at different times or intervals for a mixture of EE2 and laccase samples from the stock solutions with different ages. Everytime before measurement, the mixture was centrifuged for about five minutes because the mixture of EE2 and the enzyme was turning turbid or formed a precipitate as time elapsed. This was due to the laccase catalysed oxidation of EE2 with O₂ followed by formation of polymeric products as already has been explained in the literature [49]. Two absorption peaks were observed from the spectra in a) at different intervals. At graph b) where one week old EE2 and new enzyme was used, two sharp peaks were observed and no peaks occurred during different intervals. Observing graph c) which reperesent peak height vs time of both graph a) and b) at different intervals, red representing fresh EE2 and 2 month old enzyme, and black representing one week old EE2 and new enzyme. The conclusion observed from the graph c) is that EE2 after a week of storage must not be used, because it is no longer effective. Decline on the graph is observed when one week old EE2 was used and made. Therefore every week new solution of EE2 must be made.

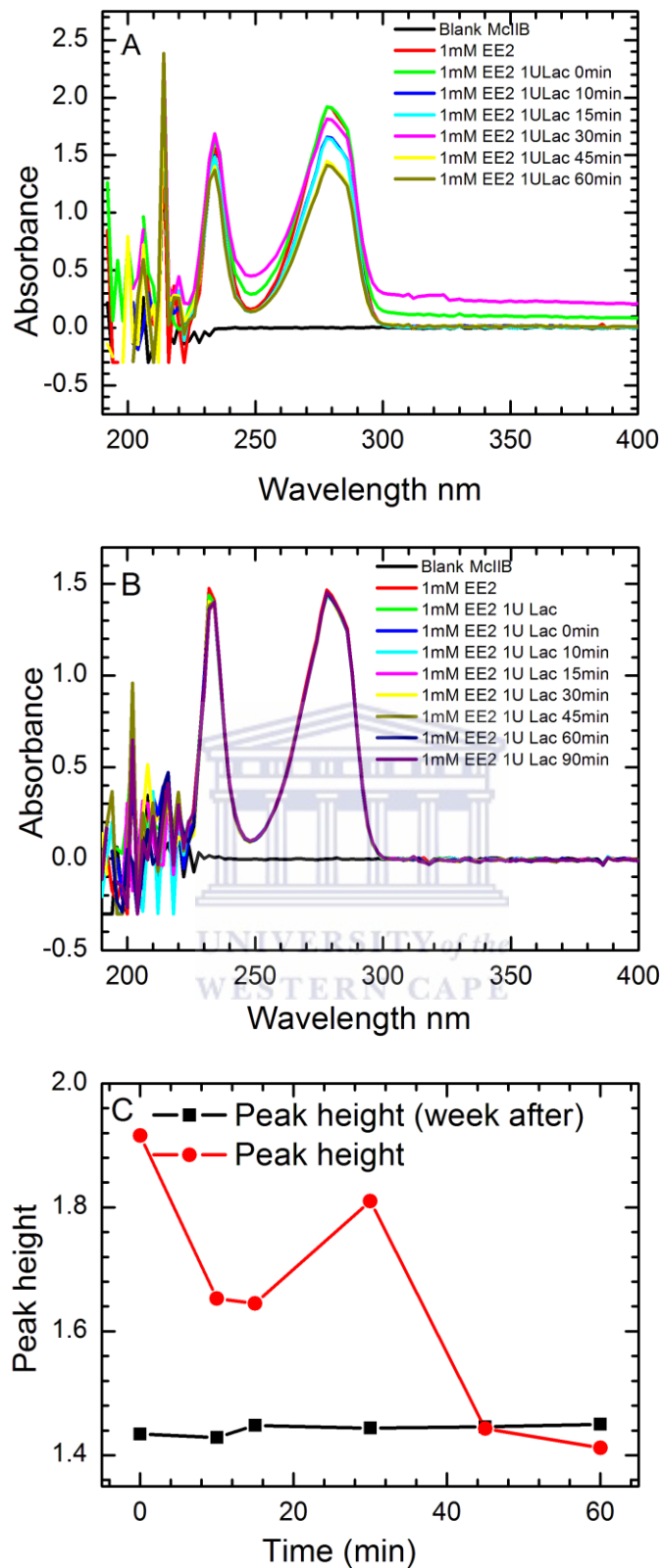


Figure 16: Time lapse UV/ Vis absorption spectra of EE2/ lac mixture in McIIB (pH 4.9): A) freshly prepared EE2 and two months old enzyme, B) one week old EE2 and freshly prepared laccase c) graph of peak height at $\lambda_{max} = 280$ nm vs time based on A and B.

5.1.1.5 Summary

The estrogens absorb at different wavelengths, from 197 nm to 293 nm with different peak intensities (absorbance). While each exhibited multiple UV/ Vis absorption peaks, they can be compared according to the most intense peak as follows: $I(E3, \lambda_{max} = 286) \approx A(E2, \lambda_{max} = 197) > A(EQ, \lambda_{max} = 284) \approx A(EE2, \lambda_{max} = 284) > A(E1, \lambda_{max} = 293)$. Each estrogen exhibited fluorescence when excited at $\lambda_{max} = 280$ nm, with intensities (I) increasing as follows: $I(EE2, \lambda_{max} = 304) \approx I(E3, \lambda_{max} = 318) > I(E2, \lambda_{max} = 305) \gg I(EQ, \lambda_{max} = 310, 362) \gg I(E1, \lambda_{max} = 309)$. EE2 was found to be irreversibly electroactive at the Au & GC electrodes, causing the passivation of both. At Pt electrode, EE2 appeared to adsorb without reaction. EE2 after a week of storage it degrade or it is no longer effective. Therefore every week new solution must be made. When checking the effect of storage for EE2, conclusion observed is that EE2 after a week of storage must not be used, because it is no longer effective. Decline on the figure 4, graph c) was observed when one week old EE2 was used and made. Therefore every week new solution of EE2 must be made.

5.1.2 Laccase

5.1.2.1 Purity and molecular weight of laccase

Electrophoretograms developed on a 10% SDS-PAGE are shown in Figure 17 for solutions of the commercial laccase used in this study in three media: pure water, phosphate buffer and ethanol. The gel revealed two bands or two components in each type of sample. The first band at approximately 97 kDa represented the major component. Hence, the molecular weight of the laccase used was 97 kDa. The second band around 55 kDa was due to a minor but significant component (about 20%), and showed that the supplied enzyme was not totally pure. The 55 kDa band also appeared even in an electrophoretogram developed with much less concentrated samples (data not shown), and the corresponding component could possibly

be because of a dislocated or de-constituted subunit of laccase or an residualy impurity. Confidently the first band belonged to laccase, since it appeared close to the 100 kDa molecular weight reported for this protein by other SDS-PAGE studies [49, 96-97].

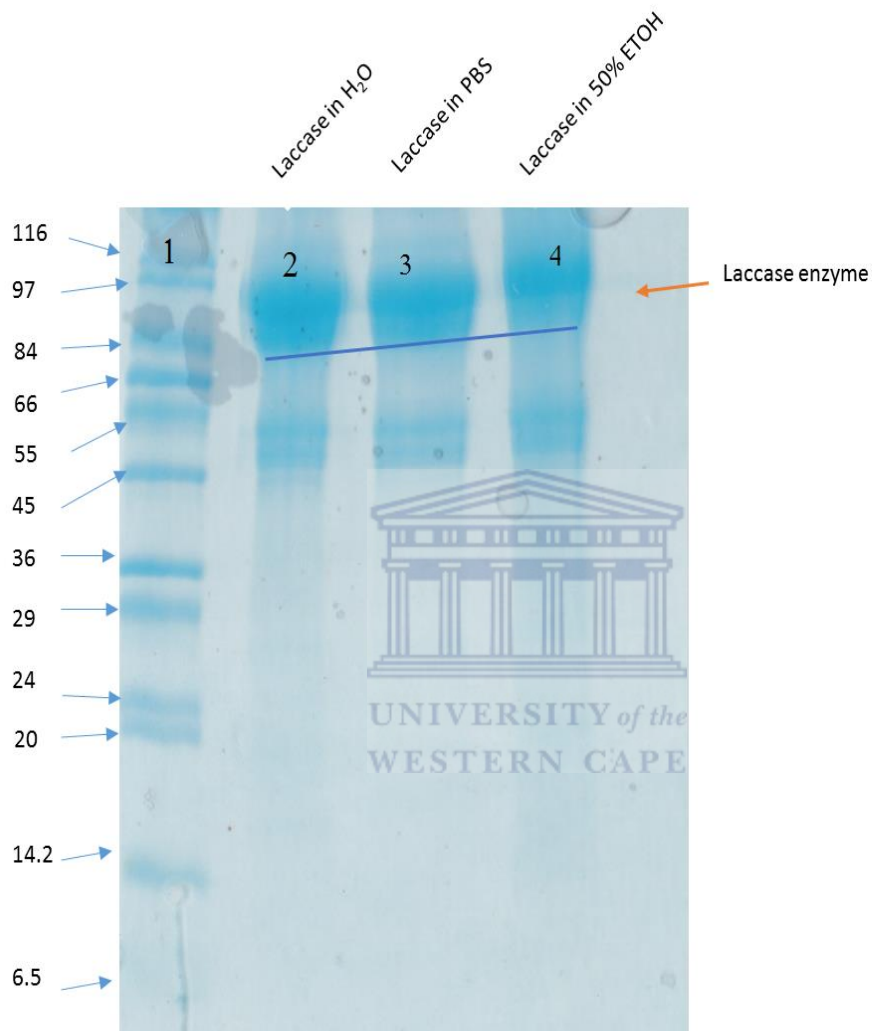


Figure 17: Electrophoretograms of laccase developed on a 10% SDS-PAGE gel: lane 1: 4 μ L of high range protein standard (marker size); lane 2: 12 μ L of 0.064 mM (6.3 mg/ mL) aq. laccase; lane 3: 12 μ L of 0.075 mM (7.53 mg/ mL) aq. laccase (phosphate buffer); lane 4: 12 μ L of 0.1 mM (10 mg/ mL) laccase in ethanol.

5.1.2.2 UV/ Vis Absorption Spectrum of Laccase in McIIB (pH 4.9)

Figure 18 shows UV/Vis absorption spectra of laccase with repeat measurements. Missing is the 604 nm absorption peak expected for a type 1 copper which gives rise to the typical blue color of the copper oxidases due to the reduction of the T_1 Cu^{2+} to Cu^+ [49]. Thus, the laccase used in this study was in its oxidised state. At around 330 nm, a shoulder was observed, representing type 3 copper which has 2 copper centres [49]. These are, however, electron paramagnetic resonance (EPR) silent due to an antiferromagnetic coupling mediated by ligand [98].

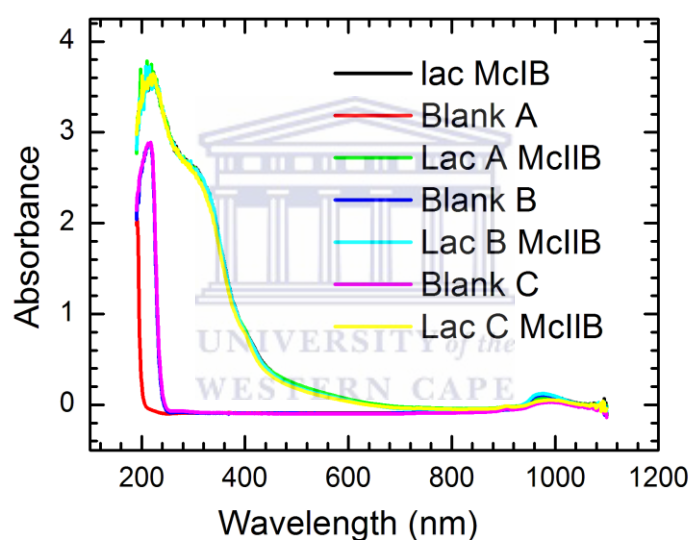


Fig. 18: UV/ Vis absorption spectrum of laccase (0.1 mM) in McIIB

5.1.2.3 Laccase Activity on EE2 in McIIB (pH 4.9) as monitored with UV/ Vis Absorption

Figure 19 shows time-lapse UV/ Vis absorption spectra of a mixture of laccase and EE2 at different intervals from 0 to 45 minutes. Before the addition of the enzyme, the EE2/ buffer solution two sharp peaks were observed about 232 nm and 280 nm. After introducing the enzyme, the intensity and width of the 280 nm peak started to increase with time showing the

occurrence of reaction. But spectra recorded on the 30th and 45th minutes did not show significant difference between them indicating the completion of the reaction, either because of over consumption of EE2 or the O₂ in the reaction medium. Slight shifts by about 1 or 2 nm in peak position was observed during the progress of the reaction, for instance 278 nm at 0 min, 280 nm in 15, 281 nm at 30 minutes. The above observation confirmed the enzyme used in this study was still active in general, and particularly towards EE2 and the buffer solution used was proved to be suitable.

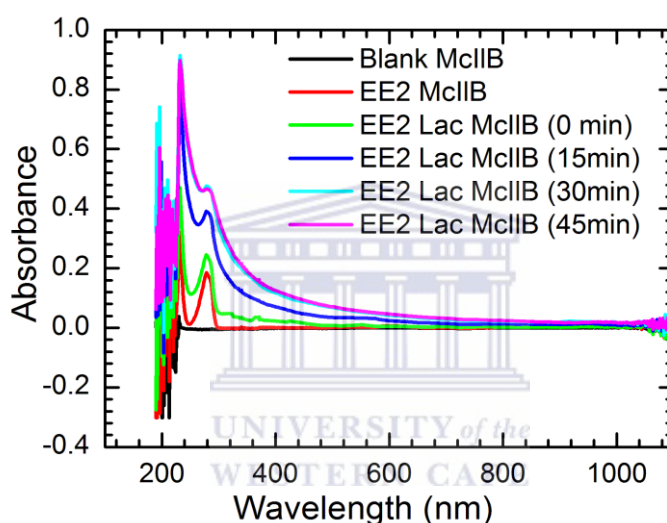


Figure 19: Time-laps UV/ Vis absorption spectra before and after addition of laccase (1 mM) to EE2 (1 mM) solution in McIlB (pH 4.9).

5.1.2.4 Laccase Activity on EE2 as Monitored with UV/ Vis Fluorescence

Figure 20 shows time-lapse UV/Vis fluorescence spectra a mixture of laccase (1 mM) and EE2 (1 mM) recorded from wavelength 295 nm to 545 nm at excitation $\lambda_{ex} = 280$ nm. No peak observed when only EE2 was added in McIlB. At 0 minute, there was a jump in the peak (high intensity) to $\lambda_{max} = 306$ nm observed due to the laccase added, catalysing the EE2. From 10 to 60 minutes $\lambda_{max} = 308$ nm was observed. Therefore as time elapsed, there was no

change on the peaks. Only after 0 min, a slight change of 2 nm was observed, due to the reaction stabilising. As the intensity at 10, 15 and 20 minutes nearly remains constant, this could be due to the reaction between the enzyme and the electrolyte stabilising. The change in peak intensity with time was not one directional and was unexplained, but the outcome of this experiment indeed confirmed the conclusion reached with UV/Vis absorption monitoring that the enzyme was active towards EE2 and the buffer solution to be used is suitable.

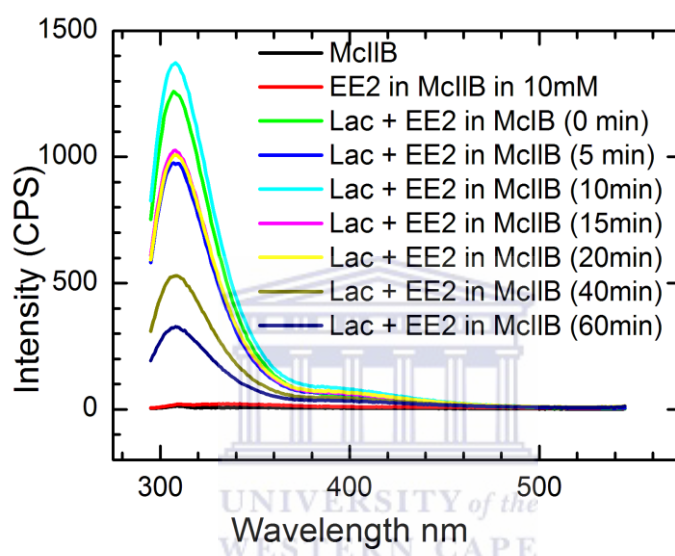


Fig. 20: Time-lapse UV/ Vis fluorescence spectra of before and after addition of laccase (0.01 mM) to a solution of EE2 (1 mM) in modified McIlB.

5.1.2.5 Electrochemical properties of laccase on GCE, AuE and PtE

Figure 21 shows CVs recorded at scan rates of 10 mV/s and 100 mV/s in the McIlvaine buffer for laccase films after drop-coating onto the surfaces of GC, Au and Pt electrodes. The CVs were run within the respective potential windows in order to test for the electrochemical activity of laccase. The potential window for GC electrode was from $E = 1.35$ to -1.4 V, for Au electrode from $E = 1.3$ to -0.8 V, and for Pt electrode $E = 1.4$ to -0.55 V.

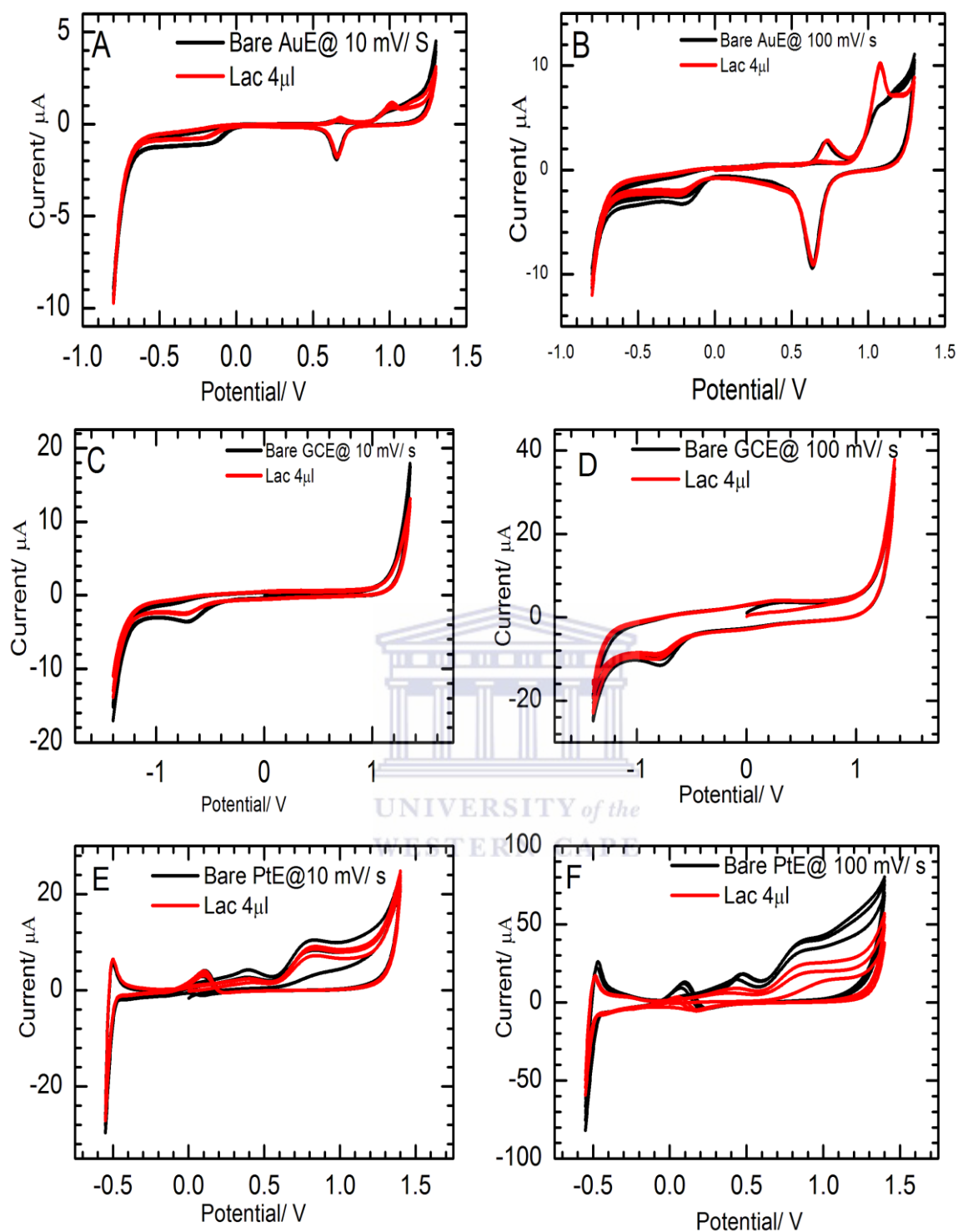


Figure 21: CVs of laccase films on Au, GC and Pt electrodes in McIIB at scan rates of 10 and 100 mV/ s. The films were cast by drop-coating 4 μL of 10 μM Lac/ McIIB solution and drying in air under a lamp for 15 minutes.

With the Au, comparison of the film's CV with the back ground CV of the electrode apparently indicated a new anodic peak about 1.2 V, but which might have also been a consequence of enhancement of the background situated at same potential. Thus further study is required to identify the origin of the new peak at this electrode. The enzyme definitely was not electrochemically active at both GC and Pt electrodes since there were no new peaks observed. Direct electron transfer between laccase and the electrode surface during CV is not observable [99]. Even the background peaks of Pt were suppressed indicating blockage of the surface with an insulating film. Thus, in this study the CVs did not show any voltammetric waves similar between 0.0 and +0.7 V range where redox reactions of blue copper proteins or multi-copper oxidases are reported to be occur [46]. This means that a direct electron transfer is not feasible between the electrode and laccase molecules.

5.1.2.6 Effect of storage on Laccase activity

Figures 22A to D show time-laps UV/ Vis absorption spectra recorded to check the effect of age on laccase activity towards EE2. Every time before measurement, the reaction mixture was centrifuged for about two minutes to remove the precipites formed due to the oxidation of EE2. Figure 22 A) shows the fresh enzyme's action on EE2 from 3 months old stock solution. EE2's absorption peak at 280 nm decreased as time passed but a rise in total absorbance was observed in the vicinity of this peak. Figure 22 B) shows when fresh EE2 was acted on by laccase from a seven weeks old stock solution. In this case the EE2 peak and the over all spetrum showed only slight changes as time elapsed. In Figure 22 C), which is for the reaction mixture composed of samples from one week old EE2 and a fresh enzyme, EE2 peaks showed a slight change and peaks were all absorbing at about the same wavelength 280 nm. Figure D), corresponding to the reaction mixture of fresh EE2 and one week old enzyme, showed positive results. Based on the above results, one may conclude that the enzyme can

be stored for a very long period of time, for more than three months and still be useful, showing the compatibility of the buffer chosen in this study.

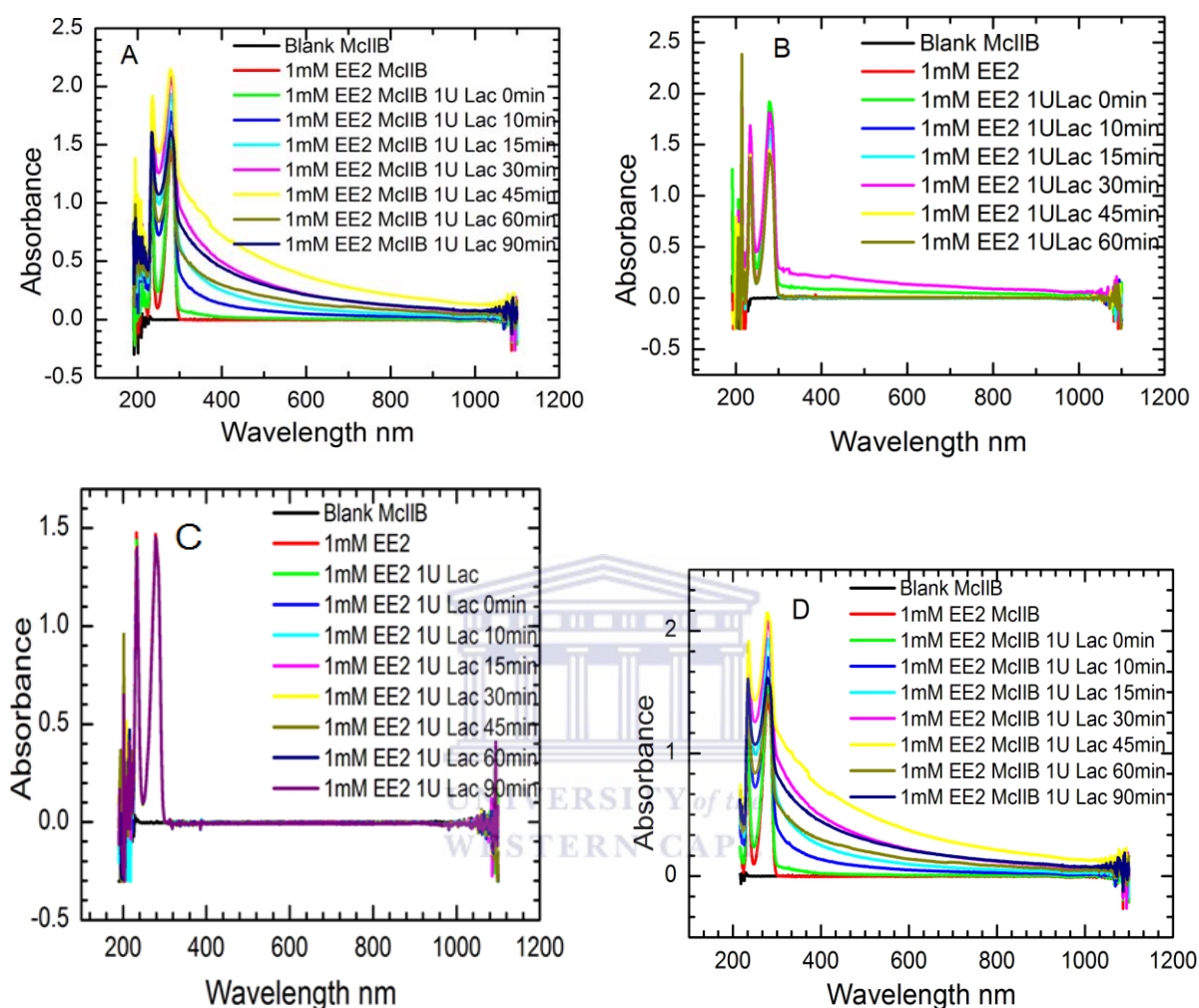
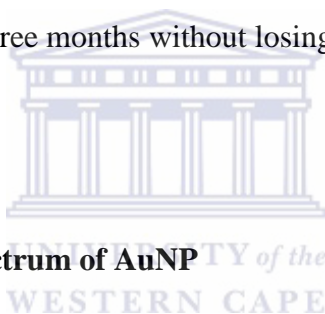


Figure 22: Time-laps UV/ Vis absorption spectra of reaction mixtures containing Laccase 1×10^{-3} mM (0.1 mg/ml) and EE2 (1 mM) from stock solutions of different ages in McIlB: A) fresh enzyme with 3 months old EE2, B) fresh EE2 with seven weeks old laccase), C) one week old EE2 with fresh laccase, and D) fresh EE2 with one week old enzyme

5.1.2.7 Section Summary

Molecular weight of laccase used in this study was successfully identified at 97 kDa. The gel revealed two bands, first band revealed molecular weight of laccase at 97 kDa and the second band around 55 kDa due to some components, and this proved the enzyme was not totally

pure. The UV/ Vis absorption spectrum of the enzyme was characterized by absence of the absorption spectra at 640 nm, thus it is in its oxidised state. When checking the activity of laccase towards EE2, results obtained show that enzyme was active towards EE2 and the buffer solution used was proved to be suitable. UV/ Vis fluorescence spectra at λ_{ex} of 280 nm showed the estrogens dominantly fluorescence at similar wavelength and that laccase solution is active towards EE2 and the buffer solution to be used is suitable. Drop-coated laccase on GC, Au and Pt electrodes when checking the electrochemical properties of the enzyme, the enzyme definitely was not electrochemically active at both GC and Pt electrodes since there were no new peaks observed. On the Au electrodes anodic peaks observed. Storage of laccase as it was observed over three months showed that the enzyme could be stored in the refrigerator for over a period of three months without losing its activity.



5.1.3 Gold Nanoparticles

5.1.3.1 UV/ Vis Absorption Spectrum of AuNP

Gold nanoparticles were obtained successfully as can be inferred from characteristic sharp absorption peak observed at 525 nm in Figure 23 A and B for the prepared stock solution, both before and after dilution. The energy of the absorbed light and hence the energy difference between the ground and excited states of the gold nanoparticles interpolated from this absorption band was found to be 3.78×10^{-19} J based on Planks Law equation:

$$\Delta E = h\nu = h \left(\frac{c}{\lambda_{\max}} \right) \text{ [100]}. \text{ This amounts to a band gap of 2.36 eV per average particle.}$$

The particle size of the gold nanoparticles was estimated using the effective mass approximation model [100]:

$$E_g = \frac{h^2}{8a^2} \left(\frac{1}{m_e} + \frac{1}{m_h} \right)$$

Where E_g is the band gap (eV), a is the particle size, $h = 6.626 \times 10^{-34}$ J s (Plank's constant, m_e is the mass of an electron = $0.17 m_o$, m_h is mass of the hole = $1.44 m_o$ ($m_o = 9.1095 \times 10^{-31}$ kg, is the mass of a stationary electron) [100]. The size of gold nanoparticles estimated using the above equation was found to be 1.7 nm

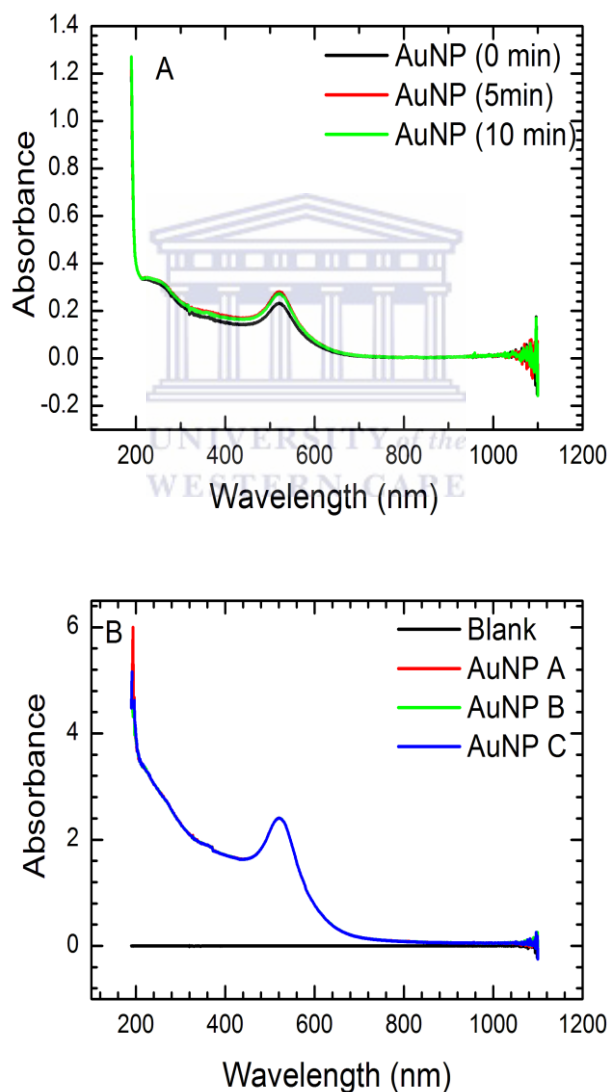


Figure 23: UV/ Vis absorption spectra of the Au nanoparticles solution used in this study: (A) after 1:10 dilution of the stock solution (repeat scans); (B) undiluted AuNP showing the typical absorption maximum at 525 nm.

5.1.3.2 TEM, SAED, EDX images and Size Distribution of AuNP

The gold nanoparticles were further characterized using transmission electron microscopy (TEM) to determine the size of gold nanoparticles. Figure 24 shows the TEM images of AuNP to have different shapes like round, spherical and rod. These nanoparticles are polydispersed. For particles that are disperse, a size distribution can be easily obtained by measuring each particle diameter at a fixed angle. The random orientation of particles allows for a statistical measure of the size distribution to be generated. The size of gold nanoparticles in percentage form is shown in Figure 24, which shows the size distribution of gold nanoparticles.

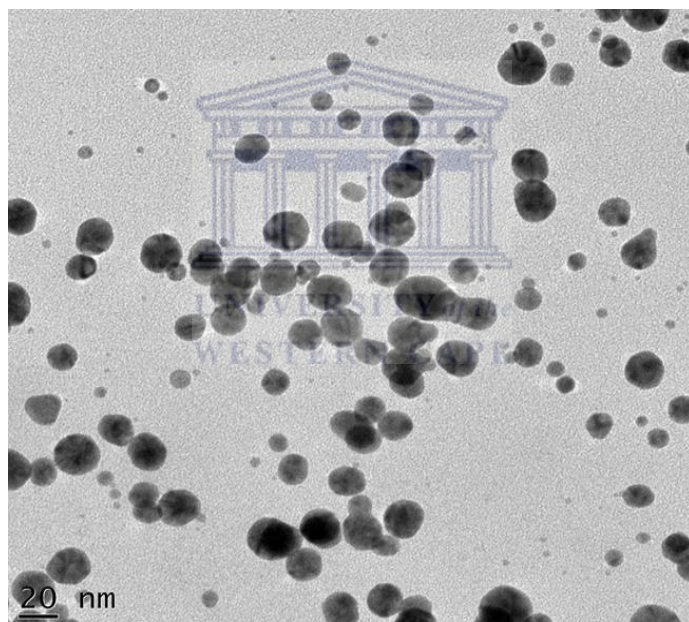


Figure 24: HR-TEM images of the gold nanoparticles

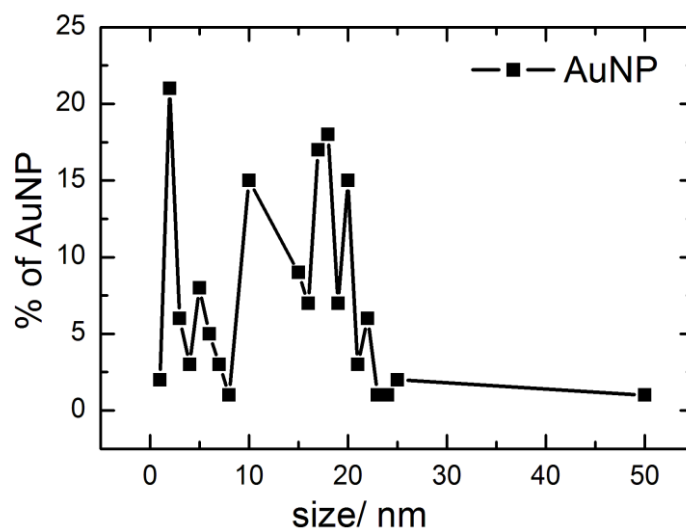


Figure 25: Graph showing size distribution of the gold nanoparticles used in the study

Figure 25 shows the size of AuNPs, estimated to be around 55% (15-22nm), 65% (10-22nm) and 30% (2-7nm). They are more scattered at these places. Graph represents the AuNP size distribution histogram, confirming the percentage of the nanoparticles. Figure 26; shows the EDX spectrum of AuNP which shows the presence of Au (due to gold chloride), oxygen and high levels of copper (which is due to the copper grid). High resolution of a single nanoparticle is shown in b) with a size of 5 nm.

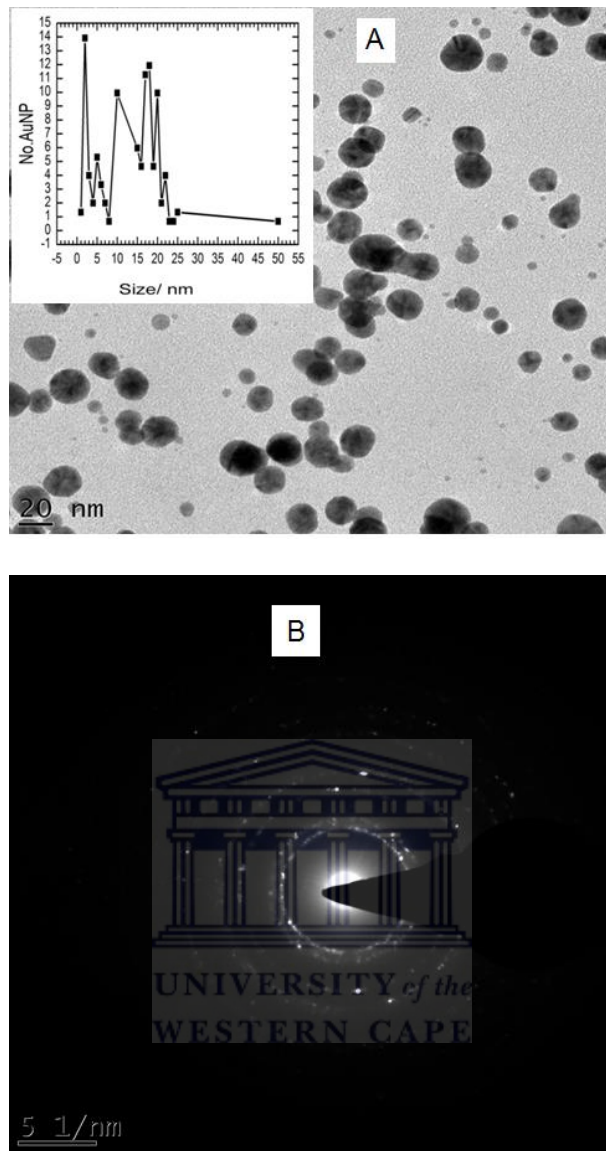


Figure 26: (A) HR-TEM images of the AuNPs (inset: size distribution histogram); (B) SAED pattern.

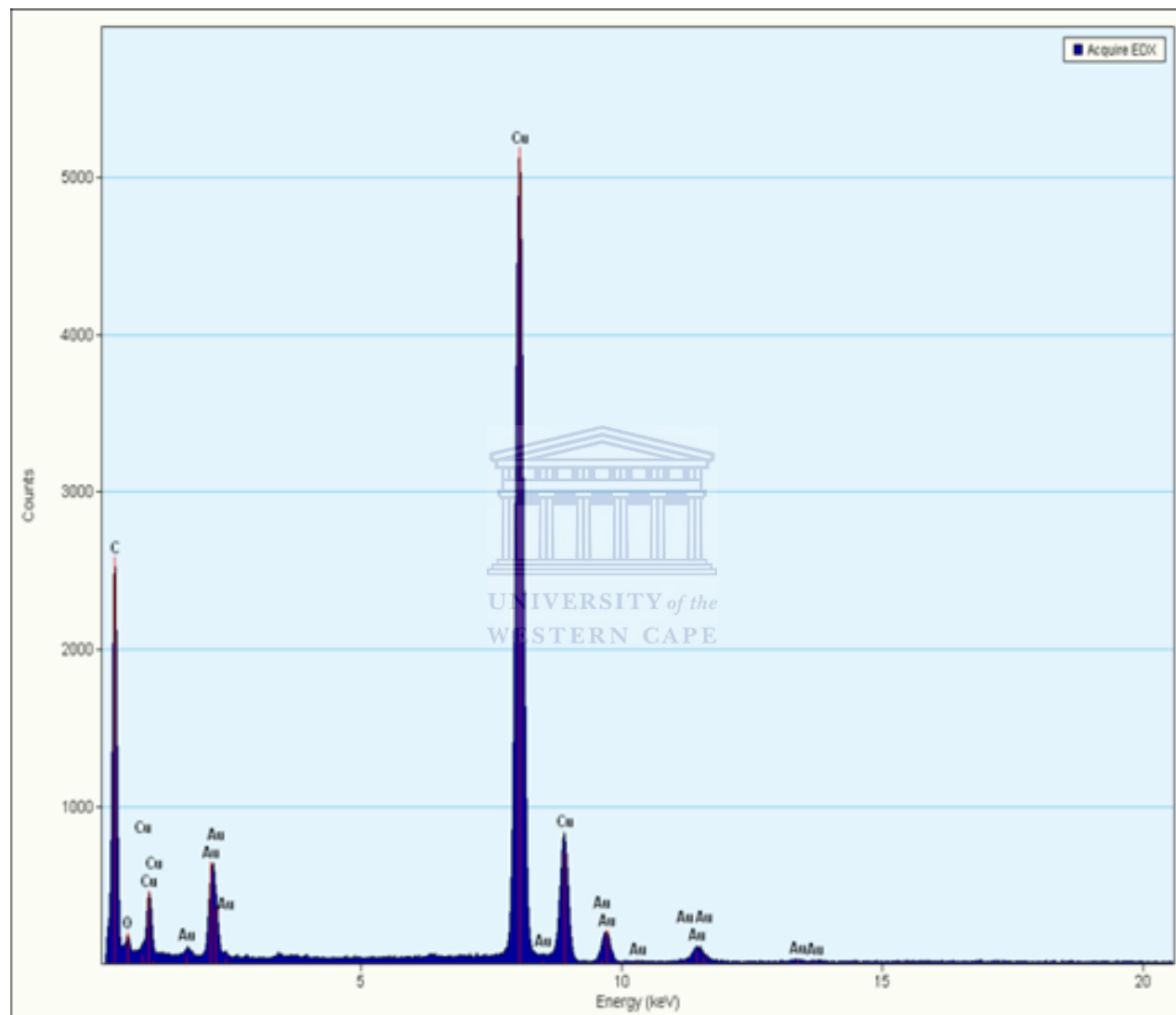
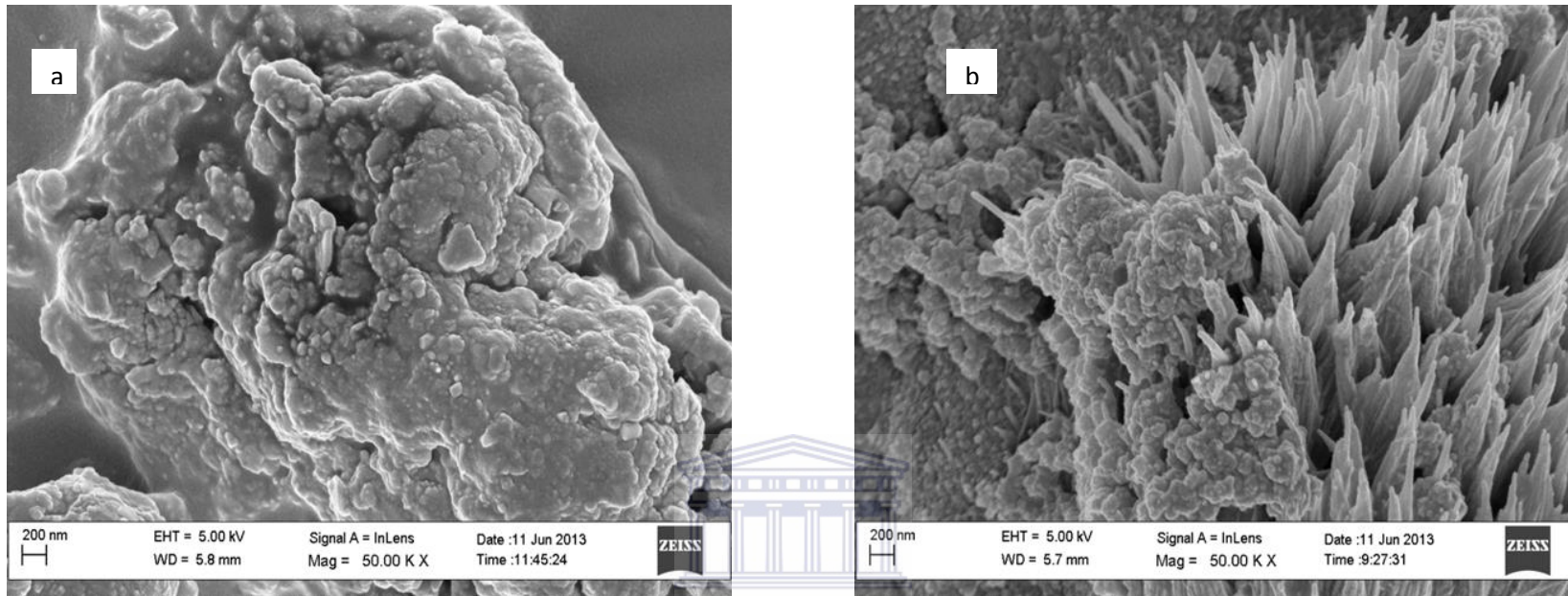


Figure 27: EDX spectrum of AuNP



UNIVERSITY of the
WESTERN CAPE

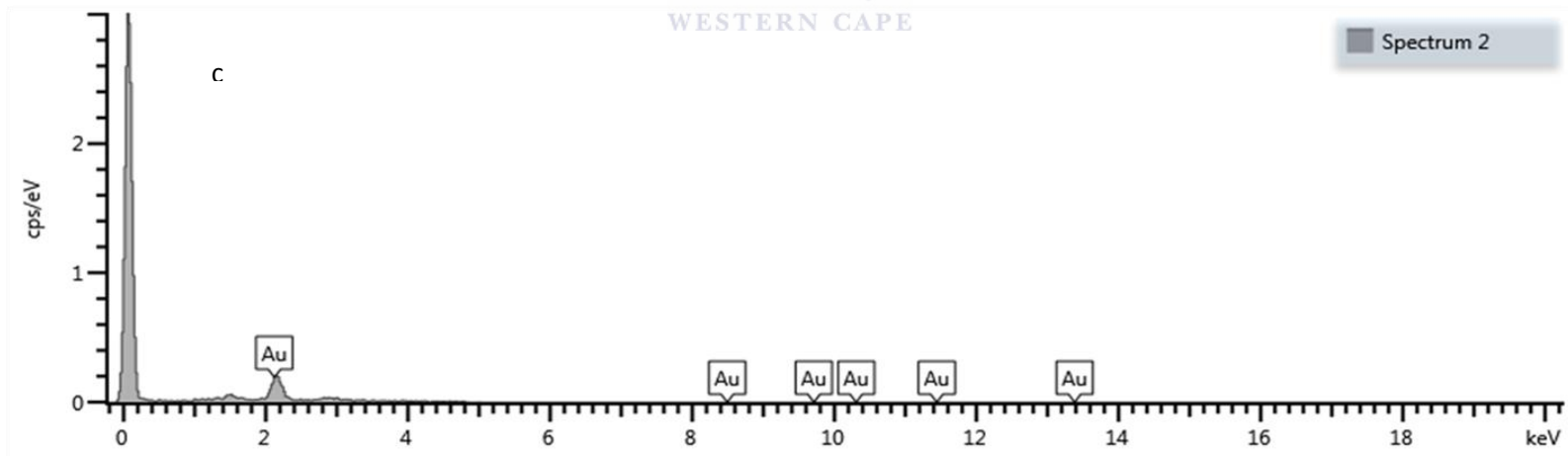


Figure 28: a) SEM images gold nanoparticle b) Laccase at 200 nm and c) EDX

Figure 27 shows EDX analysis revealed the elemental composition of the synthesized AuNP. the presence of Au (due to gold chloride), oxygen and high levels of copper which is due to the copper grid used as a TEM tray for gold nanoparticles. There is a small amount of oxygen appearing which is due to the presence of citrate in AuNP.

5.1.3.3 SEM image of gold nanoparticles, laccase and AuNP-laccase

Figure 28 shows the SEM image of gold nanoparticles in a) has shown the nanoparticles to be clustered together or is showing a particle agglomeration. This could be due to the number of reasons, could be contamination or due to the liquid used instead of solid. In b) the SEM image of laccase shows a flower more like image. The EDX has shown the presence of gold, which is due to the gold chloride used.

5.1.3.4 TEM images of Laccase, and AuNP-Laccase

Figure 29 revealed the TEM image of laccase shown doesn't show a good appearance and also the shape is not clearly visible. When laccase is mixed with gold nanoparticles, there is a visibility of gold nanoparticles and laccase appears to be clustered. The EDX of laccase and gold nanoparticles shows the presence of gold which is due to the gold chloride present in the gold nanoparticles. The EDS of Lac+AuNP- shows the presence of oxygen, nickel (due to nickel grid) carbon, sodium, and sulfur, which is due to the ethanol and the buffer used to dilute the sample.

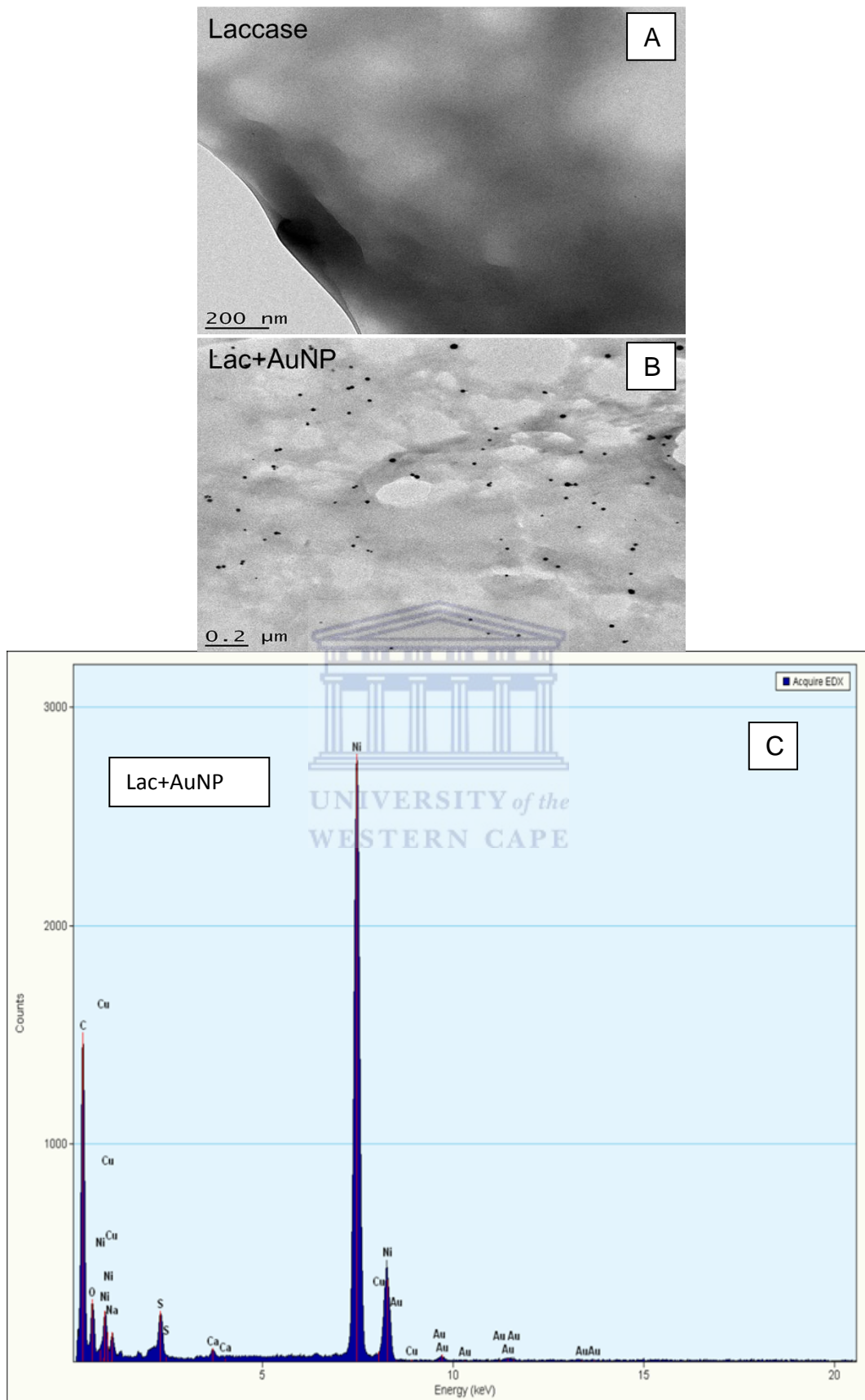


Figure 29: TEM images of laccase, (laccase + AuNP) mixture, and EDS of (laccase + AuNP)

5.1.3.5 Electroactivity of AuNP films

Figure 30 shows CVs recorded at scan rates of 10 mV/ s in the McIIB for AuNP after drop-nanoparticles after drop-coating onto the surface the GC electrode. The CVs were run within the full potential windows in order to test for the electrochemical activity of nanoparticles. Thus, in this study the CVs did not show any presence of two anodic peaks at 1.13 and 1.33 V associated with Au oxides and the cathodic peak at 0.89 V were not observed which are reported to occur [101]. The result indicates the nanoparticles were definitely not electroactive in the medium chosen for this study.

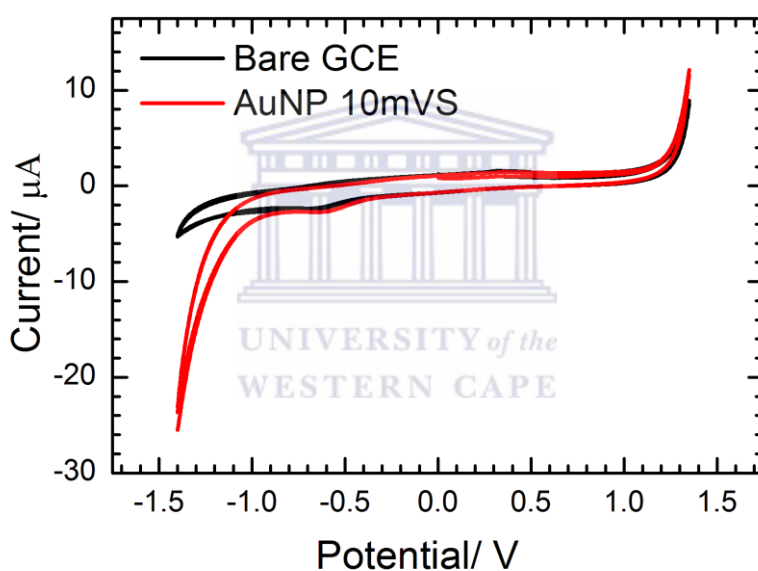


Figure 30: CV of drop coated AuNP in McIIB at 10 mV/ s

5.1.3.6 Summary

AuNPs were successfully synthesized and the size was shown to range from 2-22 nm. It was also shown to absorb at 525 nm in the UV/ Vis range. The SEM images were not successful because of aggregation of the nanoparticles. EDX showed the presence of gold, resulting from gold chloride. HRTEM images of laccase, laccase and Au nanoparticles; the shape was not clearly visible. When laccase is mixed with gold nanoparticles, there is a visibility of gold

nanoparticles and laccase appears to be clustered. Electroactivity of Au nanoparticles on CV did not show any presence of peaks, which this result indicate that nanoparticles were not electroactive in the buffer chosen for this study.

5.1.4 Polyaniline/ Polystyrene Sulfonic Acid Composite Films

5.1.4.1 Electro-co-polymerization and CV Characterization in Aq. HCl

Figure 31 shows a typical ten-cycle electropolymerization CV of aniline on the GCE in aq. HCl (1000 mM) at scan rate 50 mV/ s in the presence of PSSA (25 mM). The scan range was from $E = -0.2$ to 1.1 V. On this graph redox peaks (the anodic and cathodic peaks) which increased with cycle number were observed confirming the deposition of a conducting film.

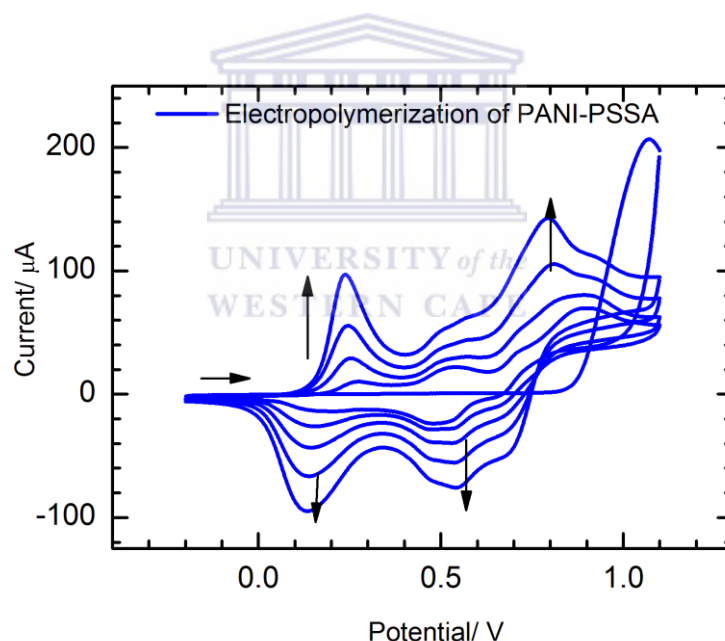


Figure 31: Electropolymerization CV (10 cycles at 50 mV/ s) of Aniline (50 mM) on GCE in presence of PSSA (25 mM) in aq. HCl (1 M). $E_{in} = -0.2$, $E_{high} = 1.1$ V, and $E_{final} = -0.2$ V

Figure 32 shows the post-polymerization, three-cycle CV of GCE/PANI-PSSA in fresh portion of aq. 1M HCl at scan rate of 50 mV/ s. The CV was run within the same respective potential window was from $E = -0.4$ to 1.1 V. The first pair of redox peaks in the more cathodic region is due to the interconversion of leucoemeraldine and emeraldine salt

(emeraldine radical cation) forms of the deposited PANI film [102] second pair which was observed in the anodic extreme region of the scan range is due to the interconversion between its emeraldine salt and the pernigraniline forms [102]. The peaks were shifting towards each other and at same time decreasing in height as the number of cycles increased. Thus, the CV of fresh GCE/PANI-PSSA was not stable in the aq. HCl medium.

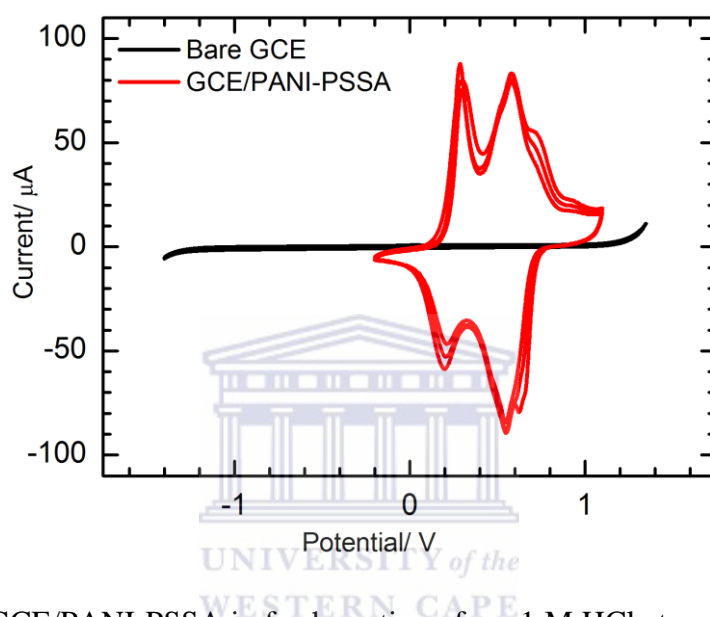


Figure 32: CV of GCE/PANI-PSSA in fresh portion of aq. 1 M HCl at scan rate of 50 mV/ s. $E_{in} = -0.2$, $E_{high} = 1.1$ V, and $E_{final} = -0.2$ V.

5.1.4.2 Electropolymerization and CV Characterization in Aq. H_3PO_4

Electropolymerisation of aniline on GCE in aq. phosphoric acid (1000 mM) was carried out potentiodynamically at the scan rate of 50 mV/ s for 10 cycles as shown in Figure 33. This resulted in a green emeraldine film on the electrode surface. The polymerisation reaction was started by the formation of resonance-stabilised aniline radical cations from the protonated aniline monomer. As the number of cycles increased the new peaks which appeared in the CV kept increasing confirming that a conductive polymer was deposited. The increase in peak heights also indicated the thickness of the polymer increased with successive potential cycles [103]. On this graph the redox peaks were observed (the anodic and cathodic peaks).

The appearance of the first anodic peak observed during all cycles was due to leucoemeraldine form of PANI being oxidized into its emeraldine or emeraldine radical cation form [103]. The second one was due to further oxidation of the polymer film into its pernigraniline form [103]. H_3PO_4 was used for electropolymerization because it has the same ions as the McIIB, which could lead to the high chance of electrochemical activity.

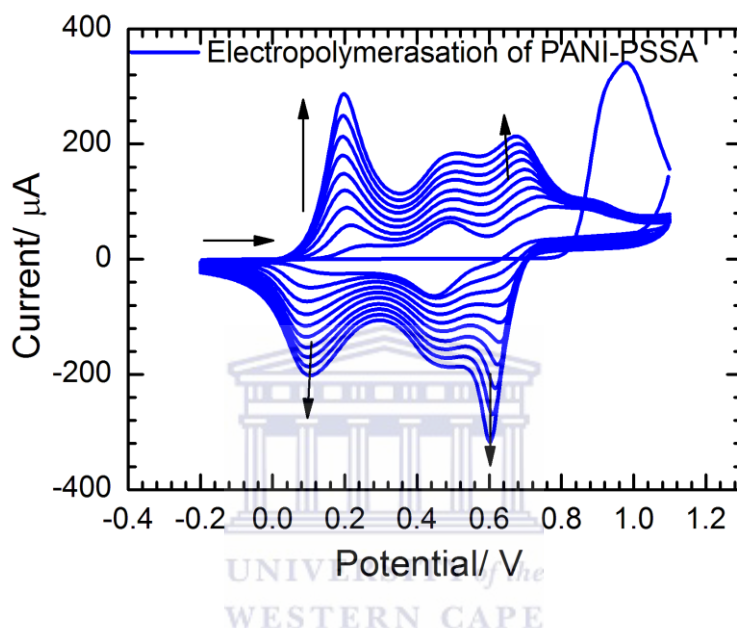


Figure 33: Electropolymerization CV (10 cycles at 50 mV/ s) of Aniline (50 mM) on GCE in presence of PSSA (25 mM) in aq. H_3PO_4 (1 M). $E_{in} = -0.2$ V, $E_{high} = 1.1$ V, and $E_{final} = -0.2$ V

Figure 34 shows post-deposition CVs of the PANI/PSSA film in fresh portion of aq. H_3PO_4 (1000 mM) at scan rates of 50 mV/ s within the potential range $E = 0.9$ to -0.4 V. This potential range was chosen because the film exhibited a very stable in CV as can be inferred from the overlaid 10-cycles and 3 cycle CVs. Therefore, proceedings to the next stage could be permitted. Every newly electropolymerized films was first tested likewise before employment in the McIIB.

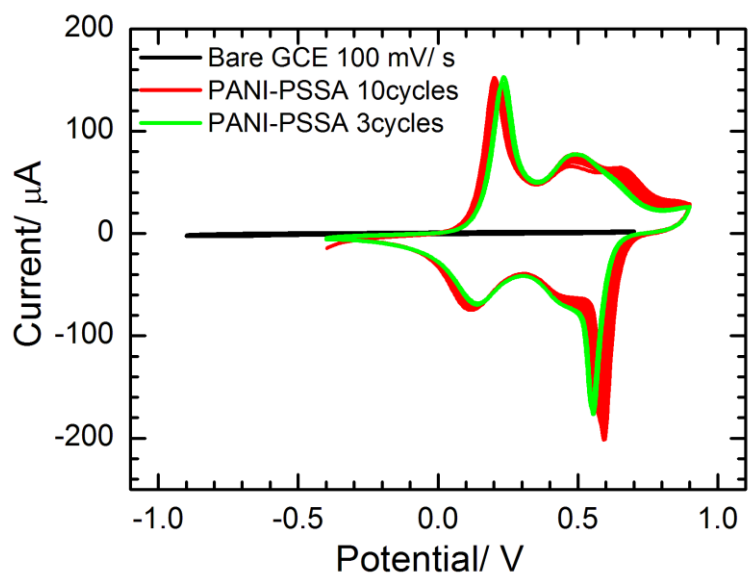


Figure 34: CV of GC/PANI/PSSA film in aq. H_3PO_4 (1000 mM) overlaid with the background CV of GCE. $E_{in} = -0.4$, $E_{high} = 0.9$ V, and $E_{final} = -0.4$ V

5.1.4.3 CV Characterization of GC/PANI-PSSA in McIlB

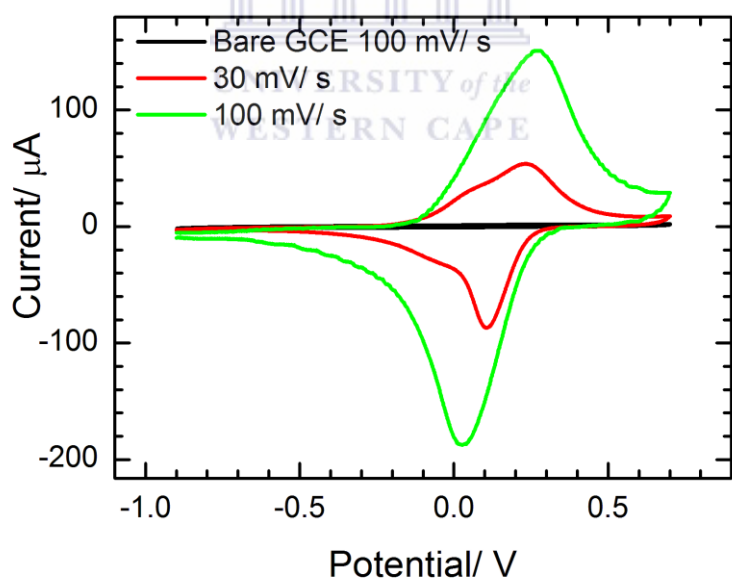


Figure 35: Overlay of three-cycle CVs of GC/PANI/PSSA film in McIlB (1 M). $E_{in} = -1$, $E_{high} = 0.7$ V, and $E_{final} = -1$ V

Figure 35 shows overlay of three-cycle CVs of PANI-PSSA recorded at 30 mV/ s and 100 mV/ s and background CV in the McIlB at scan rate of 100 mV/ s in the range $E = 0.7$ to -1

V. This range was chosen because it resulted in stable peaks. This way, the film was stable even under continuous operation; therefore the platform could be used for the biosensor.

5.1.4.4 Electroactivity of EE2 at GC/ PANI-PSSA

Figure 36 shows CV recorded with GC/PANI-PSSA at scan rate of 100 mV/ s in McIlB in the absence (Red curve) and presence (green curve) of dissolved EE2 (1 mM). CV of bare GC in the absence of EE2 (black curve) is shown for its own sake. For the GC/PANI-PSSA, a decrease in the anodic and cathodic peaks was observed on addition of the estrogen. A slight peak potential shift to the left was also observed. This could be because of its adsorption onto the surface of film with consequent passivation of some of the latter's electroactive sites. Otherwise there was no indication of any electroactivity of EE2 on GC/PANI-PSSA surface or platform.

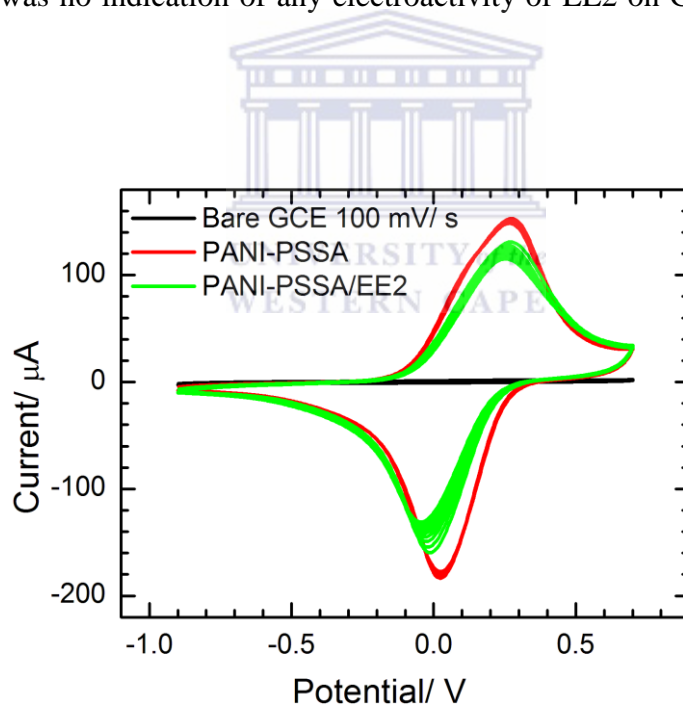


Figure 36: CV of GC/PANI-PSSA in McIlB without (red) and with (green) dissolved EE2 (1 mM). Scan rate: 100 mV/ s. $E_{in} = -1$, $E_{high} = 0.7$ V, and $E_{final} = -1$ V

5.1.4.5 Electroactivity of Dissolved Laccase on GC/ PANI-PSSA in McIIB

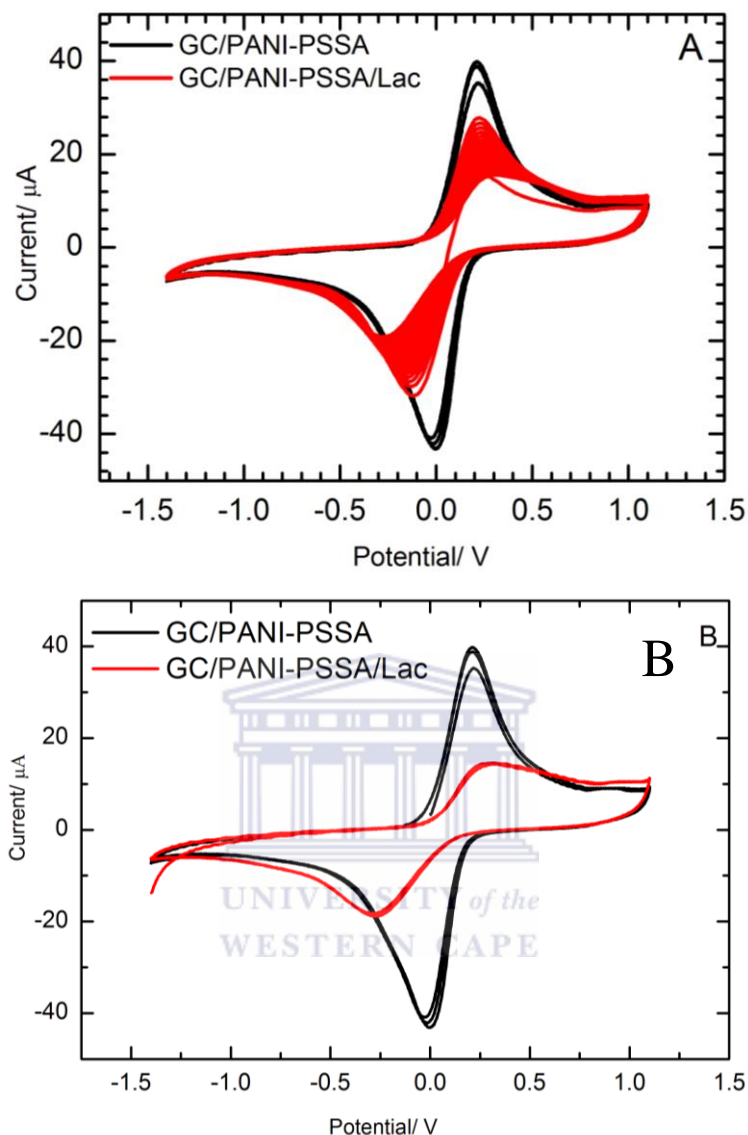


Figure 37: CVs of GC/PANI-PSSA at a scan rate of 100 mV/ s in McIIB before (black) and after (after) addition of laccase (1 mM). The CV was first run for 20 cycles and then for 3. $E_{initial} = -1.4$ V, $E_{high} = 1.35$ V, $E_{final} = -1.4$ V.

Figure 37 shows CV recorded with GCE/ PANI-PSSA at scan rate of 100 mV/ s in McIIB before (black) and after (red) adding Laccase (1 mM). The scan range was from $E = -1.4$ V to 1.35 V. The peak currents which were initially steady in the absence of EE2, started to gradually decrease and shift more negative potentials with subsequent scans once the laccase was added in the buffer. The shift in peak potential was particularly very significant for the

cathodic peak. The result showed the enzyme was adsorbed onto the GCE/ PANI-PSSA platform, but there was no any indication that the former was electrochemically active. Hence forward the resulting laccase-modified platform will be referred to as GC/PANI-PSSA/Lac. However, this approach for immobilizing the enzyme was not used in subsequent experiments in favour of the drop-coating method for economic reasons.

5.1.4.6 Electroactivity of Drop-Coated Laccase on GC/ PANI-PSSA in McIlB under Aerobic and Non-aerobic conditions

GC/PANI-PSSA/Lac was prepared by drop-coating 4 μL of laccase (0.1 mM) and run in McIlB as already described in the experimental section. Figure 38A and B are respectively overlays of multi-cyclic CVs recorded at the scan rate of 100 mV/ s between $E = 0.7$ to -0.1 V in the presence (A) and absence (B) of oxygen in the buffer to compare their electrochemical activities and responses to EE2. In the presence of oxygen (Figure 38 A), the GC/PANI-PSSA/Lac exhibited similar peak potential as GC/PANI-PSSA but an apparently higher cathodic peak current than the latter. In contrast, the differences between the peak currents and potentials of the anodic peaks of the two were not significant. Furthermore the CV of GC/PANI-PSSA/Lac was steady with cycle number. This result implies, the laccase was apparently reduced electrochemically, and then regenerated back to its oxidised normal state by chemical re-oxidation with O_2 . This conjecture is supported with result found in the absence of oxygen (Figure 38 B), because this time the GC/PANI-PSSA/Lac exhibited a slightly lower cathodic current than the GC/PANI-PSSA, but still similar anodic peak characteristics were exhibited by both. This is in accordance with literature that laccase needs oxygen [48]

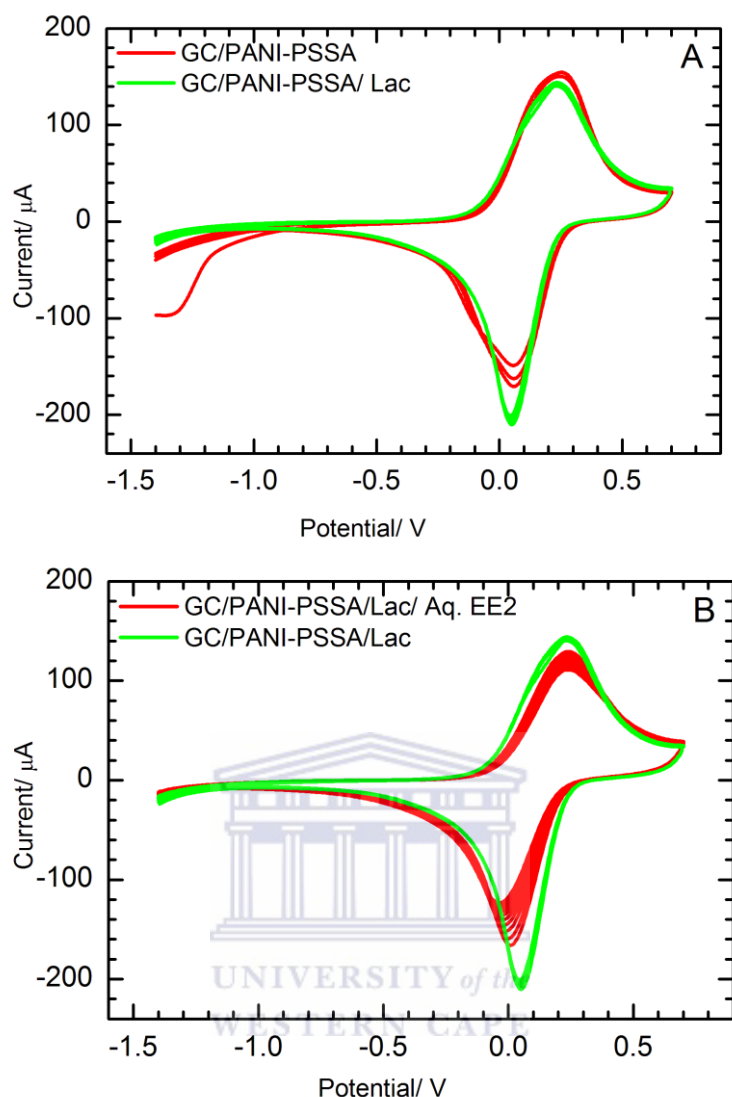
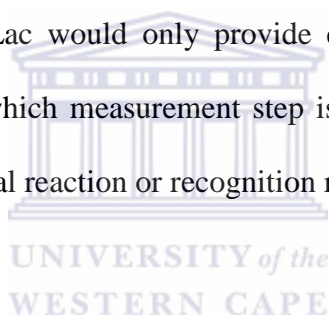


Figure 38: CVs of GC/PANI-PSSA and GC/PANI-PSSA/Lac: A) with oxygen and B) without oxygen in the McIIB. The respective curves before addition of EE2 have been shown in black and green while those after addition of EE2 (1 mM) in red and blue. Scan rate = 100 mV/ s. $E = 0.7$ to -1 V

5.1.4.7 Response of GC/PANI-PSSA/Lac to EE2 in McIIB under Aerobic and non-Aerobic Conditions

The response of GC/PANI-PSSA/Lac and GC/PANI-PSSA to EE2 in the buffer were also compared under both anaerobic (no O_2) and aerobic (O_2) conditions. The respective curves before addition of EE2 have been shown in Figure 38A and B in black (A) and green (B)

while those after its addition (1 mM) in red (A) and blue (B). As can be seen from these multi-cycle CVs, a significant and continuous decrease in cathodic peak current followed the addition of the estrogen in the presence of O₂ whereas in the absence of O₂, the change was slight and slow with increasing cycle number or time. The same was true regarding the anodic peak potential, which shifted concomitantly towards more cathodic values faster in the presence of O₂. These contrasting observations about GC/PANI-PSSA/Lac and GC/PANI-PSSA could be explained by considering the oxidative polymerization of EE2 catalyzed by laccase in the presence O₂, resulting in the deposition of an electroinactive polyphenol [34] which in turn changed the dynamics of the electrochemistry of the polymer. This could not occur in the absence of O₂. However, the non-steadiness of the CV in the presence of EE2 indicated that GC/PANI-PSSA/Lac would only provide constant signal-outputs only in a medium-exchange approach in which measurement step is carried out ex-situ in a medium different from that of the analytical reaction or recognition reaction.



5.1.4.8 Summary

Electropolymerization of aniline in HCl, the redox peak was observed (the anodic and cathodic peak) increasing with cycle number confirming the deposition of a conducting film. During the post-polymerization CV, the peaks were shifting towards each other, at same time decreasing in height as the number of cycles increased and CV showing fresh GCE/PANI-PSSA was not stable in the aq. HCl medium. During the electropolymerization of aniline in H₃PO₄, the anodic and cathodic peak was observed as expected. As the number of cycles increased, new peaks increased confirming the conductive polymer was deposited. H₃PO₄ was used for electropolymerization because it has ions as the McIIB which could lead to the high chance of electrochemical activity. Thus shows that electro-polymerization in H₃PO₄ was more suitable as compared to HCl. CV characterisation of PANI gave permission to proceed to the next stage, as stable CV was observed. When characterising PANI, the film

was found to be stable, therefore the platform could be used for biosensor. For the GC/PANI-PSSA, a decrease in the anodic and cathodic peak was observed and there was no indication of the electroactivity of EE2 on GC/PANI-PSSA surface. When the enzyme was dissolved in McIlB, the enzyme was adsorbed onto the GC/PANI-PSSA platform and no indication of the former was electrochemically active. When laccase was drop-coated on GC/PANI-PSSA in McIlB in the presence of EE2 exhibited similar peak potential with the one with absence of oxygen, but higher cathodic peak was observed in the presence of oxygen. Therefore this implies that the laccase was reduced and then regenerated back to its oxidised normal state.

5.2 Cyclic Voltammetric Amperometric Laccase Biosensor Studies

5.2.1 Response of GC/PANI-PSSA to EE2 as a Sensor

Figure 39 shows CVs of GC/PANI-PSSA recorded at scan rate of 25 mV/s from $E = -1$ to 0.7 V during eight sequential, medium-exchange-based batch measurements with a single GC/PANI-PSSA in order to obtain information on its background response and reproducibility before and after exposure to aq. EE2 (1 mM) in the McIlB. The sequence of measurements involved 1) dip in water for 60 s as a blank, 2) record CV in McIlB (water 1), 3) dip for 60 s in the aq. EE2 sample, 4) a gentle rinsing with water to remove excess EE2 molecules and loosely adhering deposits, 5) record CV in buffer, and 6) thoroughly rinse with water to regenerate surface to scrub off possible deposit. Steps 1 to 6 which constituted one experimental cycle were repeated all over again for four times. The resulting CVs have been shown overlaid in Figure 39 indicated as water 1, 2, 3, and 4 and EE2 1, 2, 3, and 4 in chronological order. According to Figure 39, there was no difference between the CV of GC/PANI-PSSA after dipping water and that after dipping in aq. EE2 solution. Therefore this shows that, in batch medium exchange mode, the background CV characteristics of GC/PANI-PSSA platform is robustly unaffected by exposure to EE2 as well as by repeated thorough

rinsing. Hence the platform is by itself re-usable, and could serve as stable immobilizing platform in laccase biosensor which is the main subject of the following sections.

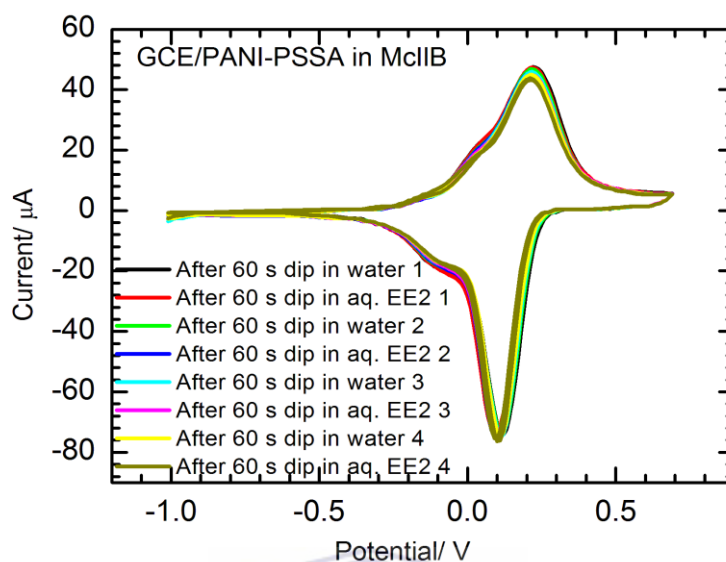


Figure 39: Set of CVs of GC/PANI-PSSA recorded at 25 mV/ s in McIIB before and after a 60 s dip in water blank or in aq. EE2 (1 mM) for four successively repeated experiments. $E_{in} = -1$ V, $E_{high} = 0.7$ V, and $E_{final} = -1$ V

5.2.2 Response of PANI-PSSA/Lac/Glu to EE2

The resulting CVs have been shown overlaid in Figure 40B indicated as water 1, 2, 3, and 4 and EE2 1, 2, 3, and 4 in chronological order. Unlike GC/PANI-PSSA, here slight differences were observed between CVs recorded after dipping the GC/PANI-PSSA/Lac/Glu in water and those after dipping it in aq. EE2 sample. The latter always reduced the cathodic peak current and shifted the cathodic peak potential to more negative values, whereas each time the biosensor was washed thoroughly with water these effects of EE2 were slightly reversed as can be seen from the CV recorded after dipping in water-blank. This is a promising observation leading to a re-usable and fast response-time laccase biosensor for EE2 and other

water estrogens. The biosensor's sensitivity should be improved in future works by optimizing its configuration and working conditions.

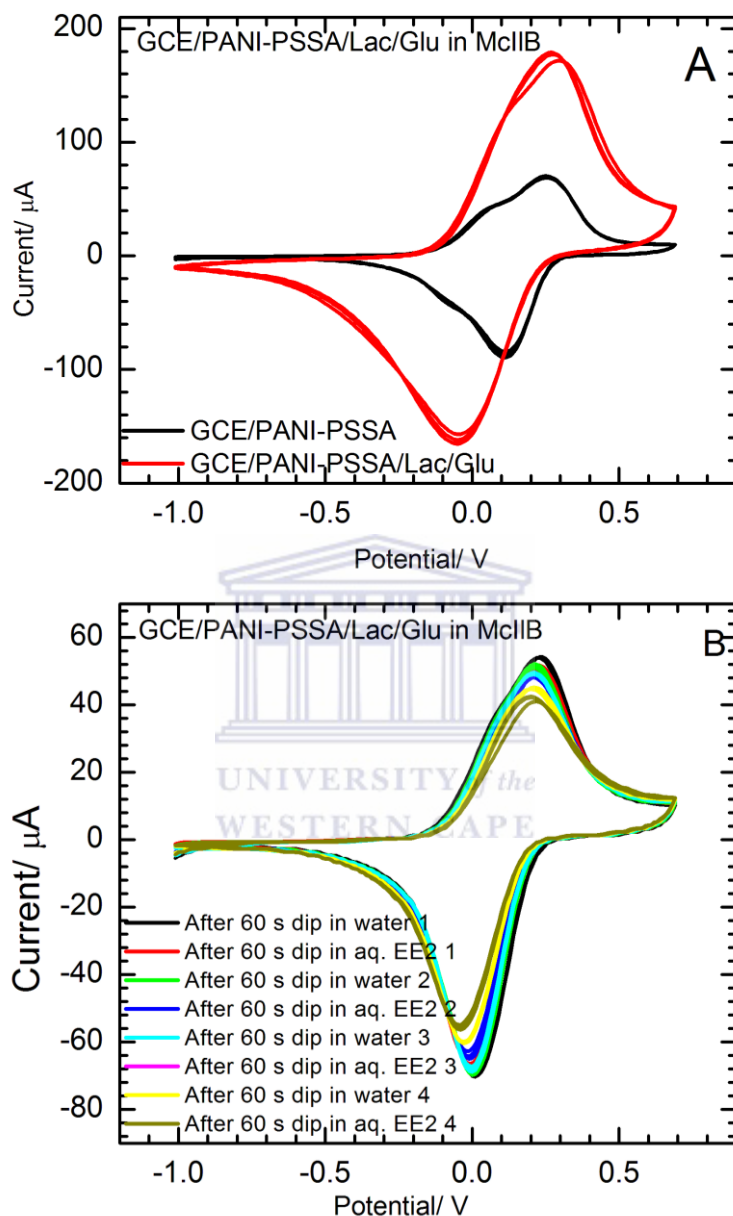


Figure 40: Set of CVs of GC/PANI-PSSA/Lac/Glu recorded at 25 mV/ s in McIIB before and after a 60 s dip in water-blank or in aq. EE2 (1 mM) sample for four successively repeated experiments A, B, C and D in that order. $E_{in} = -1$ V, $E_{high} = 0.7$ V, and $E_{final} = -1$ V

5.2.3 Response of GC/ PANI-PSSA/Au/Lac/Glu to EE2

It is obvious that AuNPs can be used to further enhance the conductivity of a polymeric film and increase the effective surface area available for immobilizing an enzyme [73]. To exploit this possibility, 4 μL of the stock solution of the prepared AuNPs was drop-coated over a fresh GC/PANI-PSSA surface. When the AuNP layer was dry, layers of laccase and glutaraldehyde were drop-cast sequentially in that order the same way described in the previous sections. The resulting biosensor (GC/PANI-PSSA/Au/Lac/Glu) was subjected the same six-step EE2-response and re-usability experiment as described for GC/PANI-PSSA and GC/PANI-PSSA/Lac/Glu in the previous two sections, but this time the experiment was repeated only for three times. The resulting CVs have been shown overlaid in Figure 40B, indicated as water 1, 2, and 3, and EE2 1, 2, and 3, in chronological order. Here as well similar observations as for GC/PANI-PSSA/Lac/Glu.

Exposure to aq. EE2 always reduced the cathodic peak current and shifted the cathodic peak potential to more negative values. However, even though thorough washing water did not appear to have reversed the effect of EE2 exposure, the results indicated that changes in CV occurred only after exposure to EE2. Thus this configuration of the biosensor seems to be inferior in its re-usability relative to the naked-laccase biosensor (GC/PANI-PSSA/Lac). While the glutaraldehyde layer would be theoretically improve stability of the biosensor, however, its presence might have made it more difficult to refresh or regenerate the biosensor as the products of the enzymatic oxidation of EE2 would remain entrapped within immobilization matrix and could not be washed off. Other strategies to address this drawback of the crosslinker agent and to improve the biosensor's sensitivity will have to be explored in future works.

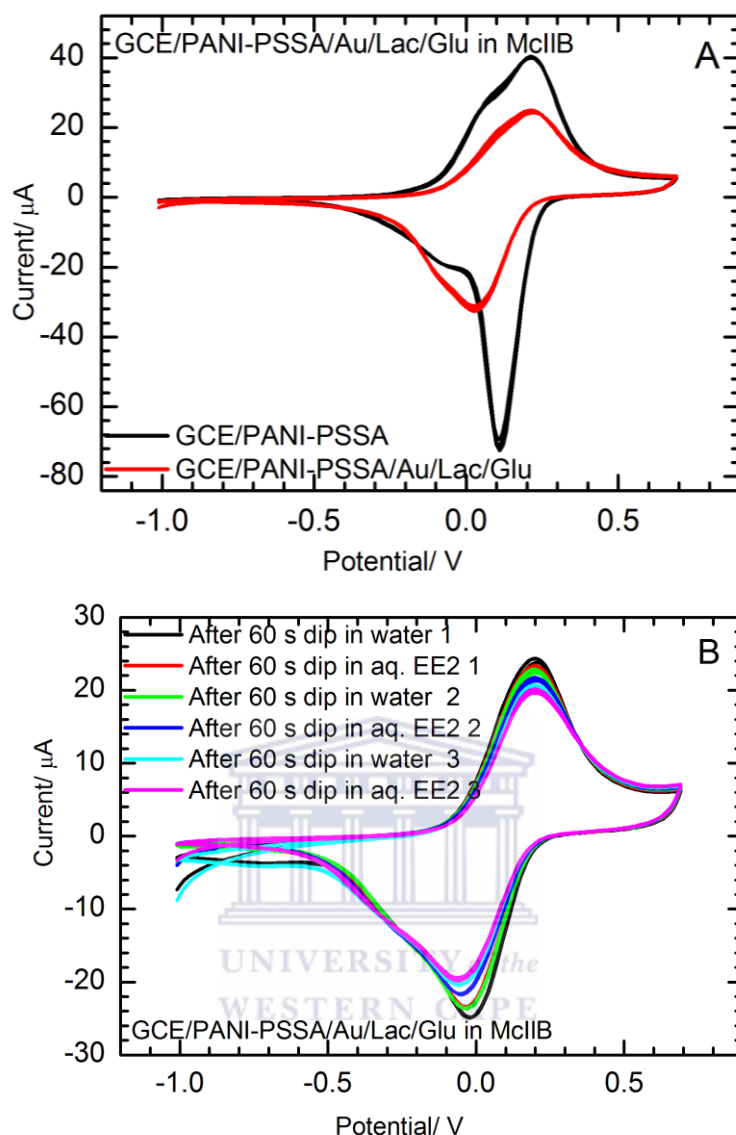


Figure 41: Set of CVs of GC/PANI-PSSA/Au/Lac/Glu recorded at 25 mV/ s in McIlB before and after a 60 s dip in water blank or in aq. EE2 (1 mM) for three successively repeated experiments A, B, and C in that order. $E_{in} = -1$ V, $E_{high} = 0.7$ V, and $E_{final} = -1$ V

5.2.4 Summary and Comparison of Platforms

CV of GC/PANI-PSSA showed no difference before and after exposure to aq. EE2 solution. Therefore this shows that the background CV characteristics of GC/PANI-PSSA platform was unaffected by exposure to EE2. This shows the platform was re-usable and could serve as stable immobilising platform in laccase biosensor. For the CV of GC/PANI-PSSA/Lac/Glu before and after dipping in aq. EE2 sample, reduced the cathodic peak and shifted peak

potential to more negative values. This shows the promising re-usable of laccase biosensor to EE2. The response of GC/PANI-PSSA/Au/Lac/Glu to EE2 when exposed to aq. EE2, the cathodic peak current and cathodic peak potential have shifted to more negative values and when thoroughly washed after exposure to EE2, it did not reverse back to the normal state. This could be due to the glutaraldehyde used. Thus this configuration of the biosensor seems to be inferior in its re-usability relative to the naked-laccase biosensor (GC/PANI-PSSA/Lac). All three platforms showed a promising re-usable effect.

5.3 Electrochemical Impedance Laccase Biosensor Studies

The studies with CVs on the changes in electrochemical properties on exposure of the biosensor to a solution of EE2 can be complemented with electrochemical impedance spectroscopic interrogation. The changes observed in peak potentials in CVs before and after exposure to EE2 could be transduced into changes in charge transfer resistance (R_{ct}) of the PANI-PSSA film to its own electron transfer reaction due to accumulation of insoluble polymeric deposits following the enzymatic oxidation of the analyte. The measurement of R_{ct} can be easily made with EIS. To this end the same sequence of experiments carried out with CV in Section 4.9 were now repeated by using EIS as the method of interrogation. Impedance spectra were obtained for GC/PANI-PSSA and then for GC/ PANI-PSSA/Lac/Glu, before and after exposure to EE2 solution, within the ac frequency range of 100 mHz - 100 kHz and amplitude of 10 mV. The Randles equivalent circuit shown in Figure 42 was used for the fitting of the experimental data. R_s is sum of uncompensated ohmic resistances due to solution and other sources if any, $CPE1$ and $CPE2$ are constant phase elements, and $R1=R_{ct}$.

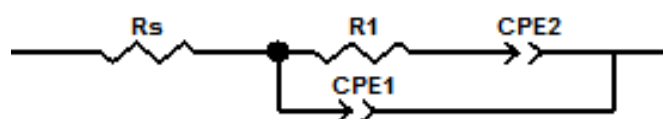


Figure 42: Equivalent circuit model for GC/PANI-PSSA and PANI-PSSA/Lac/Glu in McIIB

R_s represent the uncompensated resistance due to the solution and other resistive elements between the reference electrode and the electrical contact of the working electrode on which the biosensor has been engineered. The use of a constant phase element (CPE1) was used instead of a capacitor to represent the electrical double layer because the former resulted in a better fitting of the experimental data. R_1 represents the R_{ct} of the PANI-PSSA film, and is connected in series with a second constant phase element (CPE2) representing the behaviour of the film as a dielectric material. The experimental results and discussions in this section will mostly focus on the charge transfer resistance (R_{ct}) recorded before after EE2 exposure of the biosensors, but only briefly on other parameters. The chi-squared indicator for the goodness of EIS fitting was for every fitting runs (Z-view) were around 0.00028-0.00029.

5.3.1 Response of GC/ PANI-PSSA to EE2

Figure 43 shows the impedance (Nyquist) plots for GC/PANI-PSSA at dc bias potential (E_{dc}) of 8.5 mV in McIlB before and after 60 s exposure to water or to aq. EE2 for three consecutive cycles with thorough rinsing with water between each cycle (x1, x2, and x3). These spectra, each with a semicircle region lying on the axis followed by a curve with seemingly two linear segments and phase angle rising beyond 50 degrees, were understood as reflecting the behaviour of an electroactive thin-film of material undergoing a quasi-reversible electrochemical process [88]. The semicircle portion, observed at higher frequencies, corresponds to the electron transfer-limited process, whereas the two-segment linear part is characteristic of a partially expressed non-ideal geometric capacitor. Values of the equivalent circuit parameters estimated based on each spectrum before and after exposure to aq. EE2 have been tabulated in Table 4.

In the first cycle, after the first dipping in aq. EE2, a very slight decrease in R_{ct} was observed. In the second round, the R_{ct} was reduced again after a thorough rinsing and 60 s exposures to

water as the blank. However, on the second and third exposures to EE2, the R_{ct} increased relative to its previous values post water-exposure. Thus, one can see that these changes in R_{ct} were either random or insignificant. This is made clear by the % standard deviations (%SD) of each circuit element across the cycles of measurements across, all except one being three cycles element about the means of the values, each being with in experimental uncertainty of less 5%. Therefore the results show that the GC/PANI-PSSA platform could be used all over again and mere exposure to EE2 did not change its electrochemical impedance characteristics.

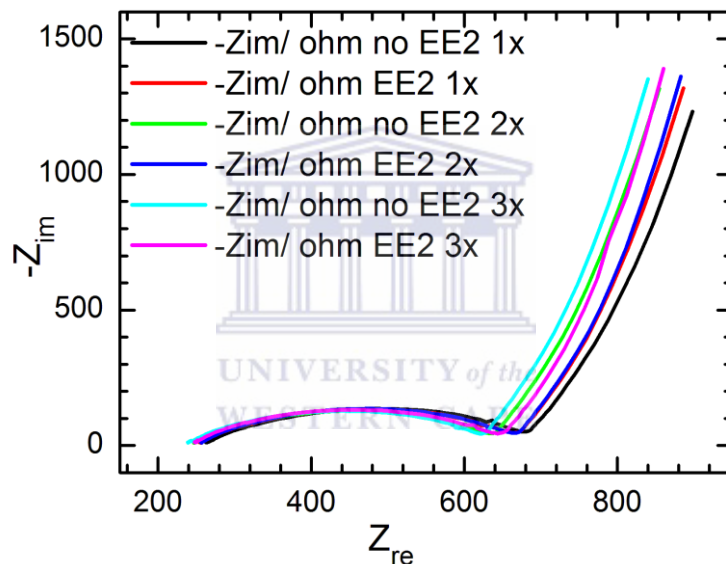


Figure 43: Impedance (Nyquist) plots for GC/PANI-PSSA at dc bias potential (E_{dc}) of 8.5 mV in McIIIB before and after 60 s exposure to water or to aq. EE2 for three consecutive cycles with thorough rinsing with water between each cycle

Table 4: Equivalent circuit and kinetic parameters estimated using the EIS data for GC/PANI-PSSA in McIIB before and after exposure to aq. EE2 solution

Parameters/ unit	Measurement cycle/ parameter/ values and error						Means across cycles/ intra- and inter-variations				
	1 st cycle		2 nd cycle		3 rd cycle		Water		EE2		EE2-Water
	Water	EE2	Water	EE2	Water	EE2	Mean±SD	%SD	Mean±SD	%SD	%Change
R_s / Ω	259.7±0.4	250.7 ±0.4	244.1±0.4	252.2±0.4	235.9±0.4	243.8±0.43	246±12	4.9%	249±5	1.8%	1.2%
$R1 = R_{ct} / \Omega$	442.9 ±1.4	435±1	410.3±1.3	431.9±0.1	405.1±1.2	419.6±1.3	419±20	4.9%	429±8	1.9%	2.4%
$CPE2-T/ 10^{-3} s^P \Omega^{-1}$	1.18±0.00	1.11 ± 0.00	1.11 ± 0.00	1.08 ±0.00	1.09±0.00	1.05 ± 0.00	1.13±0.05	4.2%	1.08±0.03	2.8%	-4.4%
$CPE2-P$	0.88 ±0.00	0.88±0.00	0.89±0.00	0.89±0.00	0.89 ±0.00	0.89 ± 0.00	0.89±0.01	0.65%	0.89±0.01	0.65%	0%
$CPE1-T/ 10^{-6} s^P \Omega^{-1}$	12.9±0.3	10.6±0.2	10.4± 0.2	9.40±0.00	9.9±0.2	9.3 ± 0.2	11.0±1.6	14%	9.8±0.7	7.4%	-11%
$CPE1-P$	0.69 ±0.00	0.7±0.00	0.70±0.00	0.71±0.00	0.71 ± 0.00	0.71±0.00	0.7±0.01	1.42857	0.71±0.01	0.82%	1.4%

5.3.2 Response of GC/ PANI-PSSA/ Lac/ Glu to EE2

Figure 44 shows the impedance (Nyquist) plots for GC/PANI-PSSA/Lac/Glu at dc bias potential (E_{dc}) of 0.11 V in McIIB before and after 60 s exposure to water or to aq. EE2 for three consecutive cycle of measurements with thorough rinsing with water between each cycle (x1, x2, and x3). Still showing the semicircle like that of GC/PANI-PSSA, the low frequency impedance line in the current case exhibited at a much lower range of frequencies and spanned only few set of data. Nevertheless the spectra were fit to the same model in Figure 42. Values of the equivalent circuit parameters estimated based on each spectrum before and after exposure to aq. EE2 have been tabulated in Table 5.

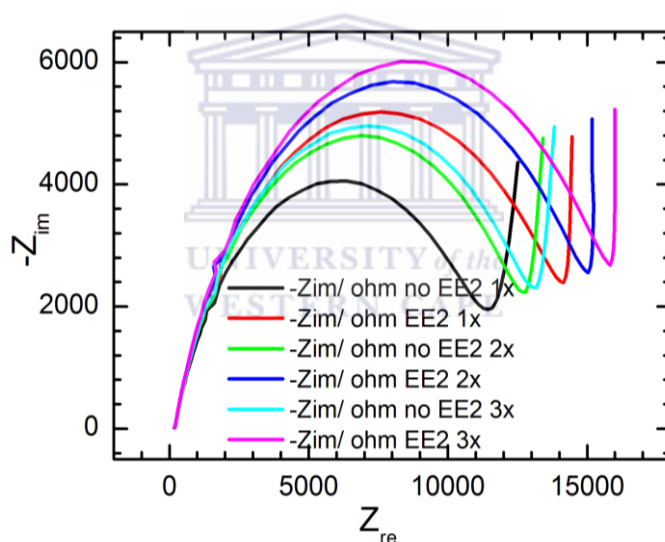


Figure 44: Impedance (Nyquist) plots for GC/PANI-PSSA/Lac/Glu at dc bias potential (E_{dc}) of 0.11 V in McIIB before and after 60 s exposure to water or to aq. EE2 for three consecutive cycles with thorough rinsing with water between each cycle

Table 5: Equivalent circuit and kinetic parameters estimated using the EIS data for GC/PANI-PSSA/ Lac-Glu in McIIB before and after exposure to aq. EE2 solution

Parameters/ unit	Measurement cycle/ parameter/ values and error						Means across cycles/ intra- and inter-variations				
	1 st cycle		2 nd cycle		3 rd cycle		After Water		After EE2		EE2-Water
	Water	EE2	Water	EE2	Water	EE2	Mean±SD	%SD	Mean±SD	%SD	%Change
$R_s/\ \Omega$	181.5±0.5	202.9±0.5	184.4±0.4	187.9±0.4	200.1±0.5	193.8±0.4	189±10	5.3%	195±8	3.9%	3.3%
$RI = R_{ct}/\ k\Omega$	12.1±0.7	15.0±0.1	13.6±0.5	16.0±0.06	14.0±0.1	16.9±0.1	13±1	7.6%	16±1	6.0%	21%
$CPE2-T/10^{-6}\ s^P\ \Omega^{-1}$	400±12	360±10	362±8	338±8	349±8	328±7	370±26	7.2%	342±16	4.8%	-7.6%
$CPE2-P$	0.90±0.02	1.05±0.02	1.02±0.02	1.09±0.02	1.02±0.02	1.09±0.02	0.98±0.07	7.1%	1.08±0.02	2.1%	9.9%
$CPE1-T/ 10^{-6}\ s^P\ \Omega^{-1}$	4.63±0.05	3.77±0.03	4.15±0.03	3.48±0.02	4.00±0.03	3.31±0.01	4.3±0.3	7.7%	3.5±0.2	6.6%	-17%
$CPE1-P$	0.76±0.001	0.78±0.00	0.8±0.0	0.78±0.00	0.78±0.00	0.78±0.00	0.78±0.02	2.6%	0.78±0	0%	0%

From the outset, GC/PANI-PSSA/Lac/Glu exhibited an R_{ct} of about $1210 \pm 70 \Omega$, which is an order of magnitude higher than the R_{ct} of GC/PANI-PSSA platform ($443 \pm 1 \Omega$). However, in the current case, an increase in R_{ct} was always observed after the 60 s exposure to the aq. EE2 sample. Also, every time the biosensor was thoroughly rinsed and dipped in water for 60 s, the R_{ct} decreased showing that it was possible to regenerate the surface of the biosensor. The EE2 sensing potential of the biosensor was demonstrated by the fact that there was an average increase of R_{ct} by about 20% after exposure to EE2, while the variation in pre-exposure R_{ct} values was only about 7.6 and that for post-exposure values was only 6%. Therefore this shows that the enzyme and hence the biosensor is functional, and a promising step towards achieving a re-usable laccase biosensor for EE2 in particular, and estrogens in general, has been demonstrated.

5.3.3 Summary and Comparison of Platforms

When interrogating the changes in electrochemical properties on exposure of EE2 using electrochemical impedance spectroscopy, only GC/PANI-PSSA and GC/PANI-PSSA/Lac/Glu platform was used. Semicircle region followed by a curve was observed on both experiments. On GC/PANI-PSSA after exposure to EE2, the R_{ct} decreased but as cycles increase, R_{ct} increase. The standard deviation also made these conclusions clearly being less than 8% for all experiments. Therefore this shows that GC/PANI-PSSA platform could be used all over again and being exposed to EE2 did not change its electrochemical impedance characteristics. Response of GC/PANI-PSSA/Lac/Glu to EE2 showed an average increase of R_{ct} of about 21% after exposure of EE2. This showed the biosensor was functional and showing a positive step of achieving a re-usable biosensor for EE2.

CHAPTER VI: CONCLUSION AND RECOMMENDATIONS

6.1 Conclusions

Firstly preliminary studies of the materials used on the experiment were studied, which were estrogens, laccase, AuNPs, laccase activity towards EE2, storage of laccase and EE2. Laccase was shown to be active towards EE2 and the enzyme could be stored for over three months. EE2 solution also could be used for over three months. Buffer used in this study was found to be suitable. H_3PO_4 was a suitable electrolyte than HCl to be used for the electropolymerization of aniline and was used because it has same ions as the McIIB which the post-deposition CVs indicated the formation of electrochemically very stable film. AuNPs were successfully synthesized and its size was identified to be less than 22 nm. The nanoparticles were used in the fabrication of a biosensor to detect EE2. McIIB used for testing electrochemical properties of AuNP. CVs of GC/PANI-PSSA and GC/PANI-PSSA/Au showed no difference before and after exposure to aq. EE2 solution, an indication of being re-usable and could also serve as stable immobilising platform in laccase biosensor. When interrogating with electrochemical impedance spectroscopy, the R_{ct} of both GC/PANI-PSSA and GC/PANI-PSSA/Lac/Glu showed an average increase by about 2.4% and 21% before and after exposure of EE2, respectively. This shows that the GC/PANI-PSSA/Lac/Glu was a functional EE2 biosensor and showing a positive step towards achieving a re-usable biosensor for EE2 as a model water estrogen.

6.2 Recommendations

The biosensor parameters should be investigated further in order to improve the methods of surface regeneration and sensitivity to EE2. This will have to be followed up with evaluation of its analytical performance and characteristics (detection, linearity, detection limit,

sensitivity, reproducibility, and selectivity) towards each water estrogen. Application to real samples and comparison with other methods will be necessary in the end.



7 BIBLIOGRAPHY

1. Bodzek, M. and M. Dudziak, *Removal of Natural Estrogens and Synthetic Compounds Considered to be Endocrine Disrupting Substances (EDs) by Coagulation and Nanofiltration*. Polish Journal of Environmental Studies 2006. **15**(1): p. 35-40.
2. Saaristo, M., J.A. Craft, K.K. Lehtonen, and K. Lindström, *An endocrine disrupting chemical changes courtship and parental care in the sand goby*. Aquatic Toxicology, 2010. **97**(4): p. 285–292.
3. Hamid, H. and C. Eskicioglu, *Fate of estrogenic hormones in wastewater and sludge treatment: A review of properties and analytical detection techniques in sludge matrix*. Water Research 2012. **46**: p. 5813-5833.
4. Mazellier, P., L. Meite, and J. De Laat, *Photodegradation of the steroid hormones 17 β -estradiol (E2) and 17 α -ethinylestradiol (EE2) in dilute aqueous solution*. Chemosphere, 2008. **73**(8): p. 1216–1223.
5. Ying, G.-G., R.S. Kookana, and Y.-J. Ru, *Occurrence and fate of hormone in the environment*. Environmental International, 2002 **28**: p. 545-551.
6. Hajkova, K., Pulkrabova J., Schurek J., *Novel approaches to the analysis of steroid estrogens in river sediments*. Analytical Bioanalytical Chemistry, 2007. **387**: p. 1351–1363.
7. Wise, A., K. O' Brien, and T. Woodruff, *Are Oral Contraceptives a Significant Contributor to the Estrogenicity of Drinking Water?* Environmental Science and Technology, 2011. **45**: p. 51–60.
8. Liu, M., E.P.C. Lai, and Y. Yang, *Removal of 17 β -Estradiol By Nylon Filter Membrane: Adsorption Kinetics And Thermodynamics*. International Journal of Research and Reviews in Applied Sciences, 2012. **11** (1): p. 67-73.

9. Caldwell, D.J., F. Mastrocco, E. Nowak, J. Johnston, H. Yekel, D. Pfeiffer, P. Anderson, *An Assessment of Potential Exposure and Risk from Estrogens in Drinking Water*. Environmental Health Perspectives, 2010. **118**(3): p. 338–344.
10. Pham, H.T.M., *Amperometric detection of hormonal activity by a yeast cell biosensor*. 2012: Germany.
11. Lucci, P., O. Nunez, and M.T. Galceran, *Solid-phase extraction using molecularly imprinted polymer for selective extraction of natural and synthetic estrogens from aqueous samples*. Journal of Chromatography A, 2011. **1218**: p. 4828– 4833.
12. Ruhland, A., N. Leal, and P.E. Kima, *Leishmania promastigotes activate PI3K/Akt signalling to confer host cell resistance to apoptosis*. Cellular Microbiology 2007. **9**(1): p. 84–96.
13. Zimmermann, K.A. *Endocrine System: Facts, Functions and Diseases*, LiveScience Contributor. 2013 [28-10-2013].
14. Hiller-Sturmhöfel, S. and A. Bartke, *The Endocrine System-An Overview*, Alcohol Health & Research World 1998. **22**(3): p. 153-164.
15. Iguchi, T. and T. Sato, *Endocrine Disruption and Developmental Abnormalities of Female Reproduction*. American Zoologist, 2000. **40**: p. 402–411.
16. Cargouet, M., D. Perdiz, A. Mouatassimsouali, S. Tamisierkarolak, Y. Levi, *Assessment of river contamination by estrogenic compounds in Paris area*. Science of the Total Environment 2004. **324**(1): p. 55–66.
17. Nagpal, N.K. and C.L. Meays, *Water Quality Guidelines for Pharmaceutically-active-Compounds (PhACs): 17 α -ethinylestradiol (EE2)*. 2009, Ministry of environment province of British Columbia,. p. 1-24.
18. Zhongboa, Z. and J. Hub, *Selective removal of estrogenic compounds by molecular imprinted polymer (MIP)*. Water Research, 2008. **42**(15): p. 4101 – 4108.

19. Elnwishy, N., A. Hanora, and R. Afifi, *A Potential 17- β Estradiol degrader Bacterium Isolated from Sewage water*. Egyptian Academic Journal of Biological Sciences., 2012 **4**(1): p. 27-34.
20. Fujii, K., N. Morita, T. Motomura, T. Tanaka, S. Kikuchi, *Novosphingobium tardaugens sp. nov., an oestradiol-degrading bacterium isolated from activated sludge of a sewage treatment plant in Tokyo*. International Journal of Systematic and Evolutionary Microbiology, 2003. **53**: p. 47–52.
21. Nxusani, E., P.M. Ndangili, R.A. Olowu, A. N. Jijana, T. Waryo, N. Jahed, R.F. Ajayi, Priscilla Baker, Emmanuel I. Iwuoha, *3-Mercaptopropionic acid capped Ga₂Se₃nanocrystal-CYP3A4 biosensor for the determination of 17-alpha-ethinyl estradiol in water*. Nano Hybrids, 2012 **1**: p. 1-22.
22. Labadie, P., T. Mader, C. Shapiro, S. Donk, D. Shelton, D. Tarkalson, T. Zhang, *Evidence for the migration of steroidal estrogens through riverbed sediments* Environmental Science and Technology 2007 **41**(12): p. 4299 -4304.
23. Colborn, T. and C. Clement, *Chemically-Induced Alterations in Sexual and Functional Development: The Wildlife Human Connection*, in *Endocrine Disruptors Part 1*, M. Metzler, Editor. 1992 p. 113-127.
24. Jobling, S., C. Tyler, and J. Sumpter, *In fish, exposure to EDCs alters their reproductive physiology and morphology : Review Endocrine disruption in wildlife: a critical review of the evidence*. Critical Reviews in Toxicology , 1998. **28**(4): p. 319-361.
25. Larkin, P., et al., *Expression Profiling of Estrogenic Compounds Using a Sheepshead Minnow cDNA Macroarray*. Environmental Health Perspectives 2003. **111**: p. 1-8.

26. Colman, J., L. Folmar, M. Hemmer, A. Poston, N. Denslow, *Effects of the synthetic estrogen, 17alpha-ethinylestradiol, on aggression and courtship behavior in male zebrafish (Danio rerio)* Aquatic Toxicology, 2009. **91**(4): p. 346–354.
27. Jobling, S., S. Coey, J.G. Whitmore, D.E. Kime, K.J. Van Look, B.G. McAllister, N. Beresford, A.C. Henshaw, G. Brighty, C.R. Tyler, J.P. Sumpter, *Wild intersex roach (Rutilus rutilus) have reduced fertility.* Biology of Reproduction. , 2002. **67**(2): p. 515-524.
28. Liu, B., F. Wu, and N.-s. Deng, *UV-light induced photodegradation of 17α-ethinylestradiol in aqueous solutions.* Journal of Hazardous Materials, 2003. **98** (1-3): p. 311–316.
29. Beecher, L.E. and S.A. White. *Assessment of Different Substrates for Removal Of Endocrine Disrupting Compounds in Wastewater and The Potential Effects on Food Chain Pathways.* in *South Carolina Water Resources*. 2012. South Carolina Institute for Environ Toxicology, Clemson University, .of the WESTERN CAPE
30. Meng , Z., W. Chen, and A. Mulchandani, *Removal of Estrogenic Pollutants from Contaminated Water Using Molecularly Imprinted Polymers.* Environmental Science and Technology, 2005 **39**: p. 8958-8962.
31. McAvoy, K., *Occurrence of estrogens in wastewater treatment plant and waste disposal site water samples.* 2008: New York.
32. Matta, M.S., A.C. Wilbraham, and D.D. Stanley, *General, Organic, and Biological Chemistry.* 1996, Canada: D.C. Health and Company.
33. ; Available from: <http://www.worthington-biochem.com/introbiochem/enzymes.pdf>.
34. Adrignola, A. *Structural Biochemistry/Enzyme/Active Site.* [cited 2013 27/10]; Available from: <http://www.saylor.org/site/wpcontent/uploads/2011/01/Enzyme-Overview.pdf>.

35. Neelam, G., S. Ray, S. Bose, V. Rai, *A Broader View: Microbial Enzymes and Their Relevance in Industries, Medicine, and Beyond*. Hindawi Publishing Corporation,, 2013: p. 18.
36. Corcuera, D., J.I. Reyes, and R.P. Cavalieri, *Biosensors*. Encyclopedia of Agricultural, Food, and Biological Engineering, 2003.
37. Starr, C. and R. Taggart, *Biology: The Unity and Diversity of Life*. 1998: Wadsworth Sworth Publishing Company.
38. Huang, C.-C., C.Y. Lin, C.W. Chang, C.Y. Tang *Enzyme Reaction Annotation Using Cloud Techniques*. Hindawi Publishing Corporation, 2013. **2013**: p. 11
39. Metin, A.U., *Immobilization of Laccase onto Polyethyleneimine Grafted Chitosan Films: Effect of System Parameters*. Macromolecular Research, Vol. 21, No. 10, pp 1145-1152 (2013), 2013. **21**(10): p. 1145-1152.
40. Yoshida, H., *Chemistry of lacquer* Journal of Chemical Society, 1883. **43**: p. 472–486.
41. Baldrian, P., *Fungal laccases-occurrence and properties*. Federation of European Microbiological Societies, 2006. **30**: p. 215–242.
42. Mayera, A.M. and R.C. Staplesb, *Laccase: new functions for an old enzyme*. . Phytochemistry 2002. **60** p. 551–565.
43. Adamafo, N.A., N.S. Sarpong, C.A. Mensah, M. Obodai, *Extracellular Laccase from Pleurotus ostreatus Strain EM-1: Thermal Stability and Response to Metal Ions*. Asian Journal of Biochemistry, 2012. **7**(3): p. 143-150.
44. Vernekar, M. and S.S. Lele, *Laccase: Properties and Applications*. Bioresources, 2009. **4**(4): p. 1694-1717.

45. Wang, X., P. Sjöberg-Eerola, K. Immonen, J. Bobacka, M. Bergelin, *Immobilization of Trametes hirsuta laccase into poly(3,4-ethylenedioxythiophene) and polyaniline polymer- matrices*. Journal of Power Sources 2011. **196**: p. 4957-4964.
46. Quan, D., et al., *Assembly of Laccase over Platinum Oxide Surface and Application as an Amperometric Biosensor*. Bull. Korean Chem. Soc 2002. **23**(3): p. 385-390.
47. Thurston, C.F., *The structure and function of fungal laccases*. Microbiology, 1994. **140**: p. 19–26.
48. Ferraroni, M., D. Llaría, M. Myasoedova, A. Leontievsky, L. Golovlela, A. Scozzafava, *Crystallization and preliminary structure analysis of the blue laccase from the ligninolytic fungus Panus tigrinus*. Acta Crystallogr Sect F Structural Biology and Crystallization Communications, 2005. **61**(2): p. 205–207.
49. Couto, C.A.M.d., *Active bionanoconjugates of laccase and gold nanoparticles: Kinetic and structural studies.*, in *B.Sc in Applied Chemistry*. 2012, New University of Lisbon.
50. Gomes, S.A.S.S. and M.J.F. Rebelo, *A new Laccase Biosensor for Polyphenols Determination*. Sensors, 2003. **3**: p. 166-175.
51. Ivnitski, D., et al., *Design and Characterization of Nano-structured Laccase Electrodes* 2013: Department of Chemical & Nuclear Engineering, UNM Center for Emerging Energy Technologies.
52. Odaci, D., S. Timur, N. Pazarlioglu, U.A Kirgoz, A. Telefoncu, *Effects of mediators on the laccase biosensor response in paracetamol detection*. Biotechnology and Applied Biochemistry, 2006. **45**: p. 23-28.
53. Haghghi, B., B. Haghghia, L. Gortonb, T. Ruzgasb, L.J. Jönssonc *Characterization of graphite electrodes modified with laccase from Trametes*

- versicolor* and their use for bioelectrochemical monitoring of phenolic compounds in flow injection analysis. *Analytica Chimica Acta*, 2003. **487** (1): p. 3–14.
54. Kunamneni, A., F.J.P.A. Ballesteros, and A. Miguel, *Laccases and their applications: A patent review*. 2007.
55. Huang, H.-w., G. Zoppellaro, and T. Sakurai, *Spectroscopic and Kinetic Studies on the Oxygen-centered Radical Formed during the Four-electron Reduction Process of Dioxygen by *Rhus vernicifera* laccase*. The American Society for Biochemistry and Molecular Biology, 1999. **1999**: p. 32718-32724.
56. Moldes, D., M. Fernández-Fernández, and M.Á. Sanromán, *Role of Laccase and Low Molecular Weight Metabolites from *Trametes versicolor* in Dye Decolorization*. . The Scientific World Journal 2012. **2012**: p. 9.
57. Hulanicki, A., S. Geab, and F. Ingman, *Chemical Sensors Definitions and Classification*. *Pure&Appl. Chem.*, 1991. **63**(9): p. 1247-1250.
58. Yoo, E.-H. and S.-Y. Lee, *Glucose Biosensors: An Overview of Use in Clinical Practice*. *Sensors* 2010. **10**: p. 4558.
59. Chambers, J.P., et al., *Biosensor Recognition Elements*. *Curr. Issues Mol. Biol.* . **10**: p. 1-12.
60. Newman, J.D. and S.J. Setford, *Enzymatic Biosensors*. *Molecular Biotechnology*, 2006. **32**: p. 249-268.
61. Ravindra, N.M., C. Prodan, S. Fnu, I. Padroni, S.K. Sikha *Advances in the Manufacturing, Types, and Applications of Biosensors*. *Journal Of Microbiology*, 2007
62. Pohanka, M. and P. Skládal, *Electrochemical biosensors – principles and applications*. *Journal Of. Applied. Biomedicine*, 2008. **6** p. 57–64.

63. Theâvenot, D.R., K. Toth, R.A. Durst, G.S Wilson. *Electrochemical Biosensors: Recommended Definitions And Classification*. Pure Applied Chemistry, 1999. **71** (12): p. 2333-2348.
64. Pumera, M., S. Sanchez, I. Ichinose, J. Tang, *Electrochemical nanobiosensors*. Sensors and Actuators B, 2007. **123**: p. 1195-1205.
65. Li, Y., L. Zhang, M. Pi, Z. Pan, D. Li, *A disposable biosensor based on immobilization of laccase with silica spheres on the MWCNTs-doped screen-printed electrode*. Chemistry Central Journal 2012, , 20012. **6**(103): p. 1-8.
66. Caseroa, E., et al., L. Vazquez, L. Ramirez-Asperilla, A.M. Parra-Alframba, F. Pariente, E. Lorenzo, *Laccase biosensors based on different enzyme immobilization strategies for phenolic compounds determination*. Talanta, 2013. **115** p. 401–408.
67. Amendola, V. and M. Meneghett, *Size Evaluation of Gold Nanoparticles by UV-vis Spectroscopy*. Journal of Physical Chemistry C 2009. **113**: p. 4277–4285.
68. Iosin, M., F. Toderas, P.L. Baldeck, S. Astilean, *Study of protein–gold nanoparticle conjugates by fluorescence and surface-enhanced Raman scattering*. Journal of Molecular Structure, 2009. **924–926**: p. 196–200.
69. Pingarron, J.m., P. Yanez-Sedeno, and A. Gonzalez-Cortes, *Gold nanoparticle-based electrochemical biosensors*. Electrochimica Acta, 2008. **53**: p. 5848-5866.
70. Sun, X., Y. Zhu, and X. Wang, *Amperometric Immunosensor Based on a Protein A/Deposited Gold Nanocrystals Modified Electrode for Carbofuran Detection*. Sensors (Basel),, 2011. **11**(12): p. 11679–11691.
71. Philip, D., *Synthesis and spectroscopic characterization of gold nanoparticles*. Spectrochimica Acta Part A 2008. **71**: p. 80–85.

72. Brondania, D., B. Souza, A. Neves, I. Vieira, *PEI-coated gold nanoparticles decorated with laccase: A new platform for direct electrochemistry of enzymes and biosensing applications*. *Biosensors and Bioelectronics*, 2013. **42**: p. 242–247.
73. Petkova, G.A., K. Zaruba, P. Zvatora, V. Kral, *Gold and silver nanoparticles for biomolecule immobilization and enzymatic catalysis*. *Nanoscale Research Letters*, 2012. **7**(287).
74. Bonanni, A., M. Pumerab, and Y. Miyahara, *Influence of gold nanoparticle size (2–50 nm) upon its electrochemical behavior: an electrochemical impedance spectroscopic and voltammetric study*. *Physical Chemistry Chemical. Physics.*, 2011, . **13**: p. 4980–49862011.
75. Hong, S. and X. Li, *Optimal Size of Gold Nanoparticles for Surface-Enhanced Raman Spectroscopy under Different Conditions*. *Journal of Nanomaterials*, 2013. **2013**.
76. Reddy, S.B., D.E. Mainwaring, M.A. Kobaisi, P. Zeepongsekul, J.V. Fecondo, *Acoustic wave immunosensing of a meningococcal antigen using gold nanoparticle-enhanced mass sensitivity*. *Biosensors and Bioelectronics*, 2012 **31** p. 382– 387.
77. Gerard, M., A. Chaubey, and B.D. Malhotra, *Application of conducting polymers to biosensors*, . *Biosensors & Bioelectronics* 2002 **17**: p. 345–359.
78. Greene, R.L., G.B. Street, and L.J. Suter, *Superconductivity in polysulfur nitride (SN)_x*. *Physical Review Letters*. , 1975. **34**: p. 577–579.
79. Vivekanandan, J., V. Ponnusamy, A. Mahudswaran, P.S. Vijayanand, *Synthesis, characterization and conductivity study of polyaniline prepared by chemical oxidative and electrochemical methods*. *Archives of Applied Science Research*, 2011. **3**(6): p. 147-153.

80. Jijana, N.A., E.I. Iwuoha, and P.G.L. Baker, *Development of electrochemical ZnSe quantum dots biosensor for low-level detection of 17 β -estradiol estrogenic endocrine disrupting compounds*, in *Chemistry*. 2012 University of Western Cape.
81. Munoz, E., A. Colina, A. Heras, V. Ruiz, S. Palmero, J. Lopez-Palacios, *Electropolymerization and characterization of polyaniline films using a spectroelectrochemical flow cell*. *Analytica Chimica Acta* 2006. **573-574**: p. 20-25.
82. Stejskal, J., *Polyaniline, Preparation of a Conducting Polymer Pure Applied Chemistry.*, Vol. 74, No. 5, pp. 857–867, 2002., 2002. **74(5)**: p. 857–867.
83. Wu, C.-G. and T. Bein, *Conducting Polyaniline Filaments in a Mesoporous Channel Host*. 1994.
84. El-Mahy, S.K., M. Dawy, and E.A. El Aziz, *Synthesis and Electrical Properties of Polyaniline - Fe₃O₄ Nanocomposite*. *Journal of Applied Sciences Research* 2013. **9(4)**: p. 2918.
85. Bocchini, S., A. Chiolerio, S. Porro, D. Accardo, N. Garino, K. Bejtka, D. Perrone, C.F. Pirri, *Synthesis of polyaniline-based inks, doping thereof and test device printing towards electronic applications*. *Journal of Materials Chemistry*, 2013.
86. Magnuson, M., J.H., Guo, S.M. Butorin, A. Agui, C. Sathe, J. Nordgren, A. Monkan *The electronic structure of polyaniline and doped phases studied by soft X-ray absorption and emission spectroscopies*. *Journal Of Chemical Physics* 1999. **111(4756)**.
87. Monk, P.M.S., *Fundamentals of Electroanalytical Chemistry*. 2001, England: John Wiley & Sons Ltd.
88. Bard, A.J. and L.R. Faulkner, *Electrochemical Methods Fundamentals and Applications*. second edition ed. 2001: John Wiley & Sons, Inc

89. Owen, T., *Fundamentals of modern UV-visible spectroscopy*. 2000, Germany: Agilent Technologies
90. Kumar, S., *Organic Chemistry Spectroscopy of Organic Compounds* 2006
91. Tanaka, T., T. Tamura T., Y. Ishizaki, A. Kawase, M. Terauchi, *Enzymatic treatment of estrogens and estrogen glucuronide*. *Journal of Environmental Sciences* 2009 **21** p. 731–735.
92. Kimling, J., M. Maier, B. Okenve, V. Kotaidis, H. Ballot, A. Plech, *Turkevich Method for Gold Nanoparticle Synthesis Revisited*. *Journal of Physical Chemistry B*, 2006. **110**: p. 15700-15707.
93. Ruh, E.L. and J.L. Rossettie, *Apparatus for Distilling Aniline*. *Analytical Chemistry*, 1947. **19**(11): p. 938-938.
94. Liu, B. and X. Liu, *Direct photolysis of estrogens in aqueous solutions*. *Science of The Total Environment*, 2004. **320**(2–3): p. 269-274.
95. Laby, K.a. [12-12-2013]; Available from: http://www.kayelaby.npl.co.uk/chemistry/3_8/3_8_7.html.
96. Shiba, T., L. Xia, T. Miyakoshi, C.L. Chen *Oxidation of isoeugenol and coniferyl alcohol catalyzed by laccases isolated from Rhus vernicifera Stokes and Pycnoporus coccineus*. *Journal of Molecular Catalysis* 2000. **10**(6): p. 605-615.
97. Sabela, M.I., N.J. Gumede, P. Singh, K. Bisetty, *Evaluation of Antioxidants in Herbal Tea with a Laccase Biosensor*. *International Journal of Electrochemical Science*, 2012. **7**: p. 4918 - 4928.
98. Piontek, K., M. Antorini, and T. Choinowski, *Crystal Structure of a Laccase from the Fungus *Trametes versicolor* at 1.90-Å Resolution Containing a Full Complement of Coppers*. *The Journal of Biological Chemistry*, 2002. **277**: p. 37663-37669.

99. Gupta, G., V. Rajendran, and P. Atanasov, *Laccase Biosensor on Monolayer-Modified Gold Electrode*. *Electroanalysis* 2003. **15**(20): p. 1577-1583.
100. Ndongili, P.M., *Electrochemical and optical modulation of selenide and telluride ternary alloy quantum dots genosensors*, in *Chemistry*. 2011, University of the Western Cape: Bellville.
101. Hezarda, T., F. Katia, E. David, C. Vincent, B. Phillipe, G. Pierre, *Gold nanoparticles electrodeposited on glassy carbon using cyclic voltammetry: Application to Hg(II) trace analysis*. *Journal of Electroanalytical Chemistry*, 2012. **664**: p. 46–52.
102. El-Mahy, S.K., M. Dawy, and E.A. El Aziz, *Synthesis and Electrical Properties of Polyaniline - Fe₃O₄ Nanocomposite*. *Journal of Applied Sciences Research*, 2013. **9**(4): p. 2918-2926.
103. Muchindu, M., *Electrochemical Ochratoxin immunosensors based on polyaniline nanocomposites template with amine and sulphate functionalised polystyrene latex beads*, in *Chemistry*. 2012, University of the Western Cape: Bellville.

